

## This is to certify that the

#### dissertation entitled

The Solubility of Xenon in Simple Organic Solvents and in Aqueous Amino Acid Solutions

## presented by

Jeffrey Frank Himm

has been accepted towards fulfillment of the requirements for

Ph.D. degree in Physics

Major professor Gerald L. Pollack

Date September 3, 1986

7-1. ....



RETURNING MATERIALS:
Place in book drop to remove this checkout from your record. FINES will be charged if book is returned after the date stamped below.

# THE SOLUBILITY OF XENON IN SIMPLE ORGANIC SOLVENTS AND IN AQUEOUS AMINO ACID SOLUTIONS

Ву

Jeffrey Frank Himm

A DISSERTATION

Submitted to
Michigan State University
in partial fulfillment of the requirements
for the degree of

DOCTOR OF PHILOSOPHY

Department of Physics and Astronomy

1986

#### ABSTRACT

## THE SOLUBILITY OF XENON IN SIMPLE ORGANIC SOLVENTS AND IN AQUEOUS AMINO ACID SOLUTIONS

Ву

#### Jeffrey Frank Himm

We have measured the Ostwald solubility (L) of 133Xe in a variety of liquids, including normal alkanes, normal alkanols, and aqueous solutions of amino acids, NaCl, and sucrose. For the alkanes and alkanols, measurements were made in the temperature range from 10-50 °C. Values of L were found to decrease with increasing temperature, and also with increasing chain length, for both series of solvents. Thermodynamic properties of solution (enthalpy and entropy of solution) are calculated using both mole fraction and number density scales. Results are interpreted using Uhlig's model of the solvation process. Measurements of L in aqueous amino acid solutions were made at 25°C. Concentrations of amino acids in solution varied from near saturation for each of the amino acids studied to pure water. In all solutions, except those with NaCl, L decreases linearly with increasing solution molarity. Hydration numbers (H), the mean number of water molecules associated with each solute molecule, were determined for each amino acid, for NaCl, and for

sucrose. Values of H obtained ranged from near zero (arginine,  $H=0.2\pm0.5$ ) to about 16 (NaCl,  $H=16.25\pm0.3$ ).

to my dad

#### **ACKNOWLEDGMENTS**

First and foremost, I would like to thank Professor Gerald L. Pollack, who generously provided guidance, encouragement, support, and friendship to make this possible.

I would like to thank all of my friends, both in the department and outside of it, whom i have come to know and love over the years.

I would like to thank Richard Kennan for his assistance in the preparation of this thesis, and Dan Edmunds for all of his help with troublesome equipment.

I would like to thank the Naval Medical Research and Development Command (Contract numbers N00014-80-C-0617 and N00014-83-K-0743) and the Exxon Corporation for their financial support.

And finally, I want to thank my family, especially Mom and Dad, for their love and support.

## TABLE OF CONTENTS

LIS	ST OF TA	BLES
LIS	ST OF FI	GURESvi
1.	INTRODU	CTION1
2.	THEORY.	
		IDEAL SOLUTION
	2.2	RAOULT'S LAW
		HENRY'S LAW11
	2.4	HARD SPHERES13
	2.5	KIRKWOOD-BUFF THEORY18
	2.6	APPLICATIONS TO EXPERIMENTS23
		2.6.1 ASSUMPTIONS2
		2.6.2 THERMODYNAMICS OF SOLUTION
	2.7	MULTICOMPONENT SYSTEMS27
3.	EXPERIM	ENTAL33
	3 1	SOLUTION COMPONENTS33
		APPARATUS
		TEMPERATURE CONTROL
		SHIELDING
		ELECTRONICS
		VOLUME DETERMINATION
		SOLVENT PREPARATION
		LOADING THE APPARATUS43
	3.9	SOLUBILITY EQUATION45
4.	RESULTS	AND CONCLUSIONS50
	jı 4	ALKANES50
		ALKANOLS
		AQUEOUS AMINO ACID SOLUTIONS
	4.3	AMOROGO AMINO ACID SOFOIIONS
5.	LIST OF	REFERENCES135

## LIST OF TABLES

TABLE 1. Solubility data for experiments with <sup>133</sup> Xe in the normal alkanes. The first row gives the Ostwald solubility measured for each alkane, and the second row is 10 <sup>2</sup> x <sub>2</sub> , where x <sub>2</sub> is the mole fraction solubility of Xe in the normal alkanes at 1 atm partial pressure of Xe
TABLE 2. Chemical potentials in the mole fraction scale, $\Delta\mu_2^0$ , and in the number density scale, $\Delta\mu_2^{\circ\rho}$ . The first row is $\Delta\mu_2^{\circ\rho}$ and the second row is $\Delta\mu_2^{\circ\rho}$ . Units are cal/mol62
TABLE 3. Entropy and enthalpy of solution in both the mole fraction scale and in the number density scale for solutions of 133 Xe in the normal alkanes70
TABLE 4. Comparison of experimental binding energies, $E_b^{\text{exp}}$ , of Xe in the normal alkanes with binding energies estimated from the heats of vaporization of the solute and solvent, $E_b^{\text{ext}}$ 76
TABLE 5. Ostwald solubility L and mole fraction solubility $x_2$ for $^{133}$ Xe in the normal alkanols. The first row for each alkanol is L, and the second row is $10^2x_2$ 78
TABLE 6.Chemical potentials in the mole fraction scale, $\Delta\mu_2^{\circ}$ , and in the number density scale, $\Delta\mu_2^{\circ\rho}$ . The first row is $\Delta\mu_2^{\circ\rho}$ and the second row is $\Delta\mu_2^{\circ\rho}$ . Units are cal/mol87
TABLE 7. Entropy and enthalpy of solution in both the mole fraction scale and in the number density scale for solutions of 133Xe in the normal alkanols. (Table 2 of reference 69)95
TABLE 8. Comparison of experimental binding energies, $E_b^{exp}$ , of Xe in the normal alkanols with binding energies estimated from the heats of vaporization of the solute and solvent, $E_b^{ext}$ 100
TABLE 9. Comparison of calculated and experimental thermodynamics of solution
TABLE 10. Comparison of calculated and experimental values for the enthalpy and entropy of solution for mixtures of Xe in some of the alkanes and alkanols. Values were calculated using Pierotti's model, and the Lennard-Jones parameters of Wilhelm and Battino

TABLE 11. List of solubilities measured for Xe in aqueous
solutions of the amino acids, sucrose, and NaCl. Also included
are the solution molarities (M), the solution pH, the volume
fraction water, and the hydration number calculated for each
experiment
TABLE 12. Hydration numbers of the amino acids

## LIST OF FIGURES

Figure 1. Solubility measurement apparatus36
Figure 2. Schematic diagram of the electronics39
Figure 3. Schematic diagram of the degassing system44
Figure 4. Schematic diagram of the gas handling system46
Figure 5. Normalized counting rate vs. time for a typical experiment(Figure 2 of reference 67). The letter A indicates the time the valve was opened, and the letter B indicates the time a run might end, about 8 hours after equilibrium has been reached
Figure 6. L vs. T for the normal alkanes. The numbers next to the symbols are the number of C atoms in the alkane molecule53
Figure 7. x <sub>2</sub> vs. T for the normal alkanes. The numbers next to the symbols <sup>2</sup> are the number of C atoms in the alkane molecule55
Figure 8. L vs. n for the n-alkanes at 5 temperatures57
Figure 9. $x_2$ vs. n for the n-alkanes at 5 temperatures58
Figure 10. L vs. n for the n-alkanes; +, 20°C, our data; Δ, 25°C, Makranczy et al
Figure 11. x <sub>2</sub> vs. n for the n-alkanes; +, 20°C, our data; Δ, 25°C, Makranczy et al
Figure 12. $\Delta\mu_0^o$ vs. T for the n-alkanes. The numbers next to the symbols are the number of C atoms in the alkane molecule64
Figure 13. $\Delta\mu_0^{\circ\rho}$ vs. T for the n-alkanes. The numbers next to the symbols are the number of C atoms in the alkane molecule66
Figure 14. $\Delta\mu_2^{\circ}$ vs. n for the n-alkanes at 5 temperatures68
Figure 15. $\Delta \mu_2^{o\rho}$ vs. n for the n-alkanes at 5 temperatures69
Figure 16. Entropy of solution for Xe in the n-alkanes71
Figure 17. Enthalpy of solution for Xe in the n-alkanes72
Figure 18. Binding energy, surface energy, and enthalpy of solution for the n-alkanes. (Figure 5 of reference 68)

Figure 19. L vs. T for the normal alkanols. The numbers next to the symbols are the number of C atoms in the alkanol molecule80
Figure 20. x vs. T for the normal alkanols. The numbers next to the symbols are the number of C atoms in the alkanol molecule82
Figure 21. L vs. n for the n-alkanols at 5 temperatures84
Figure 22. x <sub>2</sub> vs. n for the n-alkanols at 5 temperatures85
Figure 23. $\Delta\mu_2^o$ vs. T for the n-alkanols. The numbers next to the symbols are the number of C atoms in the alkanol molecule89
Figure 24. $\Delta\mu_0^{\circ\rho}$ vs. T for the n-alkanols. The numbers next to the symbols are the number of C atoms in the alkanol molecule91
Figure 25. $\Delta\mu_2^{\circ}$ vs. n for the n-alkanols at 5 temperatures93
Figure 26. $\Delta\mu_2^{o\rho}$ vs. n for the n-alkanols at 5 temperatures94
Figure 27. Entropy of solution for Xe in the n-alkanols96
Figure 28. Enthalpy of solution for Xe in the n-alkanols97
Figure 29. Binding energy, surface energy, and enthalpy of solution for the n-alkanols. (Figure 4 of reference 69)99
Figure 30. L vs. M for Xe in aqueous amino acid solutions118
Figure 31. L vs. v <sub>tw</sub> for Xe in aqueous amino acid solutions122
Figure 32. L/L $_0$ vs. v $_{tw}$ - $\bar{H}$ M/55.346 for amino acid solutions126
Figure 33. H vs. molecular weight129
Figure 34. H vs. solution pH

#### INTRODUCTION

The fundamental goal of studies on the solubility of gases in liquids is to understand solution processes from molecular first principles. Given the physical properties of a solvent 1 and a solute 2, we would like to predict the thermodynamics of solvation of 2 in 1. Although this goal is not presently attainable, we have taken a step towards understanding solubility by studying some simple gas/liquid systems.

We have measured the Ostwald solubility, L, of  $^{133}$ Xe in a variety of liquid solvents. Ostwald solubility is the equilibrium ratio of the volume concentration of solute gas in the solvent to the concentration in the gas phase. If  $\rho_2^{\xi}$ ,  $\rho_2^{g}$  are the number densities (ie the number of molecules per unit volume) of solute 2 in the liquid and gas phases, respectively, then

$$L = \rho_2^{\ell} / \rho_2^{g} . \tag{1}$$

Xenon was chosen as the solute gas because of its simplicity, because of its importance in the biological and environmental sciences, and because, as will be explained below, it is easy to work with. As an inert gas, Xe interacts weakly with other molecules (short-range, induced-dipole interactions). Due to these weak interactions, the inert

gases form prototypical solids and liquids, and have been the subject of many studies. 1,2 The general properties of these gases are well known. 3 133 Xe is an inexpensive and easy to detect radioactive isotope of Xe. This isotope is of environmental interest since it is a byproduct of nuclear power reactors. 133 Xe, along with 85 Kr, another radioactive inert gas, were the major radioactive contaminants released to the environment during the accident at Three Mile Island. 4

At a partial pressure of 0.8 atmosphere (atm), Xe is an inhalational anesthetic. The mechanism of anesthesia seems to be the same for all anesthetic agents. Although there are indications that the site of anesthetic activity is in the cell membrane, the exact mechanism is not yet known.

Cell membranes are, simply put, lipid bilayers in which proteins are imbedded. The building blocks of the bilayer are phospholipid molecules. These molecules contain a polar head group bonded to 2 nonpolar hydrocarbon chains. They are thus amphipathic; polar (or hydrophilic) at one end and nonpolar (or hydrophobic) at the other. Since the cellular environment is aqueous and highly polar, it is thought that hydrophobic effects may be important in the formation and stability of cell membranes. 6,7

The two hydrophobic tails of the lipid molecule are straight chain hydrocarbons, 16-18 carbons long. Thus, the environment inside a cell membrane is similar to that in one of the normal alkanes, i.e. both are nonpolar. This is one of the motivations for using the normal alkanes as solvent.

The normal alkanes are a homologous series of straight chain, saturated hydrocarbons. They are nonpolar, implying that interactions

with a nonpolar solute will be of the induced-dipole/induced-dipole type. Physical properties of the normal alkanes are well known and can be found in the literature. Bensity as a function of chain length is nearly constant, about 0.7 g/cm³, so that the number of carbon atoms, or  $CH_2$  groups, per unit volume is nearly constant at about 3 x  $10^{22}$ /cm³. Thus, a Xe atom in liquid n-dodecane will be surrounded by much the same microscopic environment as one in liquid n-tridecane. The difference is in the number of methyl ( $CH_3$ ) and methylene ( $CH_2$ ) groups with which it interacts and in the geometry of these groups.

A second homologous series of solvents studied are the normal alkanols. They differ from the alkanes in the replacement of a hydrogen on a terminal carbon by a hydroxyl (OH) group. Adding the polar hydroxyl group makes the longer chain alkanol molecules amphipathic. It also changes the solvent environment radically. Intermolecular interactions are stronger due to the non-zero dipole moment and due to hydrogen bonding. These stronger interactions show up in increased surface tensions, and in higher melting and boiling points for these liquids. 9

We also measured the solubility of Xe in aqueous solutions of amino acids, sodium chloride, and sucrose. In these solvents, we consider complex, three-component systems. Water, in itself, is a highly polar solvent. In addition, amino acids in solution (as the name amino acid implies) become ionized, and have both positively and negatively charged groups. Also, the amino acid side chain can be nonpolar, polar, or charged. By comparing values of L for Xe in amino acid solutions with that for Xe in pure water, we obtain information on both amino acid/water interactions and on Xe/ amino acid interactions. The former can be important in studying protein formation and conformation, while

the latter may aid in understanding Xe/protein interactions. Both types of interaction may be important in studies of anesthetic activity.

#### THEORY

There are several important relationships that we will need later and which we will now derive. In section 1, we introduce the concept of the ideal solution. All of the gas/liquid systems we studied involved dilute solutions of Xe in the solvent. These systems are known as dilute ideal solutions; i.e. solutions in which the free energy of the solute in solution is the same as that for an ideal solution.

In section 2, we derive Raoult's Law, a key property of ideal solutions. We also discuss why Raoult's Law is not applicable to our systems.

Henry's Law, which is a generalization of Raoult's Law, is introduced in section 3. We also derive here the relationships between the three quantities  $K_H$ ,  $x_2$ , and L, which are the Henry's Law constant, mole fraction solubility, and Ostwald solubility, respectively.

Section 4 is a discussion of hard-sphere models of solubility.

Our results on the solubility of Xe in the alkanes and alkanols will be compared with the predictions of some of these models.

Kirkwood-Buff theory is the topic of section 5. It may be possible to use this theory to predict deviations from Henry's Law at high pressures.

Section 6 brings together the relationships we will need to analyse our results. Section 7 discusses multicomponent systems, and

introduces the concept of hydration numbers. We also derive the equations we will use in our discussion of the Xe/amino acid/water systems.

#### 2.1 IDEAL SOLUTION

An important starting point in the study of solubility is the concept of the ideal solution. Ideal solution theory provides a framework with which real systems may be compared. As in the case of a perfect gas, it is the deviations from ideality that yield information on interactions.

Consider two liquids, A and B, at a temperature T. Let  $\bar{V}_A$  ( $\bar{V}_B$ ) be the molar volume of A (B). If we form a mixture of  $n_A$  moles of A, and  $n_B$  moles of B, then A and B form an ideal solution if  $^{10}$ :

$$\left(\Delta H_{m}\right)_{T,P} = 0 , \qquad (2)$$

$$(\Delta V_m)_{T,P} = 0 = V - n_A \bar{V}_A - n_B \bar{V}_B$$
 (3)

H is the enthalpy, and V is the volume. The subscript m stands for mixing. The first condition, that no heat is evolved or absorbed, indicates that A molecules interact with B molecules as if they were A molecules, and vice versa. The second condition, that no volume changes occur, is necessary to eliminate changes in entropy from that source, since

$$\left(\frac{\partial S}{\partial V}\right)_{T} = \left(\frac{\partial P}{\partial T}\right)_{V} . \tag{4}$$

Pressure does change with temperature if the volume is held fixed. To prevent changes in entropy on mixing, we must assume that the volume does not change, so that

$$\Delta S = \left(\frac{\partial S}{\partial V}\right)_{T} \Delta V = 0 .$$

The following conditions on the energy of mixing,  $\Delta U_m^{},$  and the free energy of mixing,  $\Delta G_m^{},$  can also be derived.

$$(\Delta U_m)_{T,P} = 0 = (\Delta H_m)_{T,P} - P(\Delta V_m)_{T,P}$$
 (5)

and

$$(\Delta G_{m})_{T,P} = -T(\Delta S_{m})_{T,P} . \tag{6}$$

Note that

$$(\Delta V_{\rm m}) = (\frac{\partial}{\partial P} \Delta G_{\rm m})_{\rm T, n} = 0 \tag{7}$$

and

$$(\Delta H_{\rm m}) = -T^2 \left[ \frac{\partial}{\partial T} \left( \frac{\Delta G_{\rm m}}{T} \right) \right]_{\rm P, n} = 0 . \tag{8}$$

We can see that equation (8) is valid by performing the differentiation, and using the relation S =  $-(\frac{\partial G}{\partial T})_{P,n}$ . If we write

$$\Delta G_{\mathbf{m}} = n_{\mathbf{A}} (\mu_{\mathbf{A}} - \mu_{\mathbf{A}}^{\circ}) + n_{\mathbf{B}} (\mu_{\mathbf{B}} - \mu_{\mathbf{B}}^{\circ})$$
 (9)

we see (assuming that equations (7) and (8) hold for each component)

$$\frac{\partial}{\partial P}(\mu_{i} - \mu_{i}^{o}) = 0$$

$$i = A,B \qquad (10)$$

$$-T^{2}\frac{\partial}{\partial T}(\frac{\mu_{i} - \mu_{i}^{o}}{T}) = 0 .$$

The  $\mu_i$  and  $\mu_i^0$  are the chemical potentials of component i in the mixture and in the standard state, respectively. The chemical potential is the free energy per molecule, and the standard state is the pure liquid. Equations (10) have as solution

$$\mu_{i} = \mu_{i}^{o} + RTln(x_{i}) , \qquad (11)$$

so that

$$(\Delta S_m)_{T.P} = -n_A R \ln(x_A) - n_B R \ln(x_B) , \qquad (12)$$

where we have  $\mathbf{x}_{A}$  and  $\mathbf{x}_{B}$  for the mole fractions, respectively, of A and B.

$$x_A = \frac{n_A}{n_A + n_B}$$
 and  $x_B = \frac{n_B}{n_A + n_B} = 1 - x_A$ . (13)

### 2.2 RAOULT'S LAW

Raoult's Law, which we will derive from the assumption of solution ideality, is a simple relation between the mole fraction solubility and the vapor pressure of a solution component. Unfortunately, as we will see below, it is only valid in a few special cases for real systems.

If the vapor phases of A and B are ideal, we have (in the gas mixture)

$$\mu_{i} = \mu_{i}^{*} + RTln(P_{i}/P_{o})$$
 (14)

where  $P_i$  is the partial pressure of i,  $\mu_i^*$  is the chemical potential of pure i in the vapor phase at unit pressure  $P_o$ .

At equilibrium, the chemical potential of i in the gas is equal to that of i in the liquid. Then,

$$\mu_i^o + RTln(x_i) = \mu_i^* + RTln(P_i/P_o). \qquad (15)$$

For pure i,  $x_i = 1$  ,  $P_i = P_i^0$  , the vapor pressure of pure i, so that

$$\mu_i^o = \mu_i^* + RTln(P_i^o/P_o) . \qquad (16)$$

Then

$$RTln(x_i) = RTln(P_i/P_o) - RTln(P_i^o/P_o) , \qquad (17)$$

or

$$P_{i} = x_{i}P_{i}^{o} . (18)$$

Equation (18), which says that the partial pressure of component i in the vapor phase is equal to the mole fraction of component i in the liquid solution times the vapor pressure of pure liquid i, is known as Raoult's law.

There are a few real systems which behave ideally. Most are isotopic mixtures, such as a mixture of  $^{16}O_2$  and  $^{18}O_2$ ,  $^{11}$  or mixtures of optical isomers.  $^{12}$  It is not surprising that these systems should be ideal. However, there are other systems, such as the benzene/toluene system at about  $90^{\circ}$  C, which behave ideally and are not in these two classes.  $^{13}$  Other possible ideal systems are mixtures of the rare gases. There are only two rare gas systems, argon/krypton and krypton/xenon, which can be studied over the entire range of composition. Davies et al.  $^{14}$  investigated solutions of argon and krypton at the triple point temperature of Kr (T = 115.77° K). They found deviations of 0-4% from Raoult's law, and volume changes of less than 1.5% from the ideal over the full range of composition. Calado and Staveley  $^{15}$  found, in a study of Kr/Xe systems, deviations of up to 12% ( $x_{Kr}$  = 0.3), and changes in volume of about 1.5%. Thus, even when interactions are weak and short range, deviations from Raoult's law are observed.

#### 2.3 HENRY'S LAW

If the temperature is above the critical temperature of one of the components, a more general form of Raoult's law, known as Henry's law, applies. Henry's law states:

$$P_{i} = K_{H} x_{i} , \qquad (19)$$

i.e., the partial pressure of component i is proportional to its mole fraction in the solution. However, the constant of proportionality,  $K_H$ , called Henry's constant, is not the vapor pressure of pure i as it is in Raoult's law. When expressed in the more general form

$$f_i = K_H x_i \tag{20}$$

where  $f_i$  is the fugacity of i, Henry's law is valid for some gases up to very high pressures, to 600 atm for N<sub>2</sub> and CH<sub>4</sub> gases in liquid solvents of H<sub>2</sub>O and of aqueous sodium chloride. <sup>16</sup>

Henry's coefficient,  $K_{\mbox{\scriptsize H}}$ , is simply related to the Ostwald solubility coefficient L. The mole fraction solubility of 2 in 1 is

$$x_2 = n_2/(n_1 + n_2) \tag{21}$$

where  $n_i$  is the number of moles of i in solution. For dilute solutions ( $x_2 << 1$ ) we can write

$$x_{2} = \frac{\frac{LP_{2}\bar{V}_{1}}{RT}}{\frac{LP_{2}\bar{V}_{1}}{RT} + 1} = \left[\frac{RT}{LP_{2}\bar{V}_{1}} + 1\right]^{-1}$$
(22)

where  $n_2 = LP_2\bar{V}_1/RT$  is the number of moles of 2 in volume  $\bar{V}_1$ ,  $P_2$  is the partial pressure of 2, and  $n_1 = 1$  is the number of moles of 1 in molar volume  $\bar{V}_1$ . Solving equation (22) for  $P_2$  we see

$$P_2 = \frac{RT}{LV_1} \frac{x_2}{1 - x_2} . {23}$$

For  $x_2 << 1$ ,

$$P_2 = (RT/L\overline{V}_1)x_2 \tag{24}$$

Comparison of equations (19) and (24) gives

$$K_{H} = RT/L\overline{V}_{1} . {(25)}$$

Deviations from Henry's law can be related to solvent-solvent, solute-solvent, and solute-solute interactions using the Kirkwood-Buff theory of solutions.<sup>17</sup> Kirkwood-Buff theory is discussed below.

### 2.4 HARD SPHERES

Besides the thermodynamic approach to solvation processes offered by ideal solution theory, there is also an approach to solubility from molecular theory. There are two models of liquids which have had some success in predicting the physical properties of liquids and the thermodynamics of liquid mixtures. Both models involve hard sphere molecules, i.e. molecules with intermolecular potentials of the form

$$V(r) = \begin{cases} \infty & r \le a \\ 0 & r > a \end{cases}$$
 (26)

where a is the radius of the molecule. The equation of state for a hard sphere liquid is the same for both models, even though they involve different assumptions and methods of derivation.

The first model is due to Percus and Yevick,  $^{18-22}$  who developed a collective coordinate description of a system of hard spheres. Percus and Yevick assumed that the pair distribution function was known, and derived from it an integral equation for the system. (The pair distribution function,  $\mathbf{g_{ij}}(\mathbf{r})$ , is the probability that there is a j molecule a distance r from an i molecule.) Thiele<sup>23</sup> and Wertheim<sup>24</sup> solved this integral equation, obtaining the equation of state of a hard sphere liquid. Lebowitz<sup>25</sup> later derived the equation of state for a Percus-Yevick mixture of hard spheres.

The other model, developed by Reiss, Frisch, Helfand, and Lebowitz,  $^{26-28}$  is known as scaled particle theory (SPT). In SPT, the pair distribution function for a system of hard spheres is constructed, and from it the equation of state is derived. This equation of state is:

$$\frac{P}{\rho kT} = \frac{1 + y + y^2}{(1 - y)^3} \tag{27}$$

where  $y = \pi a^3 \rho/6$  and  $\rho$  is the number density of the hard spheres. As noted above, this is the same as the equation of state derived from the Percus-Yevick model.

Uhlig<sup>29</sup> and Eley<sup>30</sup> proposed the following model of the solution process. First, a cavity is created in the solvent which is large enough to hold a solute molecule. Next, the solute particle is introduced into the cavity and allowed to interact with the solvent. The reversible work to create the cavity of radius r is given by

$$W(r) = 4\pi r^{3} P/3 + 4\pi r^{2} \sigma \left(1 - \frac{4a\delta}{r}\right) + K_{0}$$
 (28)

where  $\sigma$  is the surface tension of the liquid, a is the solvent diameter,  $K_0$  is a constant which is small compared to the other terms, and  $\delta$  is a factor which takes into account the non-zero curvature of the cavity surface. The first term is the work done to create the cavity against pressure P, while the second is a surface energy term.

Reiss $^{31}$  approximates W(r) for r > a/2, using scaled particle theory, by the polynomial

$$W(r) = K_0 + K_1 r + K_2 r^2 + K_3 r^3 . \qquad r > a/2$$
 (29)

For  $r \le a/2$ , the exact expression for W(r) for a hard sphere fluid is

$$W(r) = -kT[\ln(1-4\pi r^3 \rho/3)] . r \le a/2$$
 (30)

If we require continuity of W,  $\frac{\partial W}{\partial r}$ , and  $\frac{\partial^2 W}{\partial r^2}$  at r=a/2 (so that the function is at least smooth, if not well behaved, at r=a/2) then we get the following expressions for the K's  $^{22-24}$ 

$$K_{0} = kT[-\ln(1-y) + \frac{a}{2}(\frac{y}{1-y})^{2}] - \pi Pa^{3}/6$$

$$K_{1} = -(\frac{kT}{a})[\frac{6y}{1-y} + 18(\frac{y}{1-y})^{2}] + \pi Pa^{2}$$

$$K_{2} = (\frac{kT}{a^{2}})[\frac{12y}{1-y} + 18(\frac{y}{1-y})^{2}] - 2\pi Pa$$

$$K_{3} = 4\pi P/3.$$
(31)

By comparing equations (28) and (29) we see that the surface tension can be expressed as:

$$\sigma = kT/(4\pi a^2) \left[ \frac{12y}{1-y} + 18 \left( \frac{y}{1-y} \right)^2 \right] - \frac{Pa}{2}$$
 (32)

Comparisons of calculated surface tensions with experimental values yield good results (correct order of magnitude) when applied to simple liquids,  $^{27}$  and very good results ( $\pm$  10%) when applied to fused salts.  $^{32}$ 

$$\ln(K_{H}) = -5.33(\frac{\varepsilon}{kT}) + \frac{\overline{G}_{c}}{kT} + \ln(\frac{RT}{V_{1}}). \qquad (33)$$

The factor  $\epsilon^*$  is an interaction energy which is a function of the polarizabilities and susceptibilities of solvent and solute. The first term is thus related to the free energy of interaction of the solute with the solvent. In the second term, the numerator  $\bar{G}_c = W(r_{12})$ , where W(r) is given by equation (29) with the K's as in equations (31), and the mean separation is  $r_{12} = (r_1 + r_2)/2$ . The solvent and solute diameters are  $r_1$  and  $r_2$  respectively.  $V_1$  is the molar volume of the solvent. The quantity  $\epsilon^*$  can be estimated from the equation

$$\epsilon^* = (\pi \rho m c^2 / \sigma_{12}^3) [\alpha_1 \alpha_2 / ((\alpha_1 / \chi_1) + (\alpha_2 / \chi_2))]$$
 (34)

Here the  $\alpha_i$ ,  $\chi_i$  are the polarizability and susceptibility, respectively, of component i, m is the mass of the solute 2, and  $\sigma_{12}$ =  $r_{12}$  as given above. Using reasonable values for  $r_1$  and  $r_2$ , and calculating  $\epsilon^*$  from equation (34), Pierotti predicted the solubilities, heats of solution, and partial molar volumes of gases in several liquids. The agreement with experiment is good (±10% in lnK<sub>H</sub>, ±20% in  $\bar{V}_b$ , and correct order of magnitude in the enthalpy of solution).  $^{33}$ 

It is also possible to express  $\epsilon^{\mbox{*}}$  in terms of Lennard-Jones parameters. In this form we have  $^{34}$ 

$$\varepsilon_{LJ}^* = (2/3)\pi \rho \varepsilon_{12}^{3} \sigma_{12}^{3}$$
, (35)

where  $\varepsilon_{12} = (\varepsilon_1 \varepsilon_2)^{1/2}$ ,  $\sigma_{12} = (\sigma_1 + \sigma_2)/2$ , and  $\varepsilon_i$ ,  $\sigma_i$  are the Lennard-Jones energy and distance parameters for component i.

Wilhelm and Battino<sup>35</sup> have used  $\epsilon_{LJ}^*$  and equation (33) to estimate  $\epsilon_i$  and  $\sigma_i$  for several gases and solvents. We will use their Lennard-Jones parameters to predict the thermodynamics of solution for Xe in some of the alkanes and alkanols.

Yosim and Owens<sup>36</sup> calculated heats of vaporization and fusion for the inert gases, and the heats of vaporization for a number of diatomic and polyatomic gases from the hard sphere equation of state. Agreement with experiment was very good ( $\pm$ 5%) for most of the monatomic and diatomic molecules, and was good ( $\pm$ 10 to 20%) for the larger, polyatomic molecules. Yosim<sup>37</sup> calculated heat capacities at the boiling point for these gases. Calculated heat capacities were within 10% of experimental values for the symmetrical gases, and within 30% for the asymmetrical ones. Yosim<sup>37</sup> also predicted the compressibilities of Ar, H<sub>2</sub>, N<sub>2</sub>, O<sub>2</sub>, and C<sub>6</sub>H<sub>6</sub>. Agreement with experiment was good (20%).

Why should experimental results compare so favorably with such a simple model? Intermolecular potentials are essentially hard sphere, repulsive, cores with a short range attractive component. Looked at in this way, the attractive component serves primarily to determine the density of the fluid. The density,  $\rho$ , appears explicitly on the left side of equation (27), and implicitly on the right side in the parameter  $y = \pi \rho a^3/6$ . So the model does take the attractive component into account, at least in an averaged sense.

Longuet-Higgins and Widom<sup>38</sup> proposed that a hard sphere liquid be put in a uniform attractive potential, in order to make the attractive component more explicit. Snider and Herrington<sup>39</sup> used this idea in the equation of state

$$\frac{P}{\rho kT} = \chi(y) - \left(\frac{A\rho}{kT}\right) \tag{36}$$

where  $\chi(y)$  is the right hand side of equation (27), and A is an additional parameter. When generalized to binary mixtures, agreement of calculated values of  $\Delta H^E$  (excess enthalpy of mixing),  $\Delta S^E$  (excess entropy of mixing), and  $\Delta V^E$  (excess volume of mixing) with experimental values was found to be generally good (±30 to 40%) for 10 equimolar mixtures. 39

#### 2.5 KIRKWOOD-BUFF THEORY

In studies of solvation processes, and of solute and solvent interactions, we gain information by varying temperature, pressure, and composition of our systems. Temperature variations, as we will see below, yield thermodynamic quantities, such as the chemical potential, enthalpy, and entropy. Variations in pressure and composition, when analysed according to the theory of Kirkwood and Buff, tell us about other properties of the solution.

Kirkwood and Buff<sup>40</sup> developed a general statistical mechanical theory of solutions. Using integrals of the radial distribution functions of the different molecular pairs, they derived expressions not only for the partial molar volumes  $(\bar{V}_i)$  and the isothermal compressibility  $(\kappa_T)$ , but also for the osmotic pressure and the derivatives of the chemical potentials  $(\mu_{ij})$ . Their equations are applicable to multicomponent systems. For a two component system, it can be shown that  $^{17}$ :

$$\kappa_{\mathrm{T}} = \zeta/k T \eta \tag{37}$$

$$\bar{\mathbf{v}}_1 = [1 + \rho_2(G_{22} - G_{12})]/n$$
 (38)

$$\vec{v}_2 = [1 + \rho_1(G_{11} - G_{12})]/\eta$$
 (39)

$$\mu_{ij} = \frac{\rho_j kT}{\rho_i V \eta} , \quad \mu_{ii} = -\frac{kT}{V \eta}$$
 (40)

where

$$\eta = \rho_1 + \rho_2 + \rho_1 \rho_2 (G_{11} + G_{22} - 2G_{12})$$

$$\zeta = 1 + \rho_1 G_{11} + \rho_2 G_{22} + \rho_1 \rho_2 (G_{11} G_{22} - G_{12}^2)$$

$$G_{ij} = \int_{0}^{\infty} (g_{ij}(r) - 1) 4\pi r^{2} dr$$

$$\mu_{ij} = \left(\frac{\partial \mu_i}{\partial N_j}\right)_{T,P,N_j^*}.$$

In these equations,  $\rho_i$  is the number density of i,  $g_{ij}(r)$  is the i,j pair distribution function, and  $N_j$  is the number of molecules of type j in volume V. The prime (') in the expression for  $\mu_{ij}$  indicates that all  $N_i$  (except for i=j) are held constant.

For a dilute solution of B in A, we find

$$\eta = \rho_1$$
 ,  $\zeta = 1 + \rho_1 G_{11}$  . (41)

Equations (37)-(39) then become

$$\kappa_{\rm T} = (1 + \rho_1 G_{11}) / kT \rho_1$$
 (42)

$$\overline{V}_1 = 1/\rho_1 \tag{43}$$

$$\bar{V}_2 = [1 + \rho_1(G_{11} - G_{12})]/\rho_1$$
 (44)

Note that both the isothermal compressibility and the molar volume of the solvent reduce to their values for the pure solvent, as expected. It can also be shown that 41

$$\beta \left(\frac{\partial \mu_2}{\partial x_2}\right)_{T,\rho_1} = 1/x_2 + \frac{\rho_1(2G_{12} - G_{11} - G_{22})}{1 + \rho_1 x_2(G_{11} + G_{22} - 2G_{12})}$$
(45)

and

$$\left(\frac{\partial \mu_2}{\partial P}\right) = \frac{1 + \rho_1 (G_{11} - G_{12})}{\rho_1 + \rho_2 + \rho_1 \rho_2 (G_{11} + G_{22} - 2G_{12})} = \overline{V}_2. \tag{46}$$

We use the conventional symbol  $\beta$  = 1/kT in equation (45). Equation (46) is also an expression for  $\bar{V}_2$ , which is the partial molar volume of B.

Note that the second osmotic virial coefficient,  $\mathbf{B}_2$ , is related to the solute-solute radial distribution function by the equation

$$B_2 = -(1/2) \int_0^\infty (g_{22}(r) - 1) 4\pi r^2 dr = -(1/2) G_{22}. \tag{47}$$

(The osmotic pressure,  $\pi$ , is the difference in pressure across a rigid, semi-permiable membrane which separates two containers of liquid, one of which contains pure solvent A, and the second of which contains a solution of B in A. For ideal solutions, there is an ideal equation of state that is identical to the ideal gas equation of state; i.e.,  $\pi V$  = nRT . B<sub>2</sub> is the first term in the virial expansion of this equation.)

Our experiments will involve only dilute solutions. In the case of dilute solutions, equation (45) becomes:

$$\beta \left(\frac{\partial \mu_2}{\partial x_2}\right)_{T,P,\rho_1} = 1/x_2 + \rho_1 (2G_{12} - G_{11} - G_{22})$$
 (48)

Combining equations (42)-(44), (47), and (48) yields

$$\beta \left(\frac{\partial \mu_2}{\partial x_2}\right)_{T,P,\rho_1} = 1/x_2 + \rho_1 (2B_2 + \overline{V}_1 - 2\overline{V}_2 + kT\kappa_T) . \tag{49}$$

Now we can write the chemical potential of B in A by integrating equations (46) and (49),

$$\mu_{2}^{\ell}(T,P,x_{2}) = kT \ln(x_{2}) + C(T) + \bar{V}_{2}(P - P^{\circ}) + \frac{kT}{\bar{V}_{1}}(2B_{2} + \bar{V}_{1} - 2\bar{V}_{2} + kT\kappa_{T})x_{2}.$$
 (50)

Equation (50) is correct to first order in  $(P-P^{\circ})$  and  $x_b$ , where  $P^{\circ}$  is the unit of pressure  $(P^{\circ}=1$  atm), and the superscript  $\ell$  indicates the liquid phase. The term C(T) is a constant of integration which is a function of temperature. The chemical potential of B in the gas phase is

$$\mu_2^{g}(T,P) = \mu_2^{o}(T) + kT \ln\left(\frac{f_2(T,P)}{P^{o}}\right)$$
 (51)

where  $f_2(T,P)$  is the fugacity of B.<sup>10</sup> At equilibrium, the chemical potentials in the gas and liquid phases are equal. Combining equations (50) and (51) by equating  $\mu_2^2 = \mu_2^g$  gives:

$$kT \ln\left(\frac{f_{2}(T,P)}{x_{2}P^{\circ}}\right) = -\mu_{2}^{\circ}(T) + C(T) + \bar{V}_{2}(P-P^{\circ}) + \frac{kT}{\bar{V}_{1}}(2B_{2} + \bar{V}_{1} - \bar{V}_{2} + kT\kappa_{T})x_{2}.$$
 (52)

Equation (52) reduces at low pressure, and consequently small  $\mathbf{x}_2$ , to:

$$kTln(\frac{P}{x_2P^0}) = -\mu_2^0(T) + C(T) - \bar{V}_2P^0 = kTln(K_H)$$
 (53)

In equation (53),  $K_{\overline{H}}$  is the Henry's law constant for B in A. Combining equations (52) and (53) we obtain

$$\ln\left(\frac{f_{2}(T,P)}{x_{2}P^{6}}\right) = \ln(K_{H}) + \frac{1}{kT}\bar{V}_{2}P$$

$$+ (1/\bar{V}_{1})(2B_{2} + \bar{V}_{1} - 2\bar{V}_{2} + kT\kappa_{T})x_{2}. \quad (54)$$

By plotting  $\ln\left(\frac{f_2(T,P)}{x_2P^o}\right) - \frac{1}{kT} \bar{V}_2P$  as a function of  $x_2$ , we can determine the Henry's law constant,  $K_H$ , from the intercept, and the second osmotic virial coefficient,  $B_2$ , from the slope. Watanabe and

Anderson  $^{42}$  have noted an empirical relation between  $\mathrm{B}_2$  and  $\mathrm{K}_\mathrm{H}$ . They propose that

$$B_2 = a_1 \ln(K_H) + a_2 \tag{55}$$

where  $a_1$  and  $a_2$  are constants. If equation (55) is valid, it should be possible to predict deviations from Henry's law using equation (54).

#### 2.6 APPLICATION TO EXPERIMENTS

## 2.6.1 ASSUMPTIONS

We make several assumptions about the experiment in order to perform a thermodynamic analysis of the data. First, we assume that the gas phase is ideal, so that equation (14) for the chemical potential as a function of pressure is valid. This should be a good assumption, since the equation of state of Xe at 25°C, derived by Michels et al., 43 predicts a deviation of less than 1% from ideality at 1 atm pressure.

We also assume that the Xe forms a dilute ideal solution 17 in all solvents used. For dilute ideal solutions, the chemical potential can be written

$$\mu_2 = \mu_2^0 + RTln(x_2)$$
 (56)

where  $\mu_2^0$  is a constant. The quantity  $\mu_2^0$  is often interpreted as being the chemical potential of a solute B in pure B, but with molecular interactions as if the solute B molecules were surrounded by solvent A molecules. Equation (55) should be valid, since at 1 atm pressure of Xe,  $x_2$  is of the order of 0.01.

A third assumption we make is that the Ostwald solubility, L, is constant over the range of pressure from 0 to 1 atm. Considering equations (22)-(25), this assumption introduces an error of order  $x_2$ , assuming that Henry's law holds ( $K_H$  = constant). The gas phase in most of our experiments consisted of a dilute mixture of  $^{133}$ Xe in air, due to the high cost of nonradioactive Xe gas. However, some experiments were performed with mixtures of  $^{133}$ Xe in nonradioactive Xe. The value of L obtained for the system ( $^{133}$ Xe in Xe,  $_{20}$ ) differs from that for ( $^{133}$ Xe in air,  $_{20}$ ) by about  $_{1/2}$ %, which is well within experimental error (1%). This agreement, however, may be due to the low solubility of Xe in  $_{20}$  (L = 0.106 at 25°C). The corresponding mole fraction is about  $_{20}$  = 0.001, and changes in L would not be seen using our technique.

# 2.6.2 THERMODYNAMICS OF SOLUTION

At equilibrium, the chemical potential of the solute in the gas phase is equal to its chemical potential in the liquid. Equating equations (14) and (56) gives

$$\mu_2^* + RT \ln(P_2/P_0) = \mu_2^0 + RT \ln x_2$$
 (57)

At a partial pressure of 1 atm,  $P_2 = P_0$ , so that

$$\Delta \mu_2^0 = \mu_2^* - \mu_2^0 = -RT \ln(x_2) . \tag{58}$$

The entropy of solution is given by

$$\Delta S_2 = -\left(\frac{\partial \Delta \mu_2^0}{\partial T}\right)_{P,n} . \tag{59}$$

Using  $\Delta \mu_2^0 = \Delta H_2 - T\Delta S_2$  and equation (59),

$$\Delta H_2 = -T^2 \left[ \frac{\partial}{\partial T} \left( \frac{\Delta \mu_2^{\circ}}{T} \right) \right]_{P, n} . \tag{60}$$

If a plot of  $\Delta\mu_2$  as a function of temperature is linear, then the slope is  $-\Delta S_2$ , and the intercept is  $\Delta H_2$ . This is really an assumption that the temperature dependences of  $\Delta H_2$  and  $\Delta S_2$  are much slower than linear in T.

Ben-Naim et al. 44,45 advocate the use of a different formula from equation (58) for the chemical potential of solution. Their equation is derived using statistical mechanical principles. It is based on a number density scale. Our equation (58) is based on a mole fraction scale. Ben-Naim's formula for the chemical potential is

$$\Delta \mu_2^{\circ \rho} = -RT \ln(L) \tag{61}$$

where L is the Ostwald solubility. Equations (59) and (60) also hold for  $\Delta\mu_0^{\circ \rho}$ .

Unfortunately, as will be seen below, the interpretation of the data depends on which expression is used to determine the chemical potentials, and the conclusions drawn are inconsistent with each other. There is no general agreement at present as to which of the two models

is preferable, and so our results will be discussed here in terms of both equation (58) and equation (61).

The goal of these experiments is to be able to predict the solubility of a gas in a liquid from the molecular properties of the gas and liquid. This is equivalent to predicting the entropy and enthalpy of solution. Although we cannot yet predict the entropy of solution, we can estimate the enthalpy of solution using the model of Uhlig<sup>29</sup> and Eley.<sup>30</sup>

We can write

$$\Delta H_2 = E_c - E_b \tag{62}$$

where  $E_b$  is the binding energy of solute to solvent, and  $E_c$  is the amount of work done to create the cavity. The enthalpy is the heat absorbed by a system at a constant pressure.  $E_b$  may be estimated as the geometric mean of the heats of vaporization of solute and solvent. An expression for the cavity energy is  $^{31}$ 

$$E_{c} = 4\pi r_{2}^{2} \gamma_{1} N_{A} + 4\pi r_{2}^{3} P N_{A} / 3$$
 (63)

where  $r_2$  is the solute radius,  $\gamma_1$  is the solvent surface tension, P is the pressure, and  $N_A$  is Avogadro's number. The first term is the surface energy of the cavity, and the second is the work necessary to create a spherical volume of radius  $r_2$  at pressure P. At pressures of the order of 1 atm, the volume term is negligible compared to the surface term. Thus at low pressures we can estimate the enthalpy

$$\Delta H_2 = 4\pi r_2^2 \gamma_1 N_A - E_b . {(64)}$$

## 2.7 MULTICOMPONENT SYSTEMS

The solubility of a gas in a liquid is even more difficult to understand when the liquid solvent itself is made up of two or more components. Interactions between the solvent components may produce a liquid environment which is very different from the environment in either pure solvent. This thesis reports our experiments on aqueous solutions of amino acids, sucrose, and sodium chloride.

Donkersloot 46 studied the binary systems water/methanol, water/butanol, and cyclohexane/2,3-dimethylbutane using Kirkwood-Buff theory. In addition, Patil 47 applied Kirkwood-Buff theory to the system water/butanol. They found that the G<sub>ij</sub> (Kirkwood-Buff integrals) were strongly dependent on concentration, which indicates that interactions between components are also concentration dependent. Kojima, Kato, and Nomura 48 were able to approximate the results of Donkersloot for the cyclohexane/2,3-dimethylbutane system by assuming a Lennard-Jones type interaction between components. Their method, however, failed for other mixtures.

Since interactions in binary systems are so complex, changes brought about by the introduction of a third component are not easy to predict. The third component may be selectively solvated, leading to salting-in and salting out effects, <sup>49</sup> or it may be "inert" with respect to one of the components. For example, in a mixture of water and marbles, we would expect the solubility of any solute to be proportional to the volume fraction of water. An early investigator of salting-out effects was Van Slyke. <sup>50,51</sup> Van Slyke developed a method of measuring gas solubility which depends on these effects. After saturating a

solvent with the solute gas, "salts" are added to a sample to force the disolved gas out of solution. In this way, the volume of gas disolved in a known volume of solution can be determined.

Surprisingly, Yeh and Peterson  $^{52,53}$  found good agreement between measured solubilities for Kr and Xe in blood, protein solutions, and tissue homogenates, and solubilities predicted from known solubilities in each of the components. For the system Kr/blood, Yeh and Peterson obtained a value for the Ostwald solubility of  $L_{\rm exp} = 0.0455 \pm 0.0044$  at 37°C. They predicted a value of  $L_{\rm pred} = 0.0433$  by considering blood as a four-component mixture of water, hemoglobin, albumin, and lipid. They also obtained very good agreement ( $\pm 1\%$ ) for the solubility of Kr in rabbit muscle homogenate. Agreement between experiment and prediction for Xe in blood and rabbit muscle homogenate was not as good ( $\pm$  10% and  $\pm$  5% respectively).

Gas solubility in biological materials is very difficult to determine. Weathersby and Homer,  $^{54}$  in a review of the literature, found a wide disparity in published data for gas solubilities in biological fluids and tissues. This is probably due to the complexity of these many-component systems, where a small change in composition can have a large effect on gas solubility.

One of the earliest investigators of the salting out effect was Setschenow. 55 He derived an empirical relation between the solubility of a gas in an aqueous salt solution and the concentration of the salt in solution. This relation is known as the Setschenow equation:

$$\log_{10} \frac{S_0}{S} = k_S c \tag{65}$$

where S is the solubility of a gas in a salt solution of concentration c, S<sub>o</sub> is the gas solubility in pure water, and  $k_S$  is a constant known as the Setschenow coefficient. If  $k_S > 0$ , the gas solubility is less in the salt solution than in water, and salting out occurs. If  $k_S < 0$ , the gas solubility is greater, and salting in occurs.

Shoor and Gubbins<sup>56</sup> and Masterton and Lee<sup>57</sup> derived expressions for the Setschenow coefficient from scaled particle theory. Agreement with experimental values of the Setschenow coefficient was good for a variety of gases (He,Ne,Ar,Kr,H<sub>2</sub>,O<sub>2</sub>,N<sub>2</sub>,CH<sub>4</sub>,C<sub>2</sub>H<sub>4</sub>,C<sub>2</sub>H<sub>6</sub>,SF<sub>6</sub>) in several different salt solutions (NaCl, LiCl, KCl, KI). Masterton<sup>58</sup> also used scaled particle theory to predict Setschenow coefficients of 5 gases (He, Ne, Ar, O<sub>2</sub>, N<sub>2</sub>) in seawater. The average difference between observed and calculated values of  $k_S$  was of the order of 5% at 25°C. Considering the large number of components in seawater, this is very good agreement.

Eucken and Hertzberg<sup>59</sup> studied the salting out of gases in aqueous salt solutions. From their data, Eucken and Hertzberg were able to calculate hydration numbers for each salt in solution. The hydration number of a salt is the number of water molecules associated with each anion-cation pair in aqueous solution. They made several assumptions about the solutions in order to calculate the hydration numbers.

The first assumption is that water in an aqueous solution exists in one of two states, either "bound" or "free". Bound water is associated with the salt, and is unavailable to dissolve the solute gas. The rest of the water is free. The solubility of the gas in free water is the same as in pure water.

Eucken and Hertzberg also assume that the molar volume of both free and bound water is equal to that of pure water. This model is based on the excluded volume concept. The decrease in gas solubility occurs because of a decrease in the volume of water available, and the gas is excluded from the volume occupied by the salt ions and their hydration shells.

Under these assumptions, one can derive the following expression for the hydration number, H, of a salt:

$$H = (M_{H_2O}/M)(v_{tw} - \frac{L}{L_0})$$
 (66)

Here,  $\rm M_{\rm H_2O}$  is the number of moles of water per liter at temperature T, M is the molarity of the salt solution,  $\rm v_{\rm tw}$  is the volume fraction of total water for the solution, L is the Ostwald solubility of the gas in the solution at temperature T, and  $\rm L_{\rm O}$  is the Ostwald solubility of the gas in pure water at temperature T.

We can invert equation (66) and write the solubility in terms of the hydration number H.

$$L = L_0 \left[ 1 - M \left( \frac{M_{salt}}{\rho_{salt}} + \frac{HM_{H_2O}}{\rho_{H_2O}} \right) \right]$$
 (67)

where  $M_i$  and  $\rho_i$  are the molecular weight (g/mol) and density (g/l) of i, and M is the molarity. The fraction of the volume which is water, either free water or hydration water, has been written as

$$v_{tw} = 1 - \frac{M_{salt}}{\rho_{salt}}.$$
 (68)

Using equations (65) and (67), we can relate the Setschenow coefficient to the hydration number by:

$$k_{S}^{M} = -\log_{10}[1 - M(\frac{M_{salt}}{\rho_{salt}} + \frac{HM_{H_{2}O}}{\rho_{H_{2}O}})]$$
 (69)

For dilute solutions, i.e., those for which  $M(\frac{M_{salt}}{\rho_{salt}} + \frac{HM_{H_2}O}{\rho_{H_2}O}) << 1$ , we can expand the argument of the logarithm to obtain

$$k_{S}^{\dagger}M = \left(\frac{M_{salt}}{\rho_{salt}} + \frac{HM_{L_20}}{\rho_{L_20}}\right)M \tag{70}$$

from which

$$k_{S}^{\dagger} = \left(\frac{M_{\text{salt}}}{\rho_{\text{salt}}} + \frac{HM_{H_{2}0}}{\rho_{H_{2}0}}\right) \tag{71}$$

where  $k_S^* = 2.303k_S$ . Since  $k_S^*$  is of the order of 0.33 1/mol for NaCl solutions, we would not expect equation (70) to be valid for our systems. The Taylor series expansion of ln(1-x) is:

$$\ln(1-x) = x + x^2/2 + x^3/3 + \dots, \tag{72}$$

so the fraction error made in neglecting second and higher order terms is of the order of x/2. Since our solution molarities are of the order of 0.5, and  $k_S^*$  is of the order of 0.33, we make a 10% error in

neglecting the higher order terms in equation (70). We will therefore use equation (66) to interpret our results.

#### **EXPERIMENTAL**

## 3.1 SOLUTION COMPONENTS

The solute gas in our experimental system is \$^{133}\$Xe in trace amounts. The partial pressure of \$^{133}\$Xe is typically about 1 picoatmosphere (patm) usually mixed with air at 1 atm total pressure. Control experiments were also done in which \$^{133}\$Xe was mixed with naturally occuring, nonradioactive Xe gas at a total pressure of 1 atm. A variety of liquid solvents were used. These included several normal alkanes and alkanols, as well as aqueous solutions of amino acids, NaCl, and sucrose. For the experiments in which the gas phase was \$^{133}\$Xe plus nonradioactive Xe, the solvents were degassed before the run, and then saturated with nonradioactive Xe. For experiments in which \$^{133}\$Xe was mixed with air, the solvents were not degassed. In those cases, the solvents were probably saturated with air which dissolved during production and storage of the solvent. However, this had no measurable effect on our values of solubility.

Xenon is one of the noble gases. Its atomic radius is 2.23 Å, and it is therefore the largest and most polarizable atom of the 5 common inert gases (He, Ne, Ar, Kr, Xe). (A sixth noble gas, radon, has only radioactive isotopes, no stable ones. The longest lived isotope of radon is <sup>222</sup>Rn, which has a half-life of 3.8 days. <sup>60</sup> It is a product of alpha decay of radium.) The particular isotope of Xe used in our

experiments,  $^{133}$ Xe, is unstable and decays with a half-life of 5.245 days.  $^{61}$  It decays by beta emission to an excited state of  $^{133}$ Cs. This nuclear excited state decays  $^{60}$  with a half-life 6.3 × 10 $^{-9}$  sec by emitting an 81 keV gamma ray. We used the emitted radioactive intensity of these gamma rays as a measure of  $^{133}$ Xe concentration.

Xenon-133 was purchased (Medi-Physics, Plainfield, New Jersey) in 20 milliCurie (mCi) aliquots. Typical amounts of  $^{133}$ Xe used during a run are of the order of 100  $\mu$ Ci. High purity, nonradioactive Xe is commercially available (Matheson, New Jersey, 99.9+%).

The normal alkanes (Humphrey Chemical Co., New Haven, Connecticutt) are simple, nonpolar organic molecules. They are "straight" chains of carbon atoms saturated with hydrogen. Since they are nonpolar, interactions between alkane molecules, or between an alkane molecule and any other nonpolar molecule, are short range, induced dipole to induced dipole interactions. The carbon to carbon bond length is about 1.5 Å, so a Xe atom interacts directly with only a portion of a long alkane molecule.

The normal alkanols (Aldrich Chemical Co., Milwaukee, Wisconsin) differ from the n-alkanes in the addition of a hydroxyl group (OH) to a terminal carbon. <sup>62</sup> Although bond lengths are not affected, the molecule is polar. Thus we would expect stronger interactions between Xe and alkanol molecules than between Xe and alkane molecules.

For the experiments involving amino acids (Aldrich), solutions of amino acid in distilled water were made at 25.0 °C. We measured the pH of the amino acid solutions, but made no attempt to control the pH, i.e. no buffers were used since these would inevitably add yet another component to the solutions.

Physical properties (density, surface tension, etc.) for the alkanes and alkanols were taken from the literature,  $^{8,9,63}$  as were the molecular weights of amino acids, and the solubilities of amino acids in water.  $^{64}$ 

#### 3.2 APPARATUS

A diagram of the apparatus is shown in Figure 1. The apparatus can be disassembled at the threaded joint for cleaning and loading. Two valves, along with several machined brass pieces are soldered together to form the upper portion of the apparatus, i.e., above the threaded joint. The bottom portion is a Pyrex container whose mouth is joined as shown to a glass-to-metal seal. A brass nut is soldered to this seal. The nut and large ball valve form the threaded joint, which is sealed by wrapping with Teflon tape before assembly.

During a run a glass encased magnetic stirring bar runs inside the bottom vessel, which contains the solvent. Commercial stir bars are coated with Teflon. It was necessary to remove this coating since xenon concentrates in it, apparently because xenon is highly soluble in Teflon. We encase the stir bar in glass so the bare stir bar will not corrode in the experimental solvent, which is acidic in some cases. Teflon is used in two other places; in the threaded joint as tape, as noted above, and in the solid packing material in the ball valve. We ignore any contribution of these seals to the measured solubility. In both cases, the surface area of Teflon exposed to Xe is small. This, in light of the very slow diffusion rate of gases in solids

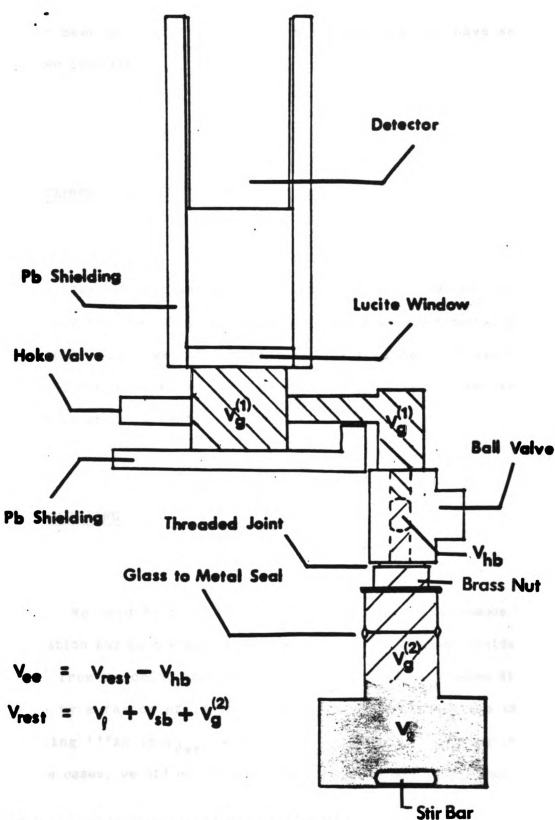


Figure 1. Solubility measurement apparatus.

 $(D \approx 10^{-9} \text{ cm}^2/\text{sec})$ , leads to a negligible contribution. Also, we have never seen any evidence of a Xe sink, which would have shown up in either leak tests or dilution runs.

## 3.3 TEMPERATURE CONTROL

Temperature was controlled to ±0.1°C (Lauda/Brinkmann K-2/RD circulator) both during a run, and in making up experimental solutions. The bath fluid was an approximately 4:1 mixture of water:ethylene glycol. The ethylene glycol decreases the problem of freeze-up of the float in the circulator.

## 3.4 SHIELDING

We used Pb shielding of thickness  $\leq$  1 cm to reduce background radiation and to prevent emissions due to  $^{133}$ Xe decays outside of volume  $v_g^{(1)}$  from reaching the detector. One cm of Pb attenuates 81 keV gamma rays by a factor of  $10^6.65$  Shielding effectiveness was checked by putting  $^{133}$ Xe in  $v_{rest}$  with the apparatus and shielding in place. In these cases, we did not observe anything above the background rate.

#### 3.5 ELECTRONICS

A diagram of the electronics is shown in Figure 2. Gamma rays of energy 81 keV are detected with an NaI(T1) scintillation detector (Harshaw, type 7SF8). A high voltage power supply (Power Designs, Inc. model 1570) supplies 1100 volts for the photomultiplier via the pre-amp (Ortec model 276). Detector output passes through an amplifier (Ortec model 485), then through a single channel analyser (SCA, Ortec model 406A). The window on the SCA is set to exclude energies below about 10 keV and above about 90 keV. The window was set by feeding signals of known amplitude into the amplifier, and observing the output on a multichannel analyser. The resulting output was then compared to a 133Xe spectrum. Two timers (Ortec model 719) are externally supplied a 0.1 sec timing pulse by a minicomputer (Micro Development Tool 1000).

The computer is programmed to take data and print out the results. It counts the number of decays in 400 sec, makes suitable corrections to the total, then prints out the result. It then waits an additional 200 sec before counting again. Each hour the average of the previous six values is printed out.

Two corrections are made to the data. Due to the nature of the electronics, a pulse into the detector is not counted at the computer if it too closely follows an earlier pulse. This "dead time" can be measured by putting signals of a known frequency into the electronics, and observing the output. In this way, we determined the dead time for our system to be about  $\tau \approx 3.33 \times 10^{-6}$  sec.

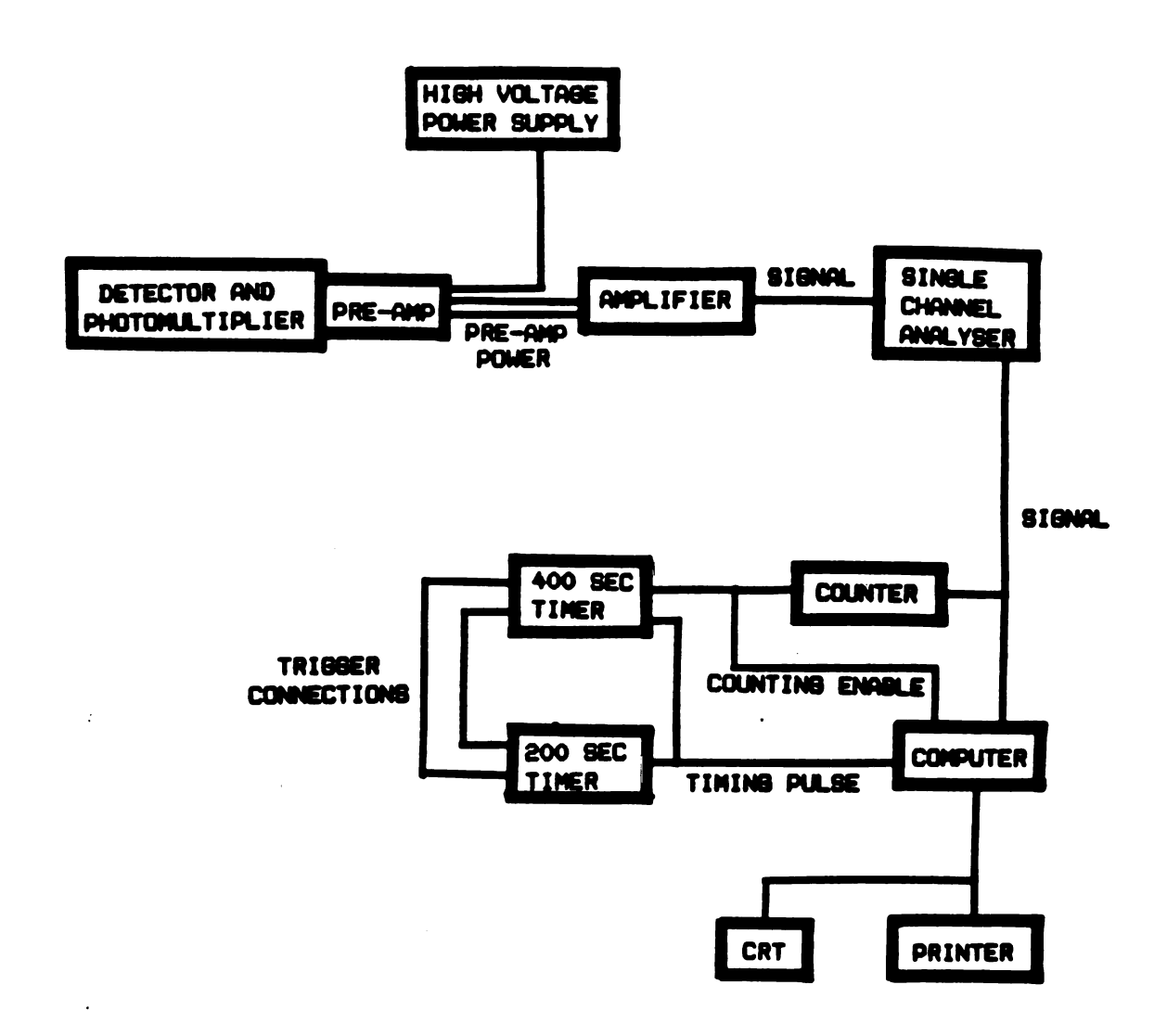


Figure 2. Schematic diagram of the electronics.

Radioactive decay is a random process, and consequently, the probability of k events, given a mean of  $\mu$  events, is given by the Poisson distribution  $^{66}$  :

$$P(k) = \frac{\mu^k}{k! e^{\mu}} . \tag{73}$$

P(k) is the probability of k events per unit time, give a mean of  $\mu$  events per unit time. If we let  $\tau$ , the dead time, be our unit of time, and  $\mu$  be the mean number of events per time  $\tau$ , then the probability that a single signal occurs within time  $\tau$  of an earlier signal is given by

$$P(1) = \frac{1}{1!e^{\mu}} = \mu e^{-\mu} . \tag{74}$$

The mean number of signals per unit time  $\tau$  is  $\mu$ , and is typically of the order of 2 × 10<sup>-3</sup>, so we may use the approximation:

$$P(1) \approx \mu(1 - \mu) \approx \mu$$
 (75)

The actual counting rate,  $N_{\text{act}}$ , can therefore be approximated by

$$N_{\text{act}} = N_{\text{obs}}(1 + \mu) , \qquad (76)$$

where  $N_{\mbox{obs}}$  is the observed counting rate. We have programmed the computer to make this correction to the data.

The second correction which must be made to the data is to remove excess counts due to natural background radiation. We measure background

radiation several times over periods of several hours with the apparatus and shielding in place, but without any  $^{133}$ Xe in the apparatus. Background is subtracted after the dead-time correction has been made. Typical backgrounds for a run are about 1100 counts in 400 sec. Counting rates due to  $^{133}$ Xe vary from about 250,000 counts/400 sec at the start of a run, to about 50,000 counts/400 sec at the end of a run.

## 3.6 VOLUME DETERMINATION

Volumes are indicated in Figure 1. There are seven volumes which must be determined for each run. Five of them,  $V_g^{(1)}$ ,  $V_{rest}$ ,  $V_{sb}$ ,  $V_{hb}$ , and  $V_{ee}$ , are the same for every run. The remaining two,  $V_g^{(2)}$  and  $V_{\ell}$ , are determined at the beginning of each run. The gas volume  $V_g^{(1)}$  is the volume above the ball valve which initially contains all of the  $^{133}$ Xe. The gas volume  $V_g^{(2)}$  is the remaining gas volume. The volume of the liquid solvent is  $V_{\ell}$ . The volume of the glass encased stirring bar is  $V_{sb}$  and  $V_{hb}$  is that of the small hole in the ball of the valve. The volume below the ball valve is designated by  $V_{ee}$ , and  $V_{rest}$  is the total volume excluding volume  $V_g^{(1)}$ .

To determine  $V_{ee}$  (ee stands for everything else), we weigh the apparatus before and after filling  $V_{ee}$  with water at a known temperature. We make a buoyancy correction for the weight of air displaced by the water. If  $m_{obs}$  is the observed mass, then the true or actual mass,  $m_{act}$ , is:

$$m_{\text{act}} = m_{\text{obs}} / \left[1 - \frac{\rho_{\text{air},T}}{\rho_{\text{H}_2,0,T}}\right]$$
, (77)

where  $\rho_{\mbox{\scriptsize i.T}}$  is the density of i at temperature T.  $\mbox{\scriptsize V}_{\mbox{\scriptsize ee}}$  is then

$$V_{ee} = \frac{m_{act}}{\rho_{H_2O,T}} . \tag{78}$$

 ${\rm V}_{\rm hb}$  (hole in ball) was calculated from measurements made on a disassembled ball valve. For  ${\rm V}_{\rm rest}$  ,

$$V_{\text{rest}} = V_{\text{ee}} + V_{\text{hb}}$$
 (79)

The volume of the glass-encased stirring bar,  $V_{\rm sb}$ , was determined by measuring the water displaced when the stirring bar was immersed in a known volume of water in a graduated cylinder.

We determined the initial gas volume  $V_g^{(1)}$ , by using a dilution measurement. Xenon-133, initially confined to volume  $V_g^{(1)}$  at a concentration of  $C_i$ , is allowed to expand throughout the volume  $V_g^{(1)}$  +  $V_{rest}$ . If the final concentration, corrected for decay of  $^{133}$ Xe is  $C_f$ , we define the ratio  $\alpha$  to be:

$$\alpha = \frac{C_f}{C_i} = \frac{V_g^{(1)}}{V_g^{(1)} + V_{rest}},$$
 (80)

from which

$$V_{g}^{(1)} = \frac{\alpha}{1-\alpha} V_{rest}. \tag{81}$$

#### 3.7 SOLVENT PREPARATION

Alkanes (99% pure) and alkanols (purities: methanol,99.9%; propanol and butanol, 99+%; pentanol, octanol, decanol, and undecanol. 99%: hexanol, heptanol, and dodecanol, 98%; nonanol and tetradecanol, 97%; 200 proof ethanol) were used as purchased. Amino acid solutions were prepared in 250.0  $\pm$  0.1 cm<sup>3</sup> volumetric flasks in the following way. To a predetermined mass of amino acid, we added distilled water to fill the flask to within 1 cm $^3$  of the 250.0 cm $^3$  mark. For experiments involving Xe atmospheres, the water was first degassed by boiling under vacuum (Figure 3), then was saturated with Xe under a Xe pressure of 1 atm. The amino acid and water were also mixed under a Xe atmosphere. After temperature equilibration at 25.0°C, enough water was added to bring the total solution volume to 250.0 cm<sup>3</sup>. The outside of the flask was carefully dried, then the flask and solution were weighed, with the usual buoyancy correction being made for the weight of displaced air or Xe. Solution density was calculated, along with the volume fractions of both water and amino acid. A small sample, about 5 cm<sup>3</sup>, of the solution is used to determine the pH (Brinkmann pH meter with combination electrode).

## 3.8 LOADING THE APPARATUS

With the ball valve closed, air is evacuated from volume  $V_g^{(1)}$  through the Hoke valve. A trace amount of  $^{133}$ Xe is allowed to expand into  $V_g^{(1)}$ , and then air or Xe is let in to bring the pressure to 1 atm.

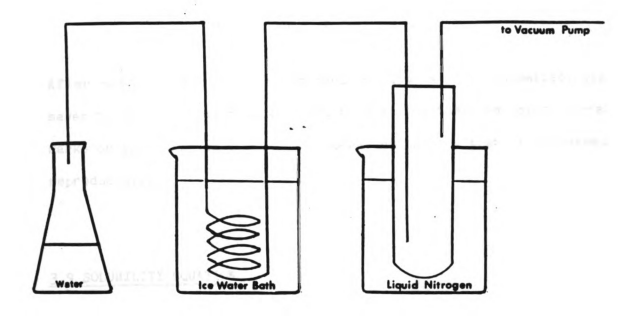


Figure 3. Schematic diagram of the degassing system.

When using nonradioactive Xe,  $V_g^{(1)}$  was loaded using the gas handling system shown in Figure 4. The Hoke valve is then closed.

Approximately 220 cm<sup>3</sup> of solvent is poured into the glass portion of the apparatus, and is weighed. The gas handling system of Figure 4 was also used to load the solvent under a Xe atmosphere. The buoyancy corrected weight divided by the solvent density yields the volume of the liquid solvent,  $V_q$ . The secondary gas volume,  $V_q^{(2)}$ , is:

$$V_{g}^{(2)} = V_{rest} - V_{sb} - V_{\ell}$$
 (82)

After putting in the stirring bar, the apparatus is assembled. Six to seven turns of Teflon tape are used to seal the threaded joint. Scratch marks on the ball valve and on the brass nut ensure that it is assembled reproducibly.

## 3.9 SOLUBILITY EQUATION

Solubility is calculated using conservation of  $^{133}$ Xe. Initially,  $^{133}$ Xe is confined to volume  $V_g^{(1)}$  at a concentration of  $C_i$ . When equilibrium has been reached, the  $^{133}$ Xe is distributed throughout volumes  $V_g^{(1)}$  and  $V_g^{(2)}$ , as well as throughout the solvent. The total amount of  $^{133}$ Xe in the solvent is  $C_f L V_g$ , where L is the Ostwald solubility of  $^{133}$ Xe in the solvent, and  $C_f$  is the equilibrium concentration of  $^{133}$ Xe in volume  $V_g^{(1)}$ . Then

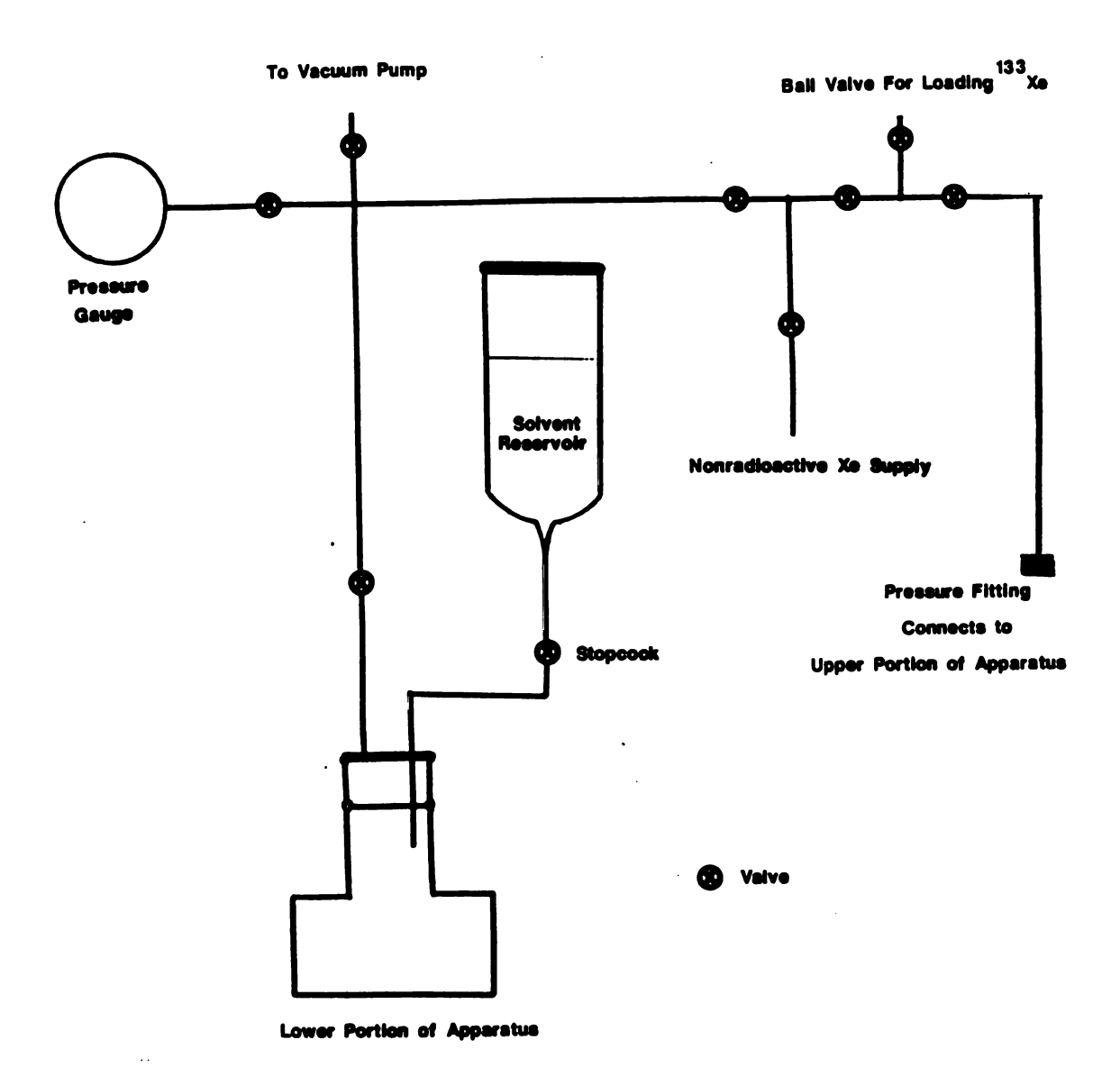


Figure 4. Schematic diagram of the gas handling system.

$$c_i v_g^{(1)} = c_f e^{\lambda \Delta t} (v_g^{(1)} + v_g^{(2)} + L v_g)$$
, (83)

where  $\lambda$  is the decay constant for  $^{133}$ Xe ( $\lambda$  = 0.9177 × 10<sup>-4</sup> min<sup>-1</sup>), and  $\Delta$ t is the time elapsed between measurement of  $C_i$  and  $C_f$ . The term  $e^{\lambda\Delta t}$  is a correction for the decay of  $^{133}$ Xe atoms. We can also see that LV  $_{\ell}$  is the "effective gas volume" of the liquid solvent.

Rearrangement of equation (81) gives

$$L = \frac{c_1}{c_f} e^{-\lambda \Delta t} \frac{v_g^{(1)}}{v_g} - \frac{v_g^{(1)} + v_g^{(2)}}{v_g}.$$
 (84)

Equation (84) is valid for measurements at a single temperature. Experiments involving the alkanes and alkanols were done at a variety of temperatures. The temperature dependent form of equation (84) is:

$$L(T) = \frac{C_{1}}{C_{f}} e^{-\lambda \Delta t} \frac{V_{g}^{(1)}}{V_{g}} R(T) - \frac{V_{g}^{(1)} + V_{g}^{(2)}}{V_{g}} R(T) + 1 - R(T)$$
 (85)

where  $R(T) = \rho(T)/\rho(T_{\ell})$  is the ratio of the solvent density at temperature T to the solvent density at temperature  $T_{\ell}$ , the loading temperature. For the alkanes and alkanols,  $T_{\ell}$  was usually taken to be 20.0°C, except for those which were solid (heptadecane, octadecane, nonadecane, and eicosane) at that temperature. In these cases,  $T_{\ell}$  was taken to be either 30°C or 40°C, depending on the melting point of the alkane.

During a run,  $C_1$  is measured hourly for six to eight hours. Each value is corrected for decay, and the mean value is calculated. After the gas is uniformly distributed in  $V_g^{(1)}$ , as determined from the

observed decay rate, the main valve is opened and the stirrer is started. We calculate the Ostwald solubility, L, each hour. When L reaches a constant value, equilibrium has been reached. Time to equilibrium is typically 12 hours. We wait an additional 8 to 12 hours to be sure of equilibrium (see Figure 5. Figure 5 appears as Figure 2 in reference 67). The equilibrium values of L are averaged to determine the Ostwald solubility. For amino acid experiments, a second pH sample is taken at the end of the run.

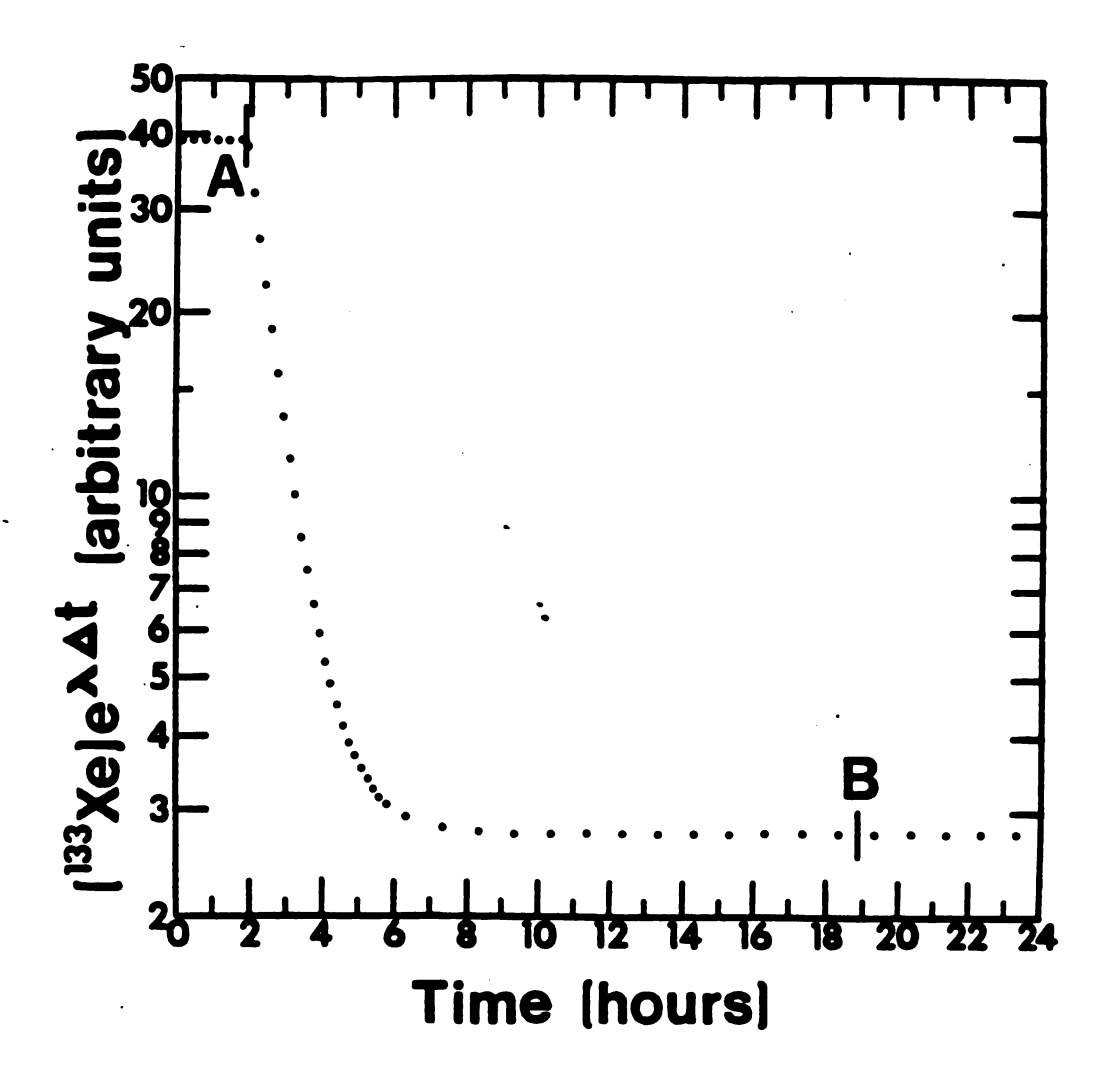


Figure 5. Normalized counting rate vs. time for a typical experiment (Figure 2 of reference 67). The letter A indicates the time the valve was opened, and the letter B indicates the time a run might end, about 8 hours after equilibrium has been reached.

#### RESULTS AND CONCLUSIONS

The results for Xe solubility in the normal alkanes and normal alkanols have been previously published.  $^{68,69}$  In addition, some of the results on the solubility of Xe in aqueous amino acid solutions have also recently appeared.  $^{70}$ 

## 4.1 ALKANES

We measured the Ostwald solubility, L, of \$^{133}\$Xe in normal alkanes at five temperatures in the range from 10°C to 50°C. \$^{68}\$ Values of L, and the mole fraction solubility, x2, are listed in Table 1. Mole fraction solubilities were calculated using equation (21). Figures 6 and 7 are plots of L versus Temperature (T) and x2 versus T, respectively, for the normal alkanes. Figures 8 and 9 show L versus n, the number of carbon atoms, and x2 versus n, respectively, at five different temperatures. The Ostwald solubility decreases with both increasing T and increasing n, while the mole fraction solubility decreases with T, and increases with n. Thus, even though the number of Xe atoms per unit volume decreases with increasing n, the number of Xe atoms per alkane molecule increases with n. The decrease of Xe solubility with increasing temperature is typical of gas/liquid systems.

TABLE 1. Solubility data for experiments with  $^{133}$ Xe in the normal alkanes. The first row gives the Ostwald solubility measured for each alkane, and the second row is  $10^2$ x<sub>2</sub>, where x<sub>2</sub> is the mole fraction solubility of Xe in the normal alkanes at 1 atm partial pressure of Xe.

3.18 2. 7 5.41±0.03 4. 3.26 2. 8 4.99±0.03 4. 3.34 2. 9 4.70±0.02 4.			
x <sub>2</sub> = 3.03 2.5 5.91±0.03 5.7 3.18 2.6 7 5.41±0.03 4.7 3.26 2.6 8 4.99±0.03 4.7 3.34 2.6 9 4.70±0.02 4.8			
3.18 2. 7 5.41±0.03 4. 3.26 2. 8 4.99±0.03 4. 3.34 2. 9 4.70±0.02 4.			
3.26 2. 8 4.99±0.03 4. 3.34 2. 9 4.70±0.02 4.		5±0.03	
3.34 2.	_	3.75±0	.07 3.37±0.0
9 4.70±0.02 4.		2.15	1.90
		0±0.02 3.47±0 2.20	3.31±0.06 1.95
3.45 2.	14±0.03 3.70	0±0.03 3.32±0	2.99±0.03
	99 2.62	2.30	2.04
10 4.42 3.		2±0.04 3.14	2.84
3.54 3.		2.38	2.11
	72±0.03 3.35	3.00	2.71
	16 2.79	2.45	2.18
	59±0.02 3.22	2±0.01 2.90±0	2.64
	28 2.88	3 2.55	2.28
	44±0.01 3.09	9±0.02 2.80	2.53
	37 2.96	5 2.63	2.34
	35±0.02 3.02 49 3.08	2±0.01 2.72 2.73	2.49 2.44

TABLE 1 (cont'd.).

Temperature	10°C	20°C	30°C	40°C	50°C
Number of carbons in n-alkane					
15 L = x <sub>2</sub> =		3.24±0.02 3.59	2.92±0.01 3.17	2.64 2.81	2.41 2.51
16		3.14±0.01 3.67	2.85±0.03 3.26	2.57±0.0 2.89	2.35±0.0 2.59
17			2.76±0.03 3.34	2.51±0.01 2.98	2.30 2.68
18			2.71±0.01 3.45	2.47±0.01 3.08	2.25±0.01 2.76
19				2.42±0.01 3.17	2.21±0.01 2.84
20				2.36±0.0 3.24	2.17±0.0 2.92

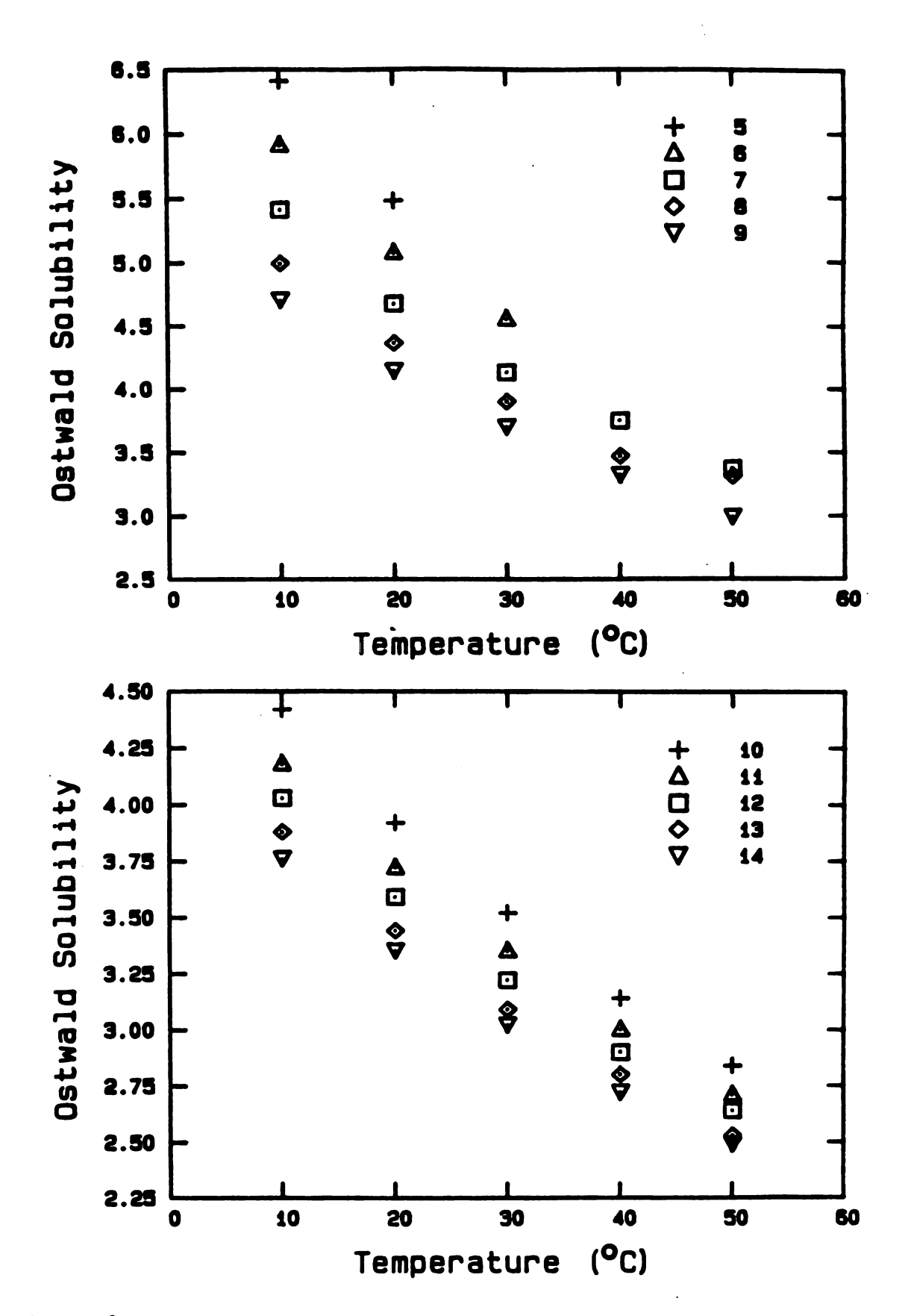


Figure 6. L vs. T for the normal alkanes. The numbers next to the symbols are the number of C atoms in the alkane molecule.

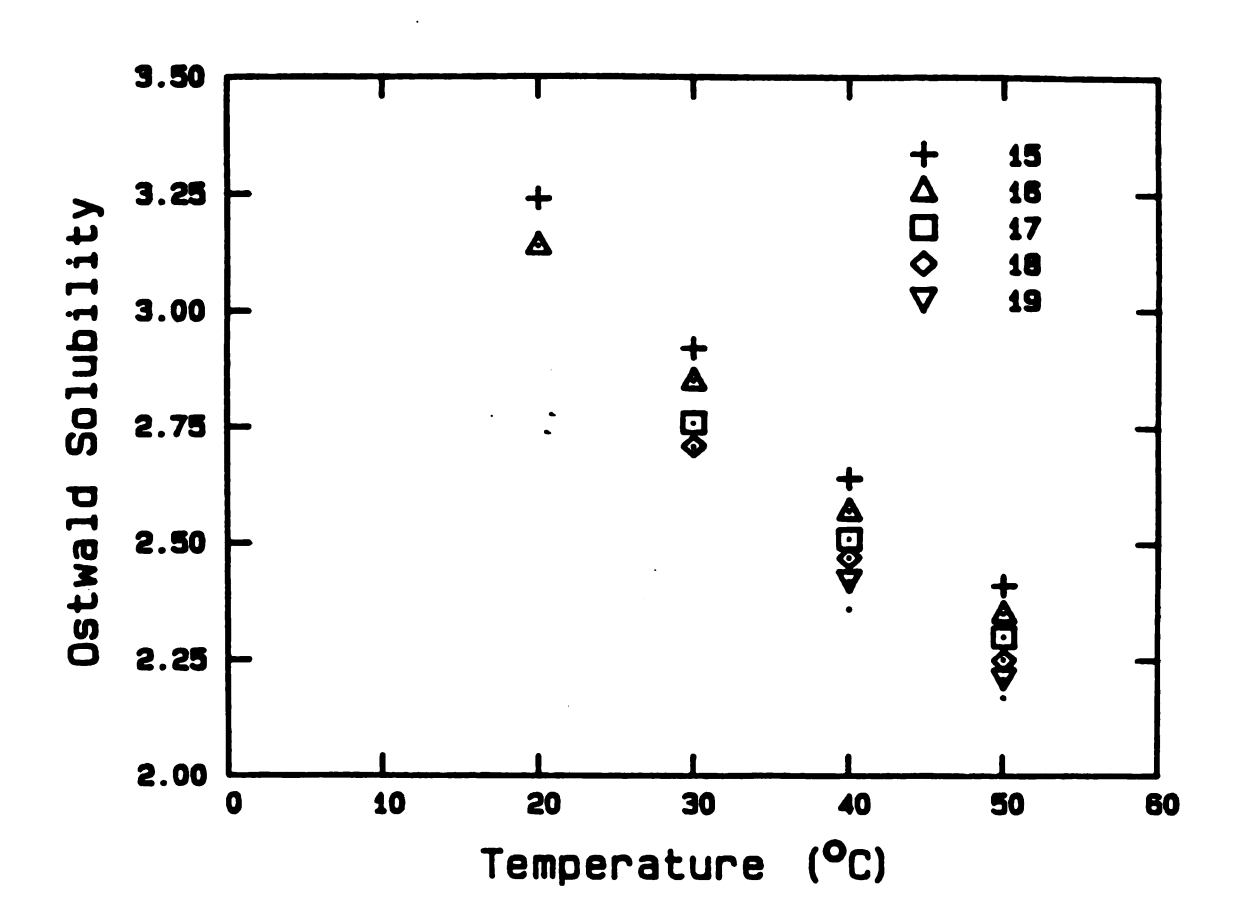


Figure 6. (cont'd.).

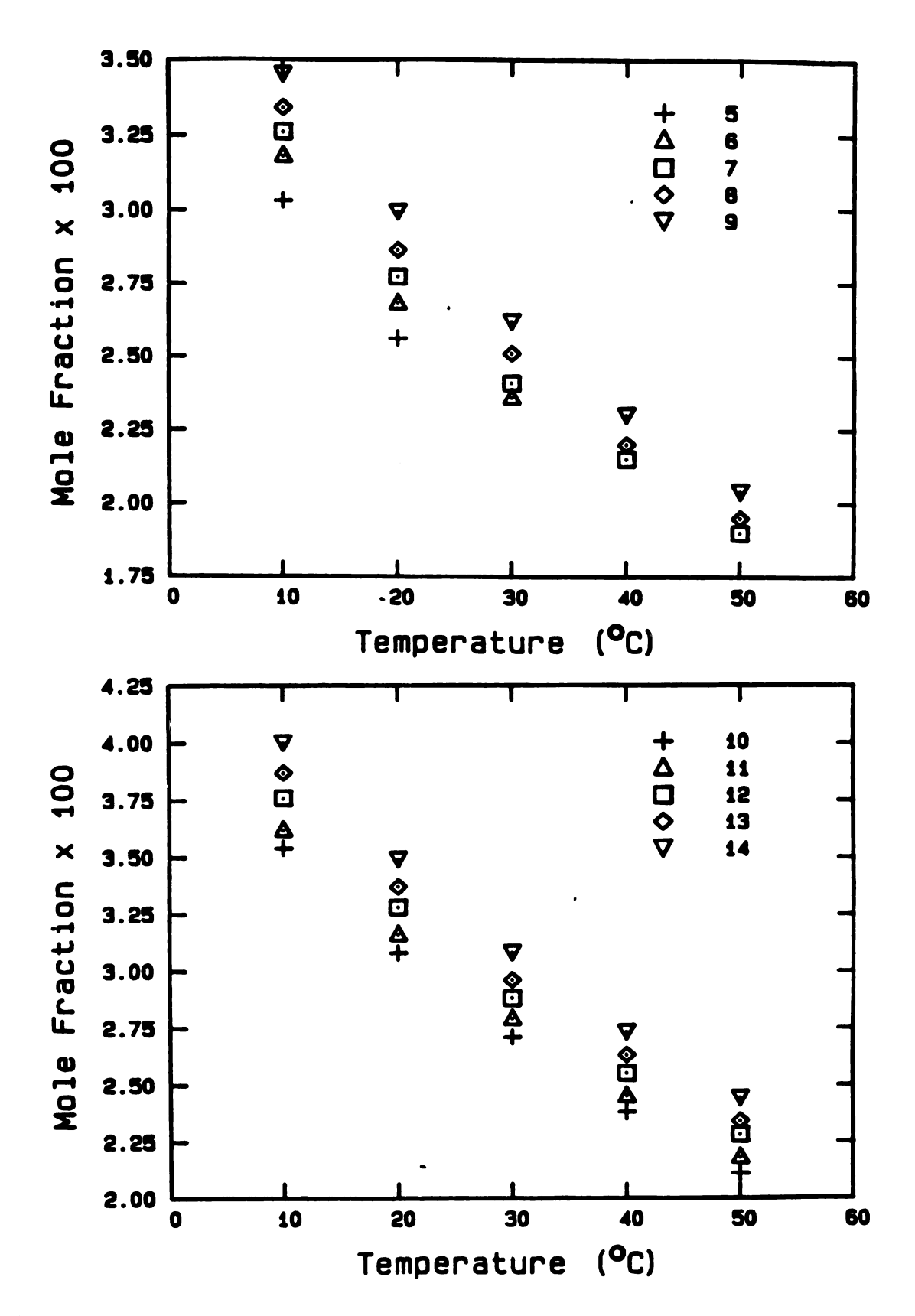


Figure 7.  $\times$  vs. T for the normal alkanes. The numbers next to the symbols are the number of C atoms in the alkane molecule.

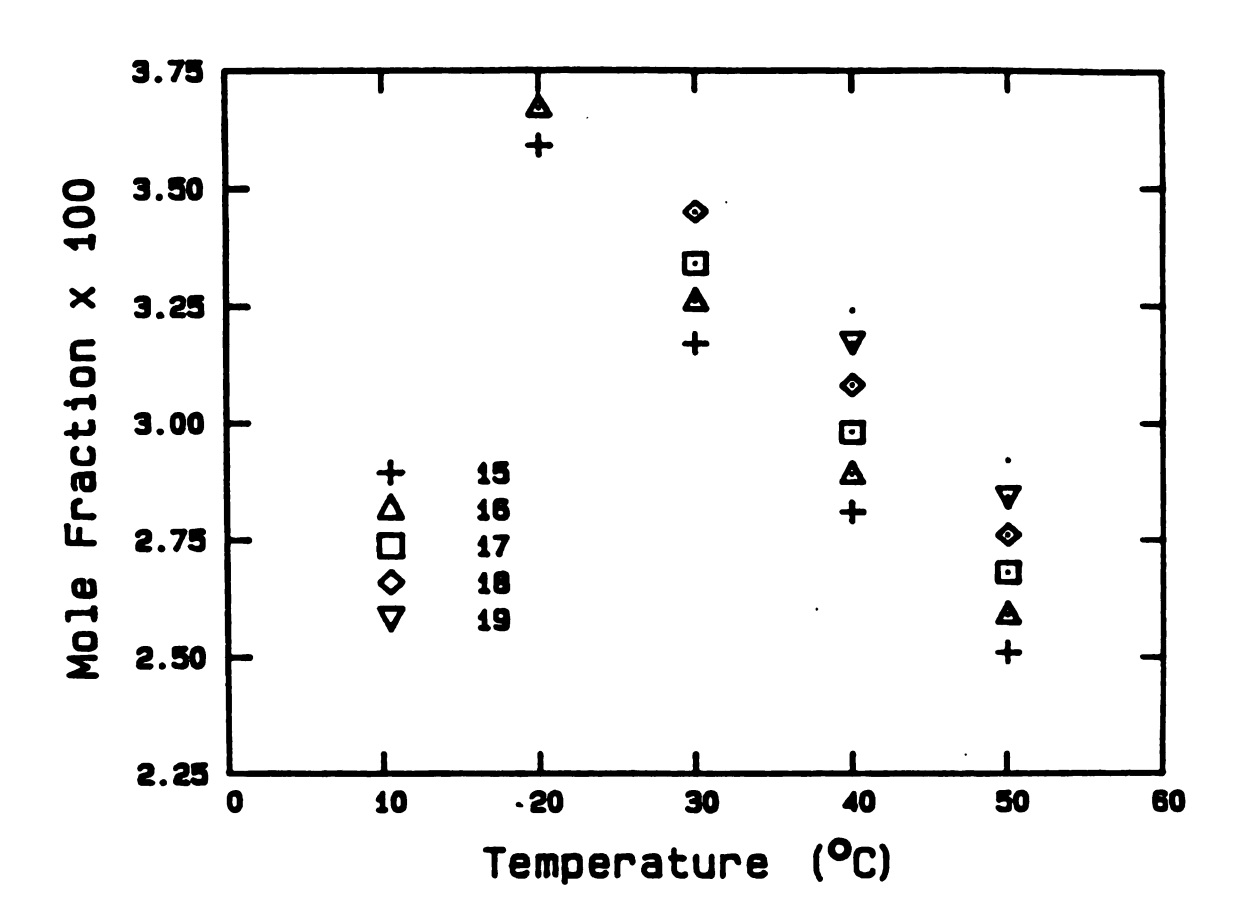


Figure 7. (cont'd.).

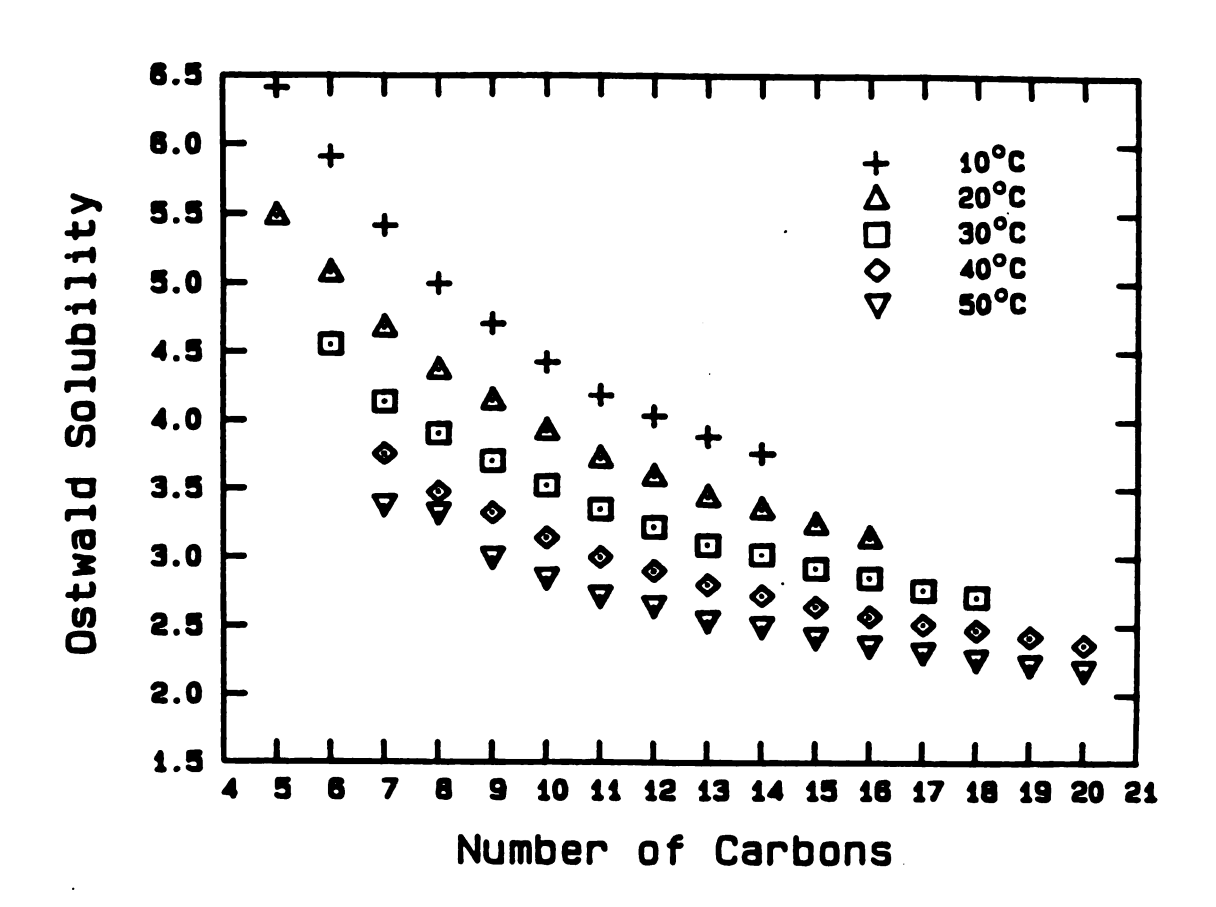


Figure 8. L vs. n for the n-alkanes at 5 temperatures.

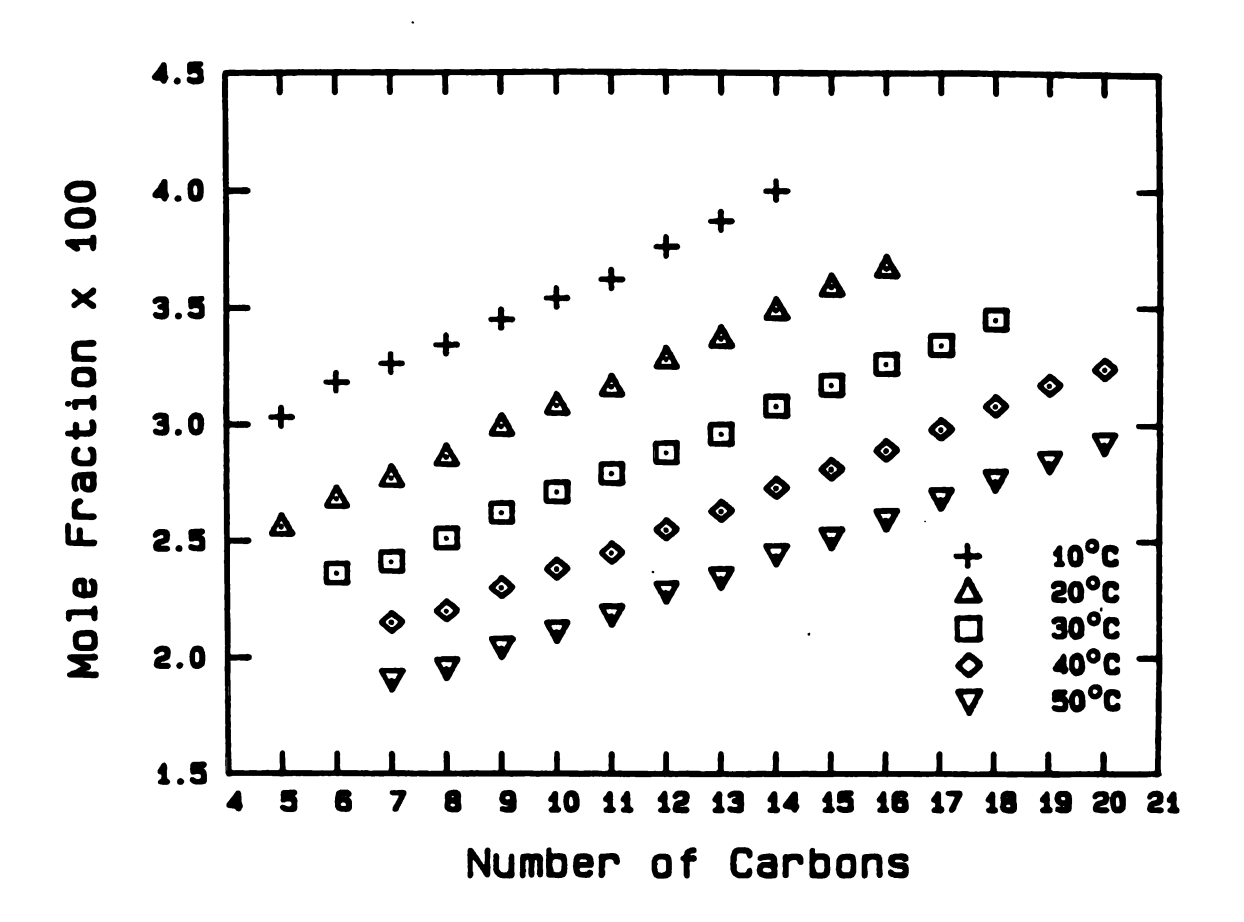


Figure 9.  $x_2$  vs. n for the n-alkanes at 5 temperatures.

Makranczy et al.  $^{71}$  measured the Ostwald solubility of Xe in the normal alkanes n-pentane through n-hexadecane. Their data are plotted, along with our data for 20°C, in Figure 10. The mole fraction solubilities are shown in Figure 11. It is interesting to note the differing behavior of  $x_2$  as a function of n. The data of Makranczy et al. show a decrease in the mole fraction solubility with n.

Clever et al.  $^{72}$  measured the solubility of He, Ne, Ar, and Kr in the normal alkanes n-hexane through n-decane, n-dodecane, and n-tetradecane at several different temperatures. Their data show a decrease in  $\mathbf{x}_2$  with with increasing n for He and Ne, but Ar shows an initial decrease in  $\mathbf{x}_2$ , followed by an increase for the longer chains. The mole fraction solubility of Kr in the n-alkanes increases with increasing n. This would lead you to believe that the mole fraction solubility of Xe in the normal alkanes should increase with increasing n.

In table 2 are values for  $\Delta\mu_2^0$ , calculated using equation (58), and  $\Delta\mu_2^{00}$ , calculated using equation (61). The chemical potentials as a function of temperature, and as a function of n, are shown in Figures 12, 13, 14, and 15. A least squares fit of the  $\Delta\mu_2$  versus T data for both  $\Delta\mu_2^0$  and  $\Delta\mu_2^{00}$ , yields straight lines ( $r \ge 0.999$ ) for each of the alkanes. It is from the slope and intercept of these straight lines that we obtain the entropies and enthalpies of solution.

The entropy of solution, obtained via equation (59), is the negative of the slope of the best fitting line, and the enthalpy is the intercept on the ordinate axis. Values of the entropy and enthalpy are listed in Table 3, and are plotted versus n in Figures 16 and 17.

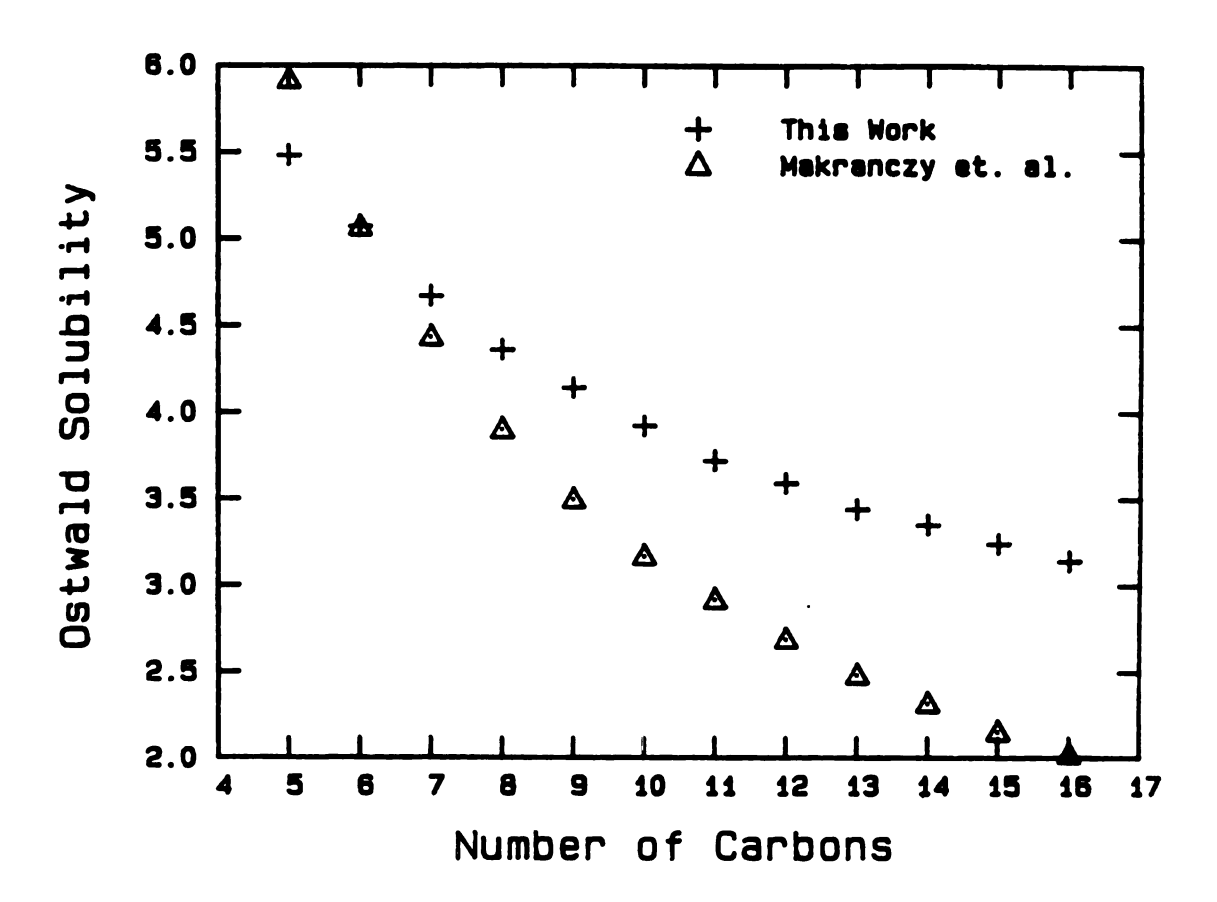


Figure 10. L vs. n for the n-alkanes; +,  $20^{\circ}$ C, our data;  $\Delta$ ,  $25^{\circ}$ C, Makranczy et al.

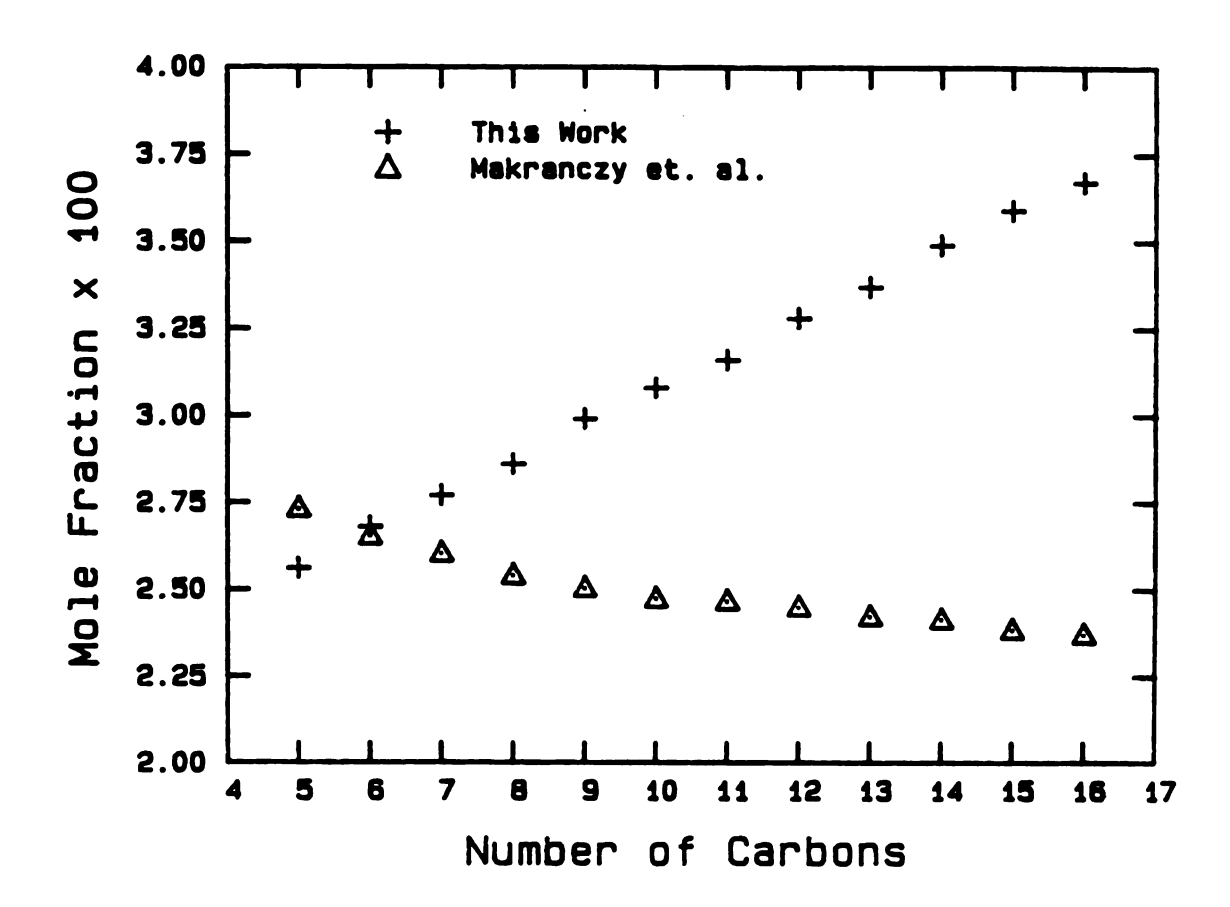


Figure 11.  $x_2$  vs. n for the n-alkanes; +, 20°C, our data;  $\Delta$ , 25°C, Makranczy <u>et al</u>.

TABLE 2. Chemical potentials in the mole fraction scale,  $\Delta\mu_2^o$ , and in the number density scale,  $\Delta\mu_2^{o\,\rho}$ . The first row is  $\Delta\mu_2^o$  and the second row is  $\Delta\mu_2^{o\,\rho}$ . Units are cal/mol.

Temperature	10°C	20°C	30°C	40°C	50°C
Number of carbons in n-alkanes					
5 Δμ <sup>ο</sup> = Δμ <sup>ο ρ</sup> =	1967±8.4 -1045±8.4	2136±8.7 -991±8.7			
6	1941 -999	2109 -945	2257±9.0 -913±9.0		
7	1926	2089	2246	2390±9.3	2546±9.6
	<del>-</del> 950	-898	-854	-822±9.3	-780±9.6
8	1913	2071	2218	2376	2529
	-904	-858	-820	-774	-769
9	1894	2045	2195	2347	2498
	<del>-</del> 871	-828	-788	-747	-703
10	1879	2027	2173	2327	2477
	-836	<del>-</del> 796	<del>-</del> 758	-712	-670
11	1867	2012	2157	2307	2458
	-805	-765	-728	-684	-640
12	1847	1991	2136	228 <b>3</b>	2429
	-784	-744	-704	-662	<del>-</del> 62 <b>3</b>
13	1830	1976	2120	2264	2411
	-763	-720	-679	-641	<del>-</del> 596
14	1811	1955	2096	2241	2383
	-745	-704	-666	-623	-586
			•		

TABLE 2 (cont'd).

emperature	10°C	20°C	30°C	40°C	50°C
iumber of carbons in n-alkane					
$5  \Delta \mu_2^{\circ}  =  \\ \Delta \mu_2^{\circ \rho}  =  $		1939 <b>-</b> 685	2080 -645	2223 <b>-</b> 604	2366 -565
6		1926 -667	2062 <b>-</b> 631	2204 -587	2345 -549
7			2048 -612	2186 -573	2325 -535
3			2027 <b>-</b> 601	2166 <b>-</b> 563	2306 <del>-</del> 521
9				2149 -550	2286 <del>-</del> 509
0				2134 -534	2270 -498

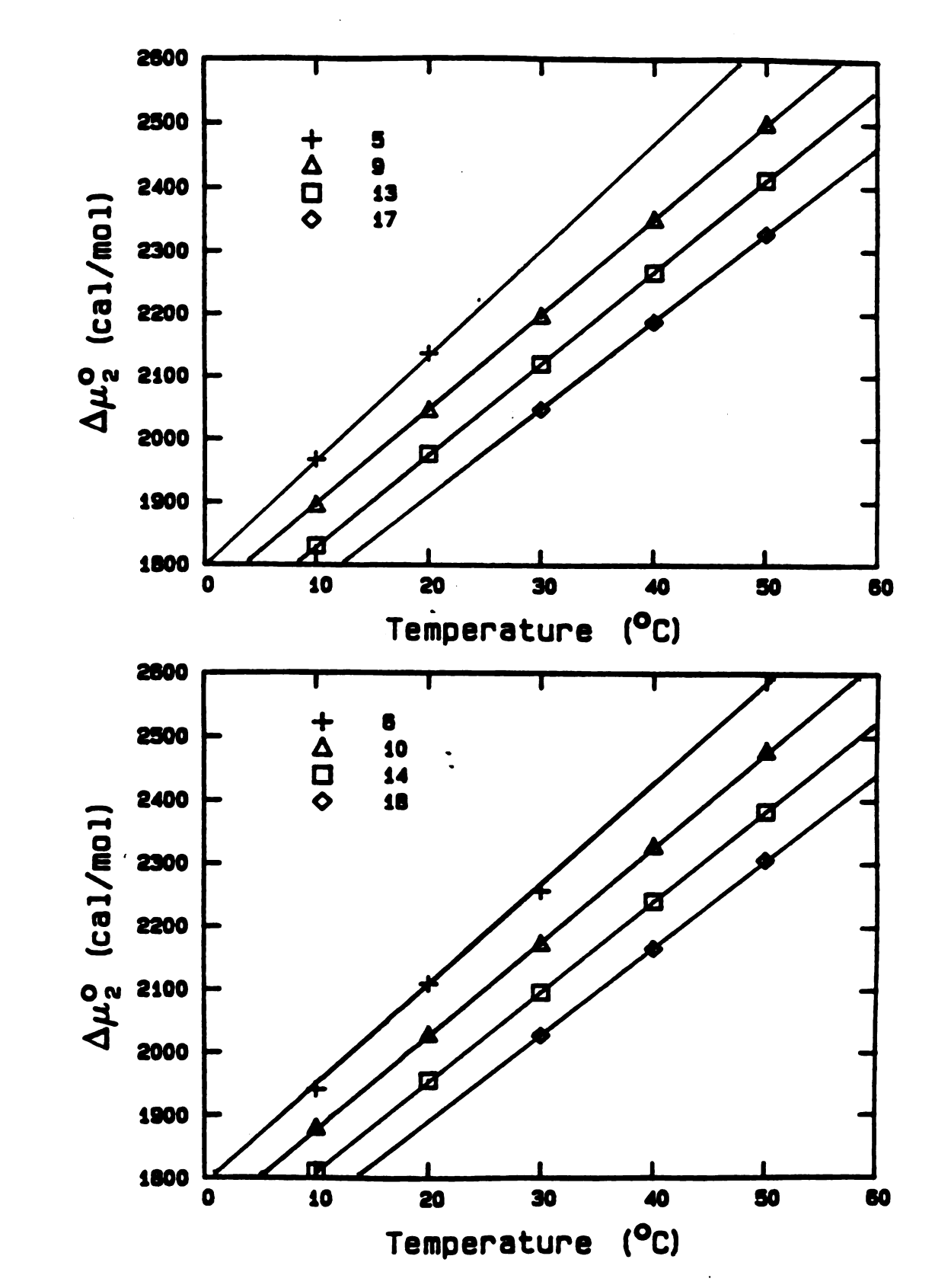


Figure 12.  $\Delta\mu_2^o$  vs. T for the n-alkanes. The numbers next to the symbols are the number of C atoms in the alkane molecule

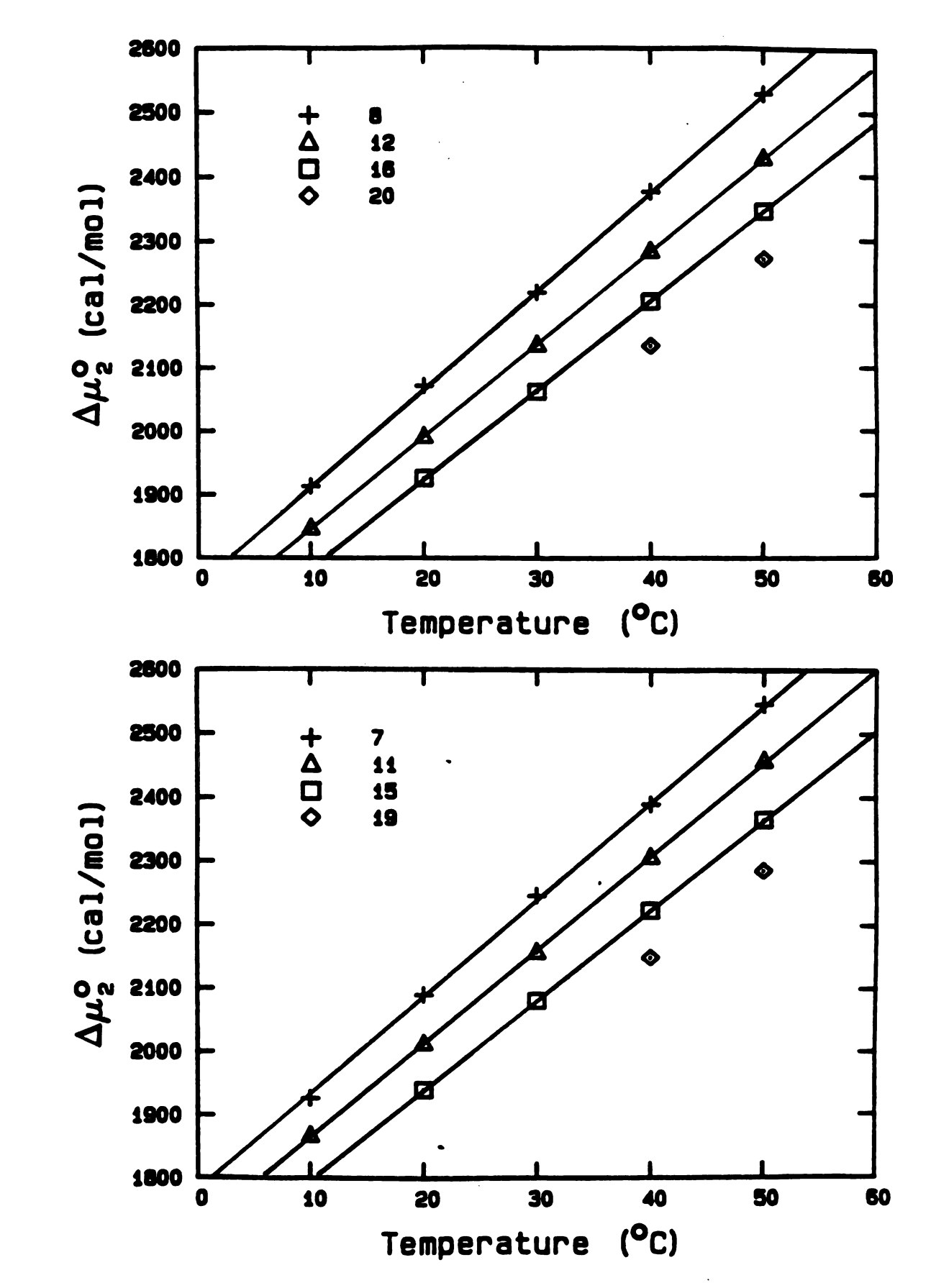


Figure 12. (cont'd.).

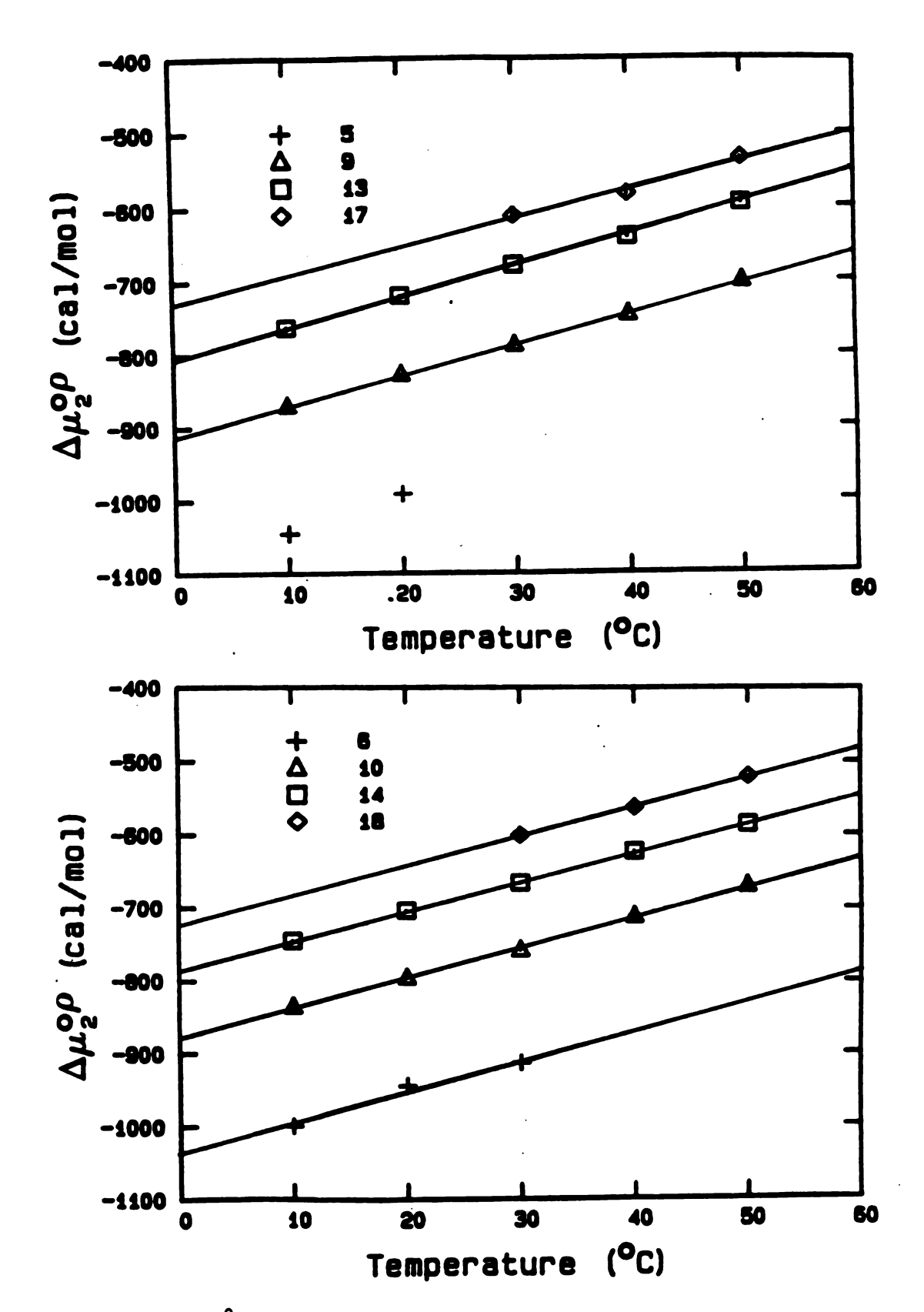


Figure 13.  $\Delta\mu_2^{e\,\rho}$  vs. T for the n-alkanes. The numbers next to the symbols are the number of C atoms in the alkane molecule

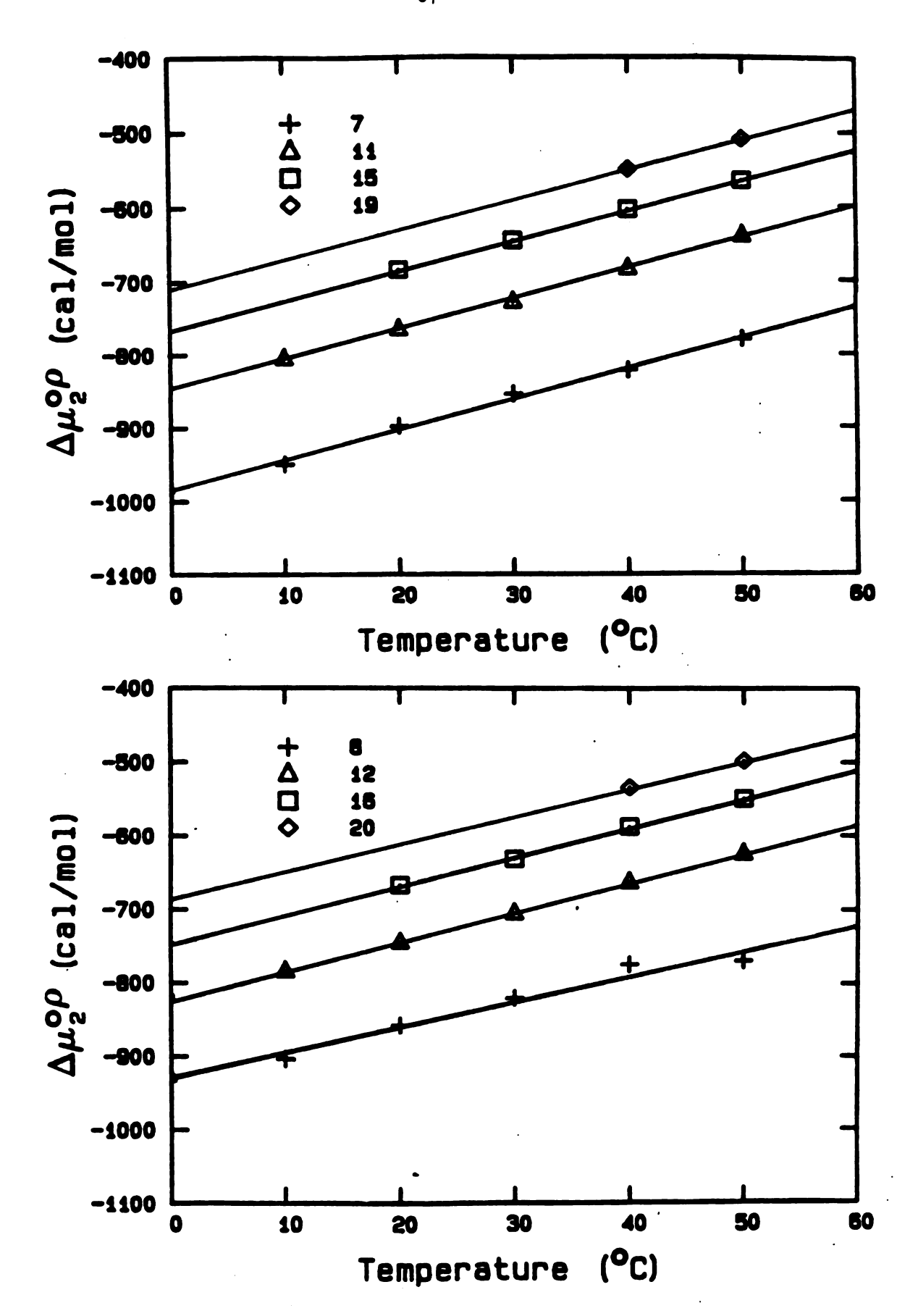


Figure 13. (cont'd.).

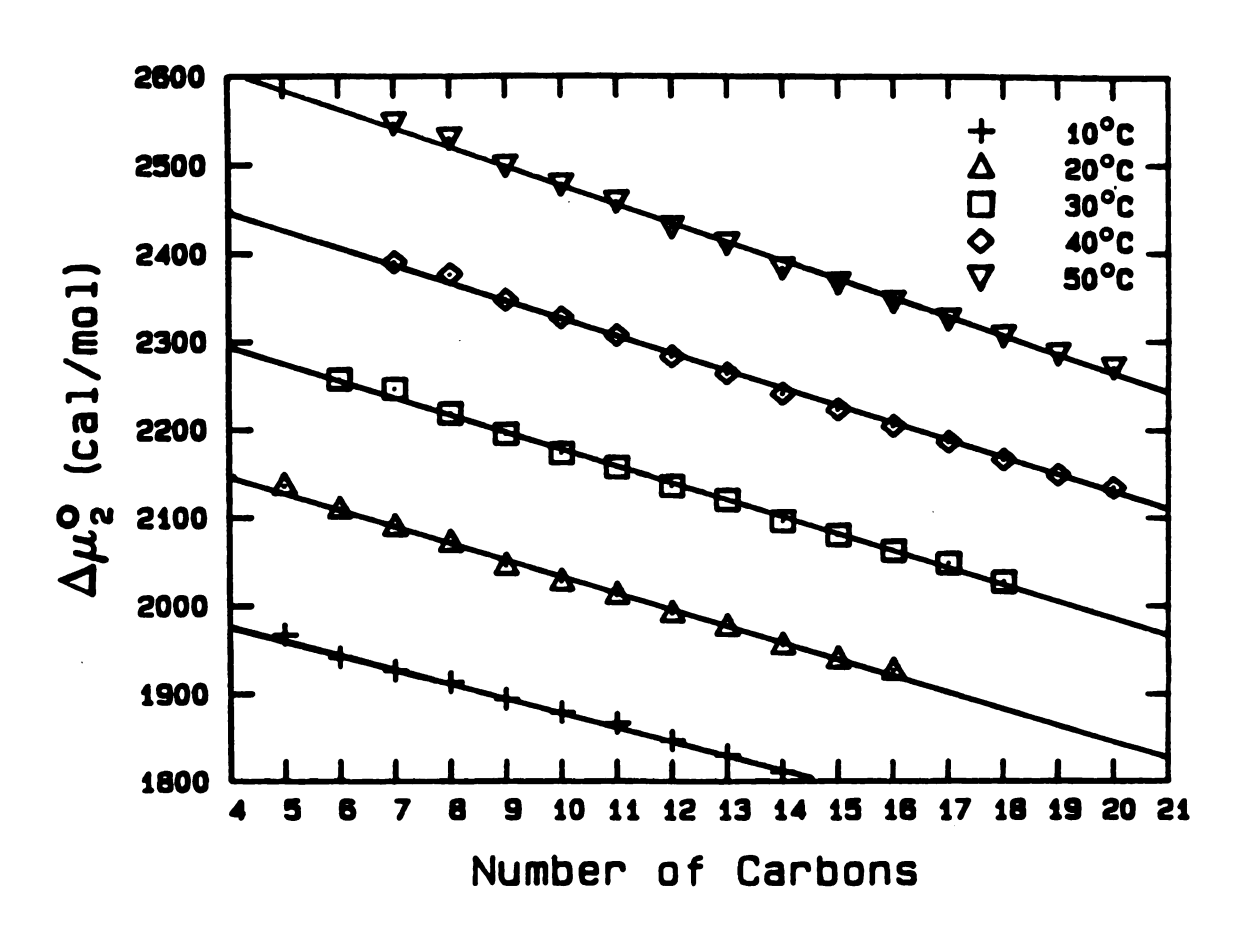


Figure 14.  $\Delta\mu_2^{0}$  vs. n for the n-alkanes at 5 temperatures

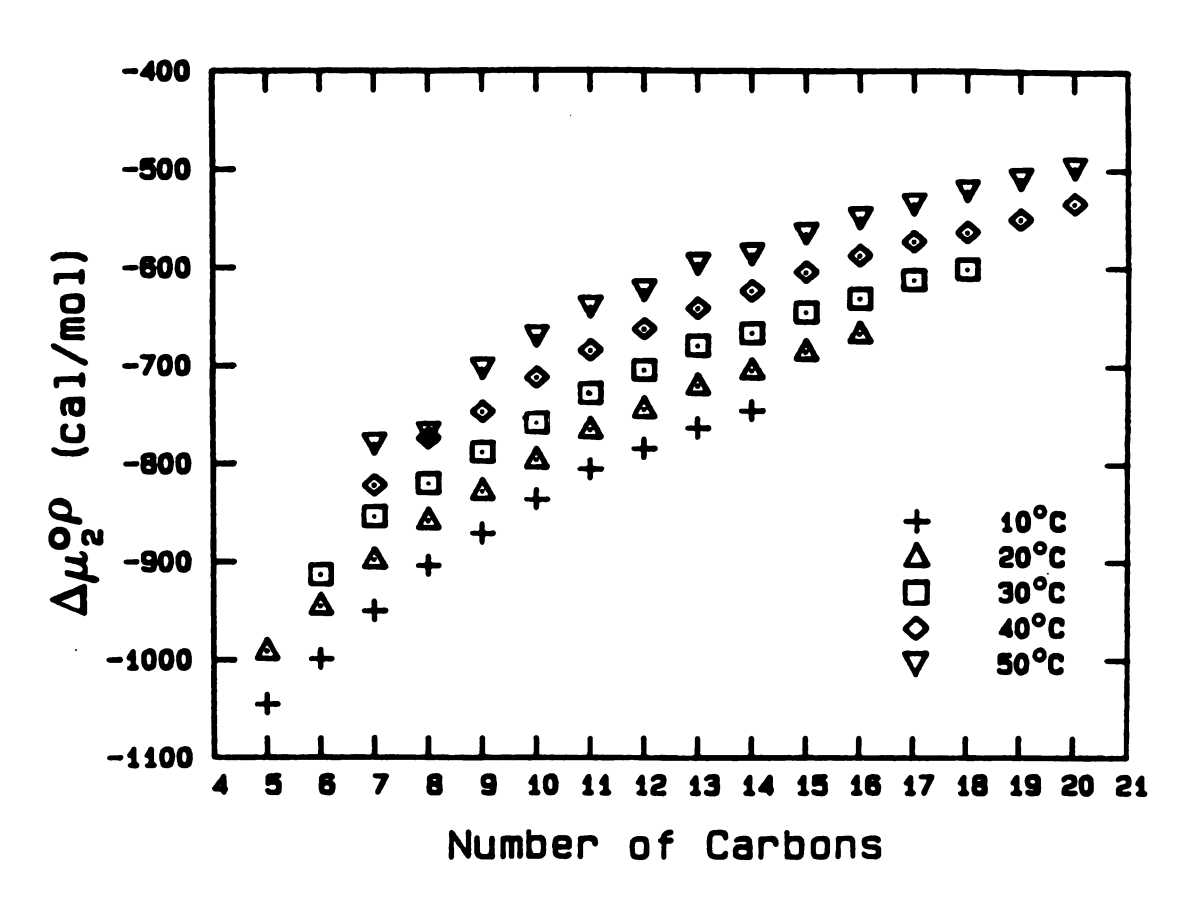


Figure 15.  $\Delta\mu_2^{\mathfrak{op}}$  vs. n for the n-alkanes at 5 temperatures

TABLE 3. Entropy and enthalpy of solution in both the mole fraction scale and in the number density scale for solutions of  $^{133}$ Xe in the normal alkanes.

	Mole Fracti	on Scale	Number Densi		
Number of Carbons	Enthalpy of Solution AH <sup>o</sup> (cal/mol)	Entropy of Solution $\Delta S_2^{\circ}$ (cal/mol K)	Enthalpy of Solution	Entropy of	Temperature Range of Experiments
5 6	-2818 ± 200	-16.90 ± 0.69	-2574 ± 200	-5.40 ± 0.69	10 - 20°C
	-2691 ± 132	$-16.37 \pm 0.45$	-2230 ± 132	$-4.35 \pm 0.45$	10 - 30°C
7	-2415 ± 61	$-15.36 \pm 0.20$	-2120 ± 61	$-4.14 \pm 0.20$	10 - 50°C
8 9	$-2429 \pm 77$	$-15.34 \pm 0.26$	-2120 ± 77	$-4.29 \pm 0.26$	10 - 50°C
	-2378 ± 45	$-15.09 \pm 0.15$	-2050 ± 45	$-4.16 \pm 0.15$	10 - 50°C
10	-2351 ± 51	$-14.93 \pm 0.17$	-2010 ± 51	$-4.16 \pm 0.17$	10 - 50°C
11	-2308 ± 55	$-14.74 \pm 0.18$	-1970 ± 55	$-4.11 \pm 0.18$	10 - 50°C
12	-2278 ± 24	-14.56 ± 0.08	-1930 ± 24	$-4.04 \pm 0.08$	10 - 50°C
13	-2278 ± 32	-14.51 ± 0.11	-1930 ± 32	$-4.13 \pm 0.11$	10 - 50°C
14	-2239 ± 23	$-14.30 \pm 0.08$	-1860 ± 23	-3.93 ± 0.08	10 - 50°C
15	-2233 ± 30	$-14.23 \pm 0.10$	-1860 ± 30	$-4.01 \pm 0.10$	20 - 50°C
16	$-2180 \pm 40$	$-14.00 \pm 0.13$	-1830 ± 40	$-3.97 \pm 0.13$	20 - 50°C
17	$-2154 \pm 102$	$-13.68 \pm 0.33$	$-1770 \pm 102$	$-3.84 \pm 0.33$	30 - 50°C
18	$-2191 \pm 38$	$-13.91 \pm 0.12$	-1810 ± 38	$-3.99 \pm 0.12$	30 - 50°C
19	$-2152 \pm 97$	$-13.73 \pm 0.31$	$-1820 \pm 97$	$-4.07 \pm 0.31$	40 - 50°C
20	-2117 ± 24	$-13.58 \pm 0.08$	$-1690 \pm 24$	$-3.68 \pm 0.08$	40 - 50°C

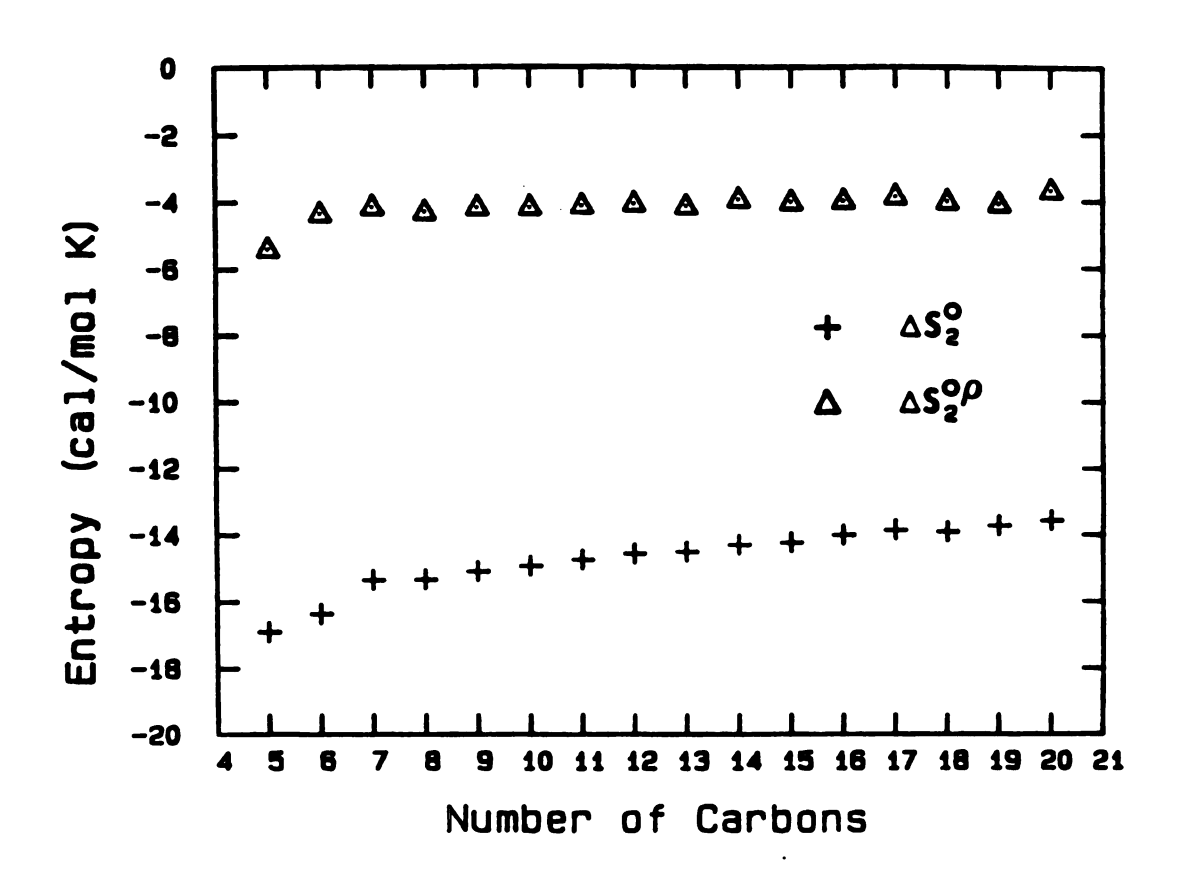


Figure 16. Entropy of solution for Xe in the n-alkanes

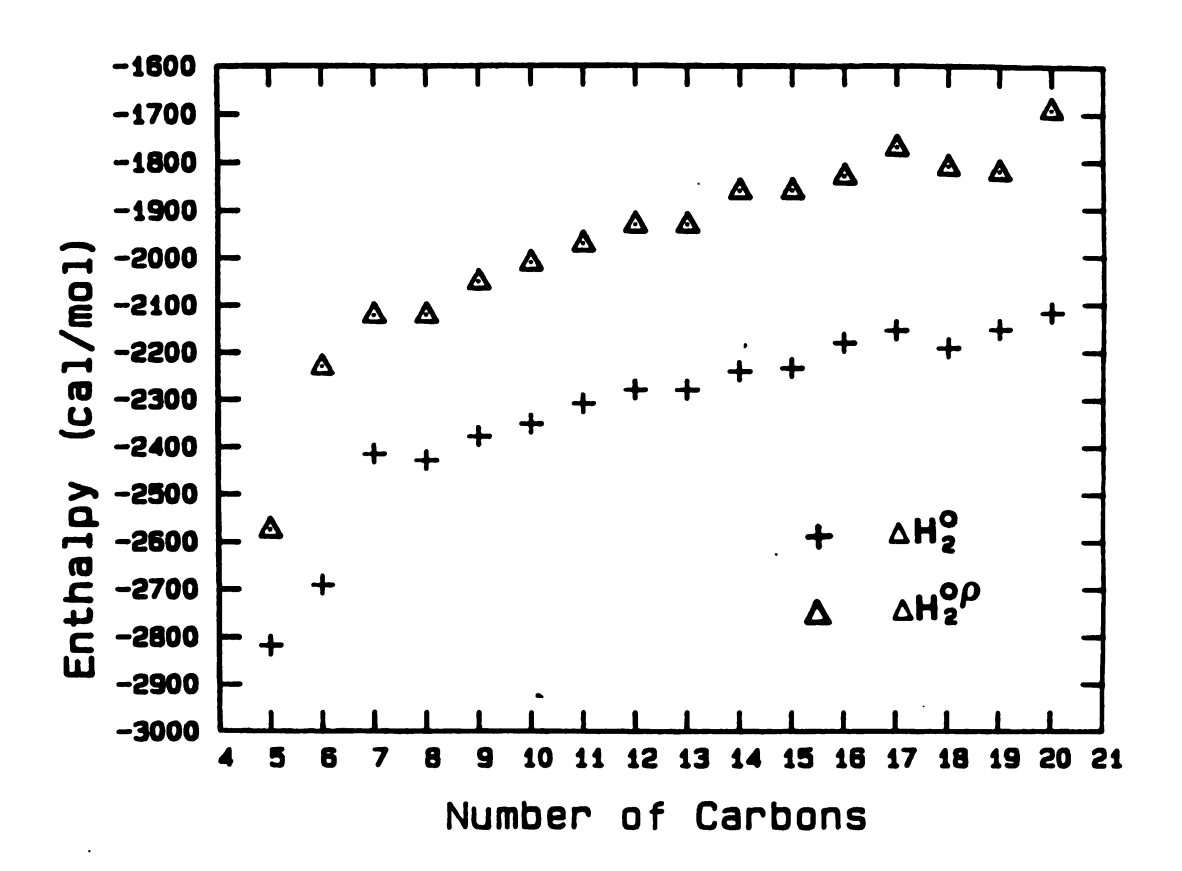


Figure 17. Enthalpy of solution for Xe in the n-alkanes

From Figure 16, we see that both  $\Delta S_2^0$  and  $\Delta S_2^{0\rho}$  are negative, and increase slowly with n for  $n \le 8$ . We can interpret this in several different ways. One explanation is that the Xe has more freedom of movement, or is less constrained in solution, for larger n. A second interpretation is that the Xe has a greater disordering effect on the liquid molecules for large n. The actual situation is probably a combination of these two.

Clever  $^{73}$  has calculated the entropy of solution of Xe in n-hexane, n-dodecane, and isooctane. He obtained values of -15.92, -15.54, and -15.51 cal/(mol K), respectively. The agreement with our results is good. Clever et al.  $^{72}$  calculated the entropy of solution for He, Ne, Ar, and Kr in the normal alkanes n-hexane through n-decane, n-dodecane, and n-tetradecane. All exhibit nearly constant  $\Delta S_2^{\circ}$  (He, -10.4  $\pm$  0.7; Ne, -10.8  $\pm$  0.4; Ar, -13.0  $\pm$  0.4; and Kr, -13.7  $\pm$  0.2 all in dimensions of cal/mol K). For Xe in the same seven solvents, we determined  $\Delta S_2^{\circ}$  = -15.13  $\pm$  0.25 cal/mol K. This is about the value we would expect if we view the inert gases as a homologous series.

Like the entropies, the enthalpies,  $\Delta H_2^{\circ}$  and  $\Delta H_2^{\circ \rho}$ , are negative and generally increase with increasing n. This is the proper qualitative effect we would expect according to the cavity formation model of Uhlig<sup>29</sup> and Eley.<sup>30</sup> Assuming the Xe/alkane interaction is nearly constant as a function of n, we would expect this increase in  $\Delta H$ , since the surface tension of the alkanes increases with chain length, and it is more difficult to create a cavity in a liquid of higher surface tension.

Clever  $^{73}$  calculated  $\Delta H_2^{\circ}$  for Xe in n-hexane, n-dodecane, and isooctane. His values are -2582, -2273, and -2489 cal/mol, respectively.

Our values for these same quantities are  $-2691 \pm 132$  for n-hexane and  $-2278 \pm 24$  for n-dodecane, taken from Table 3. Our value for n-octane,  $-2429 \pm 77$ , also compares favorably with his value for isooctane. The agreement with our data is good.

Figure 18 is a plot of the three quantities in equation (64) for the alkanes n-pentane through n-hexadecane. The binding energy shown has been calculated from the enthalpy,  $\Delta H_2^0$ , and the surface energy,  $4\pi r_2^2 \gamma_1 N_A$ . As expected, the binding energies are nearly constant, varying by a few percent from the mean of 4500 cal/mol. The gradual increase in E with n is consistent with the stronger interactions between Xe and alkane at large n.

A plot similar to Figure 18 can also be made for  $\Delta H_2^{\circ \rho}$ . However, the difference in enthalpies,  $\Delta H_2^{\circ \rho}$  -  $\Delta H_2^{\circ}$ , is nearly constant, about 350 cal/mol, and the behavior of  $E_h$  will be much the same.

Table 4 lists values of E<sub>b</sub> calculated from equation (64), and the binding energy estimated as the geometric mean of the heats of vaporization of Xe and the alkanes at their normal boiling points. Agreement is good, within 20%, for all of the alkanes shown. The estimated binding energy also shows an increase with increasing n, much as the values obtained from experiment. However, the estimated values increase at a greater rate.

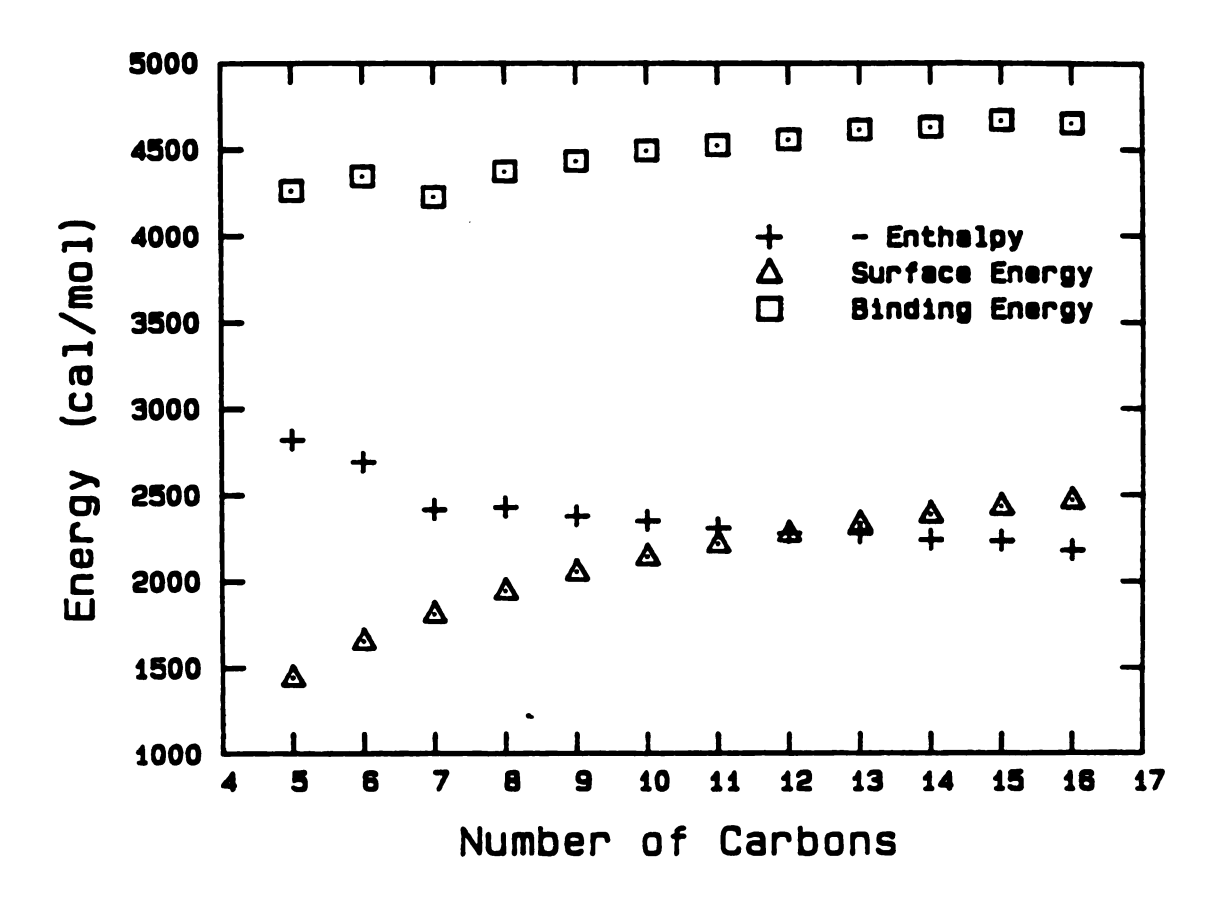


Figure 18. Binding energy, surface energy, and enthalpy of solution for the n-alkanes. (Figure 5 of reference 68).

TABLE 4. Comparison of experimental binding energies,  $E_b^{\text{exp}}$ , of Xe in the normal alkanes with binding energies estimated from the heats of vaporization of the solute and solvent,  $E_b^{\text{est}}$ .

Number of Carbons per n-alkane	Eexp b (cal/mol)	Eest b (cal/mol)	
	(Call mol)	(cal/mol)	
5	4261	4071	
6	4346	4307	
	4226	4514	
7 8	4373	4701	
9	4433	4860	
10	4494	5026	
11	4526	5167	
12	4558	5299	
13	4615	5414	
14	4628	5539	
15	4668	5636	
16	4651	5751	

## 4.2 ALKANOLS

We also measured the Ostwald solubility of  $^{133}$ Xe in the normal alkanols at five temperatures in the range from 10°C to 50°C. The values we obtained for L and  $x_2$  are listed in Table 5.

Figures 19 and 20 are plots of L versus T and  $x_2$  versus T. As with the alkanes, both L and  $x_2$  decrease with increasing temperature.

Komarenko and Manzhelii $^{74}$  measured the solubility of Xe in n-propanol in the temperature range from -80°C to -30°C. They found that the mole fraction solubility decreased with increasing temperature, not only for Xe in n-propanol, but also for a variety of gas/alcohol systems. Solute gases were spherically symmetric (Ar, Kr, Xe, CH<sub> $\mu$ </sub>, and CF $_{\mu}$ ) and solvents included methanol, ethanol, n-propanol, and n-butanol.

The behavior of L and  $\mathbf{x}_2$  as a function of n is more complicated for the alkanols than for the alkanes. Figure 21 shows L versus n at five different temperatures. The sharp initial increase, followed by the slow decrease, is probably due to the change from the highly polar environment of methanol to one which is becoming more alkane-like for large n.

Figure 22 shows  $x_2$  <u>versus</u> n at five temperatures for Xe solubility in the normal alkanols. As with the alkanes, the number of dissolved Xe atoms per alkanol molecule increases with increasing n. The mole fraction solubility also has its greatest rate of change at small n, when the liquid environment is presumably changing most rapidly.

TABLE 5. Ostwald solubility L and mole fraction solubility  $x_2$  for  $^{1\,3\,3}$ Xe in the normal alkanols. The first row for each alkanol is L, and the second row is  $10^2x_2$ .

Tempe	rature	10°C	20°C	30°C	40°C	50°C
Numbe carbo n-alk	ns in					
1	L = x <sub>2</sub> =	2.46 0.423	2.20±0.01 0.370	1.98±0.02 0.325	1.79 0.288	
2		2.79±0.00 0.689	2.47±0.02 0.597	2.22±0.00 0.525	2.02±0.02 0.466	1.85±0.01 0.420
3		3.02±0.01 0.953	2.65±0.05 0.817	2.38±0.06 0.716	2.16 0.637	1.98±0.01 0.572
4		3.04 1.17	2.68±0.01 1.01	2.40 0.884	2.17 0.782	1.98 0.699
5		2.97 1.35	2.62±0.00 1.17	2.36 1.02	2.13±0.00 0.903	1.95 0.809
6		2.97 1.55	2.61±0.02 1.33	2.34 1.17	2.12 1.04	1.92 0.920
7		2.91 1.73	2.57±0.01 1.49	2.31 1.31	2.09 1.16	1.91 1.03
8		2.86 1.89	2.52±0.03 1.62	2.25±0.02 1.42	2.05 1.26	1.88 1.13
9		2.79 2.04	2.49±0.00 1.77	2.24 1.55		

TABLE 5 (cont'd.).

Tempe	rature	10°C	20°C	30°C	40°C	50°C
Number carbor n-alk	ns in					
10	L = x <sub>2</sub> =	2.74 2.19	2.43±0.02 1.89	2.20 1.67	2.00 1.49	1.83 1.33
11			2.34±0.01 1.98	2.11±0.01 1.74	1.92 1.55	1.76 1.39
12			•	2.12±0.02 1.89	1.94±0.01 1.68	1.78 1.51
14					1.91±0.01 1.91	1.76±0.01 1.72

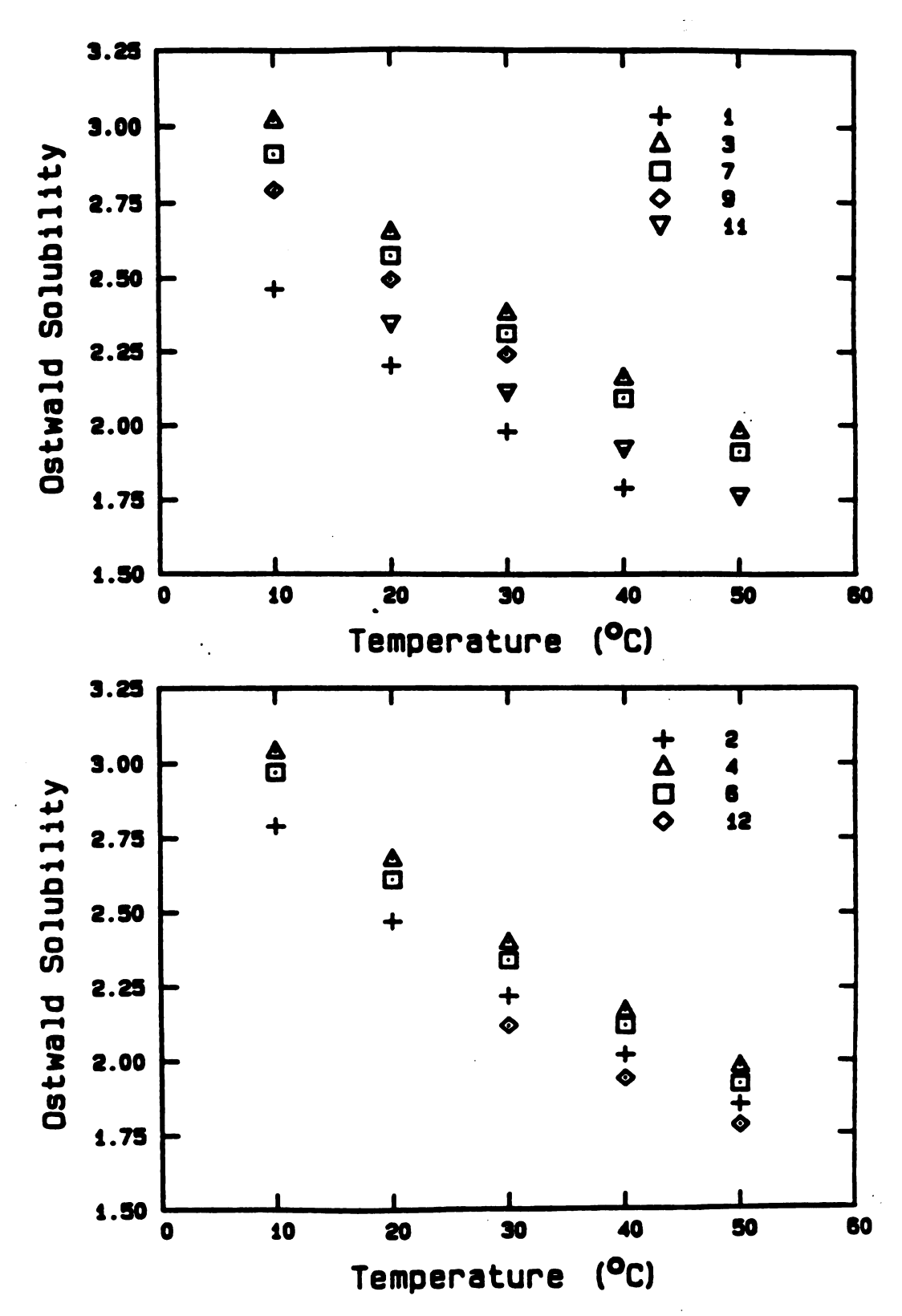


Figure 19. L vs. T for the normal alkanols. The numbers next to the symbols are the number of C atoms in the alkanol molecule.

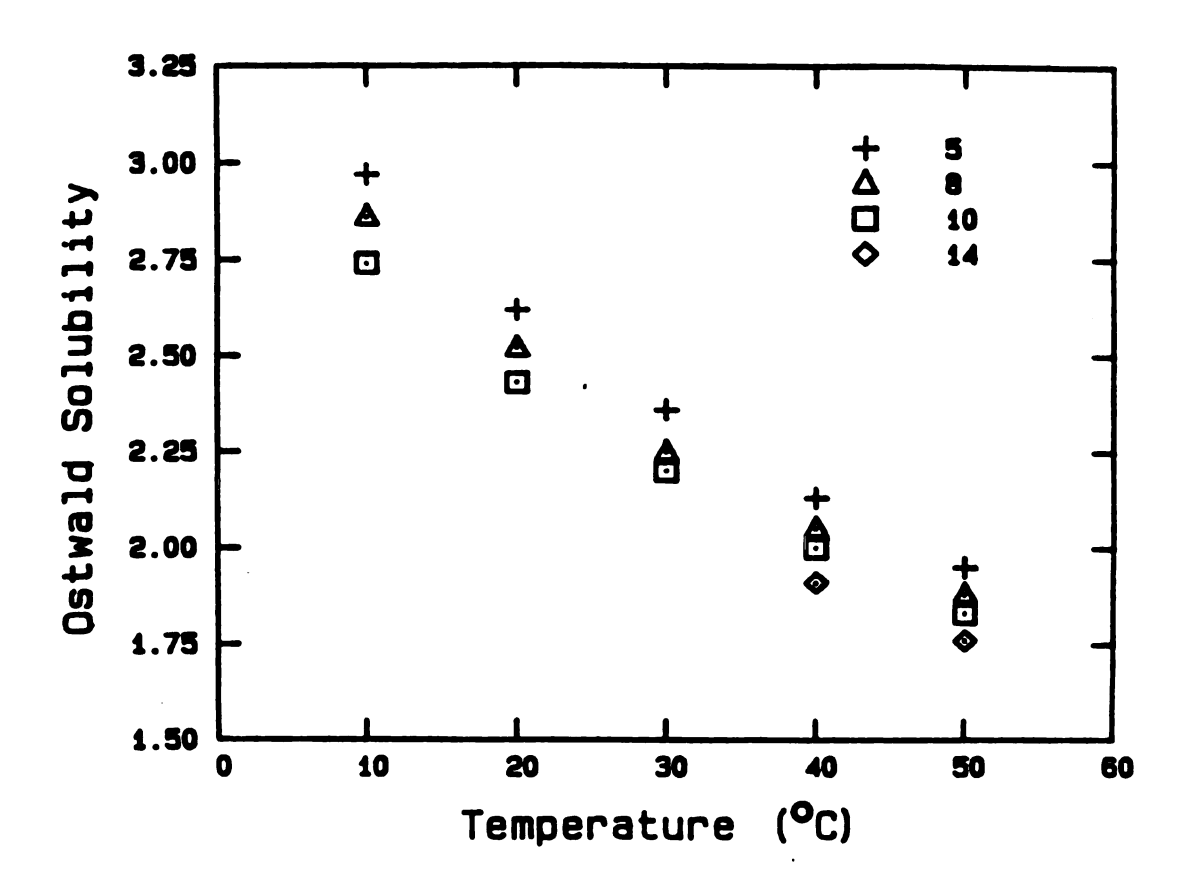


Figure 19. (cont'd.).

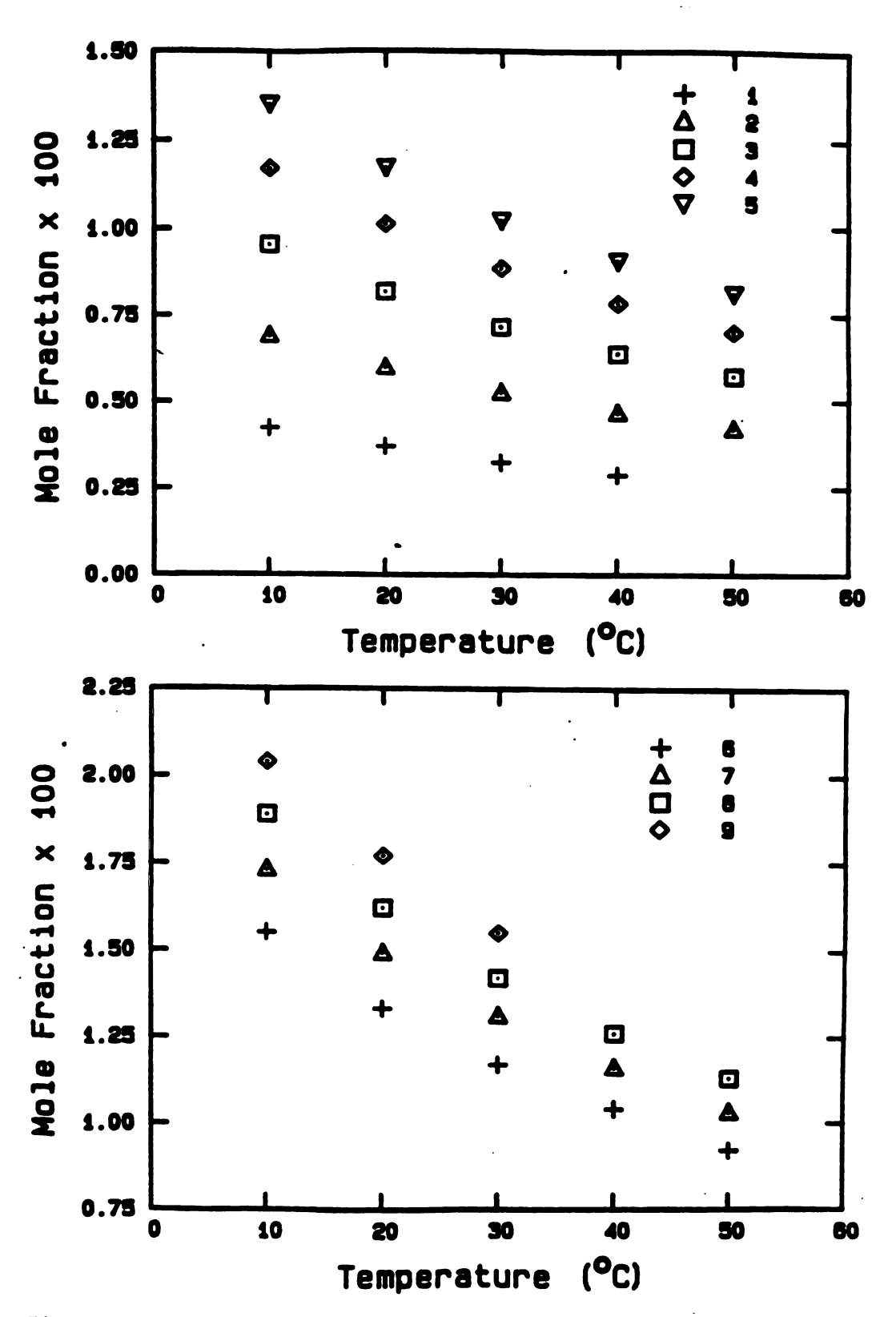


Figure 20.  $x_2$  vs. T for the normal alkanols. The numbers next to the symbols are the number of C atoms in the alkanol molecule.

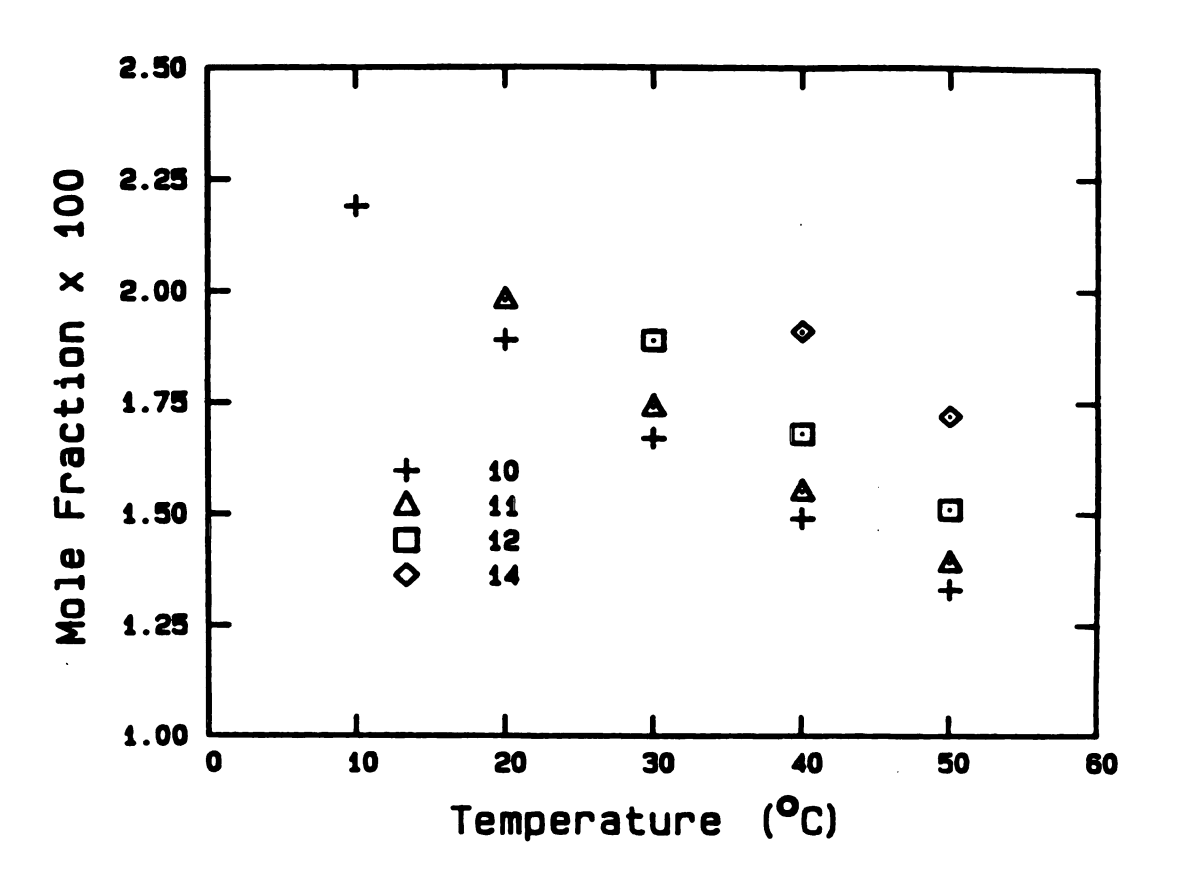


Figure 20. (cont'd.).

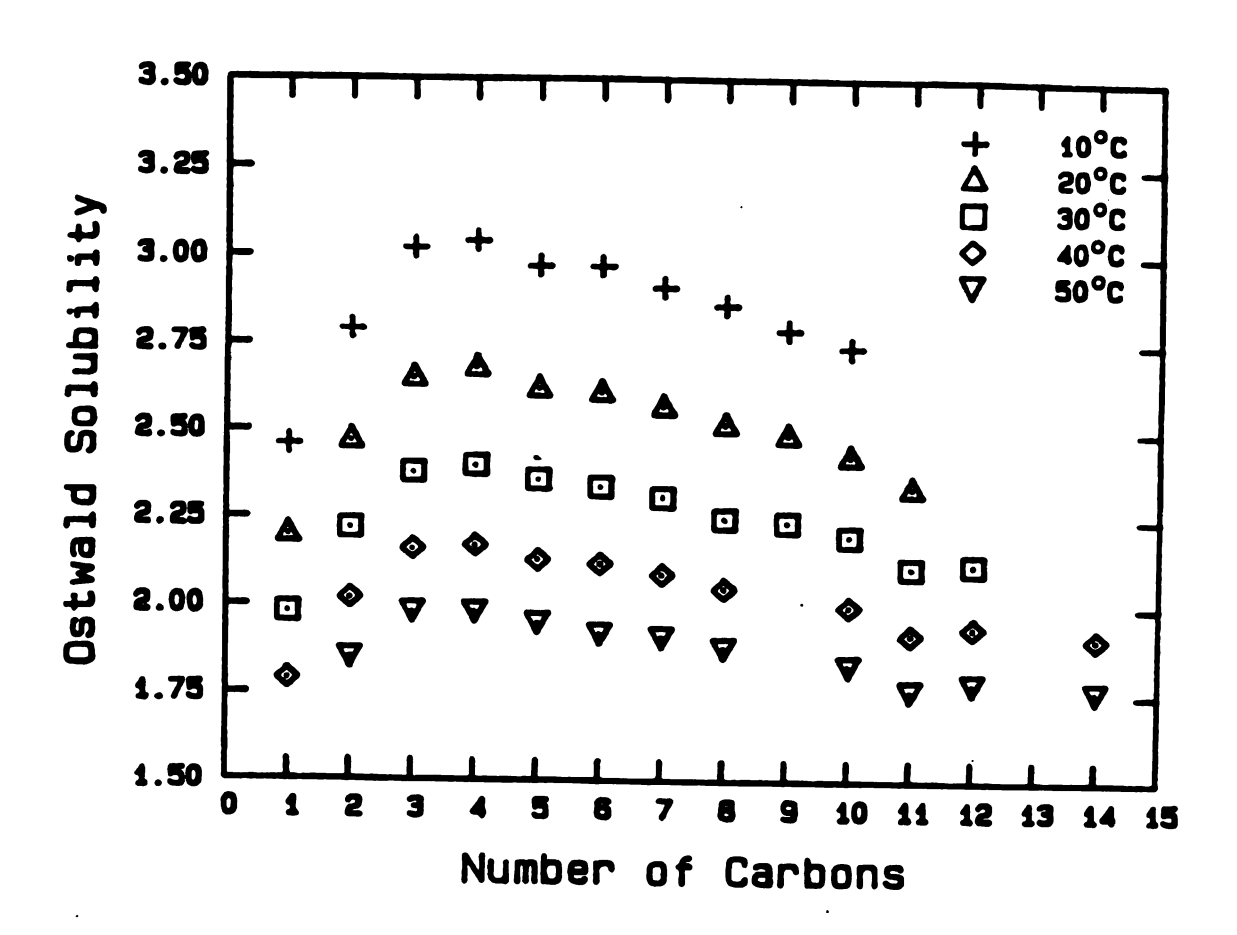


Figure 21. L vs. n for the n-alkanols at 5 temperatures.

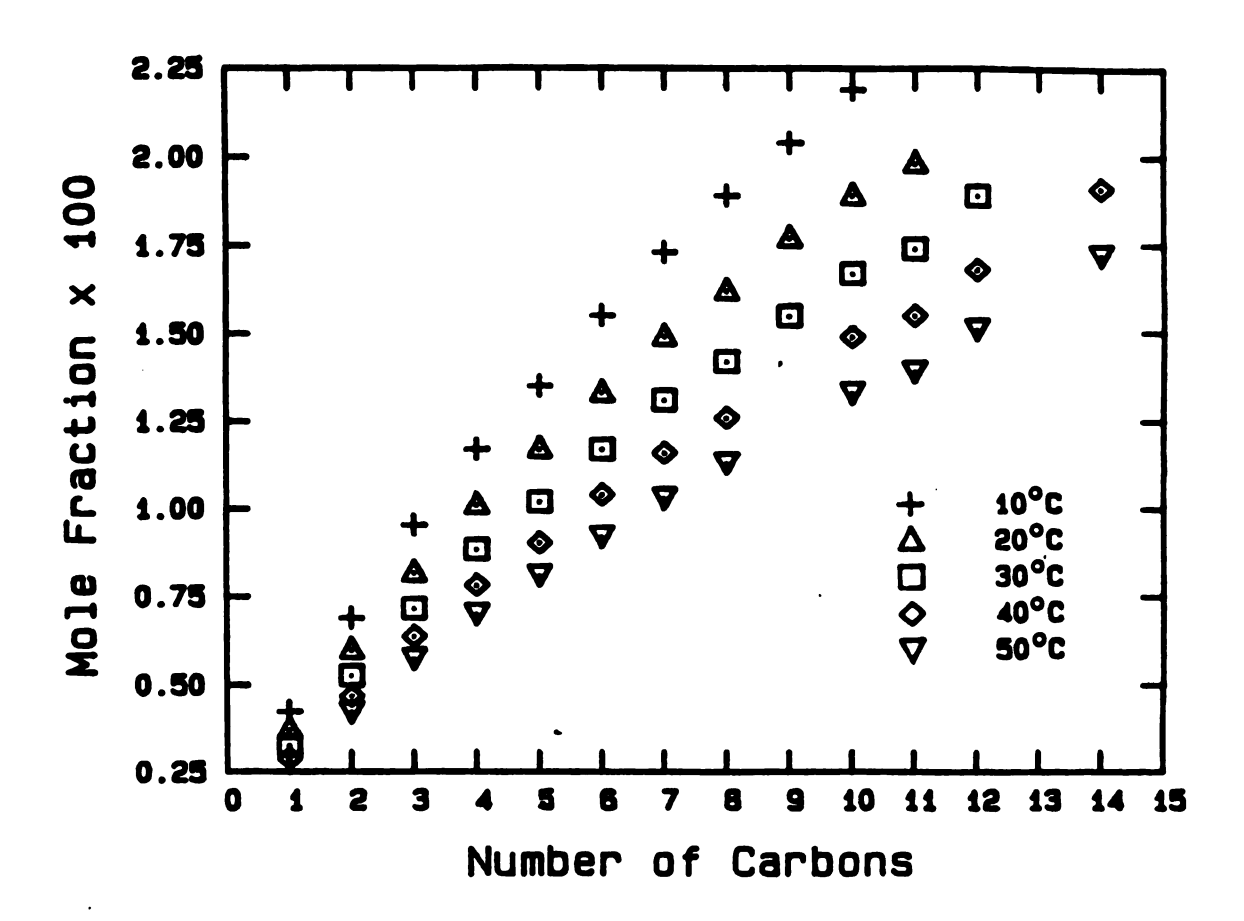


Figure 22.  $x_2$  vs. n for the n-alkanols at 5 temperatures.

Komarenko and Manzhelii<sup>74</sup> observed similar behavior for solutions of Kr in methanol, ethanol, n-propanol, and n-butanol at a variety of temperatures.

Table 6 also contains  $\Delta\mu_2^0$  and  $\Delta\mu_2^{0\rho}$  for the Xe/alkanol systems. Figures 23 and 24 show  $\Delta\mu_2^0$  and  $\Delta\mu_2^{0\rho}$ , respectively, as a function of T. Figures 25 and 26 show the same chemical potentials as a function of n.

As with the alkanes, least squares fits to the  $\Delta\mu$  versus T data yield straight lines with slope  $-\Delta S$  and intercept  $\Delta H$ . Entropies and enthalpies of solution are listed in Table 7 (Table 2 of reference 69), and are plotted versus n in Figures 27 and 28.

We see the same type of transitional behavior in the  $\Delta\mu$  versus n graphs as we saw in the solubility versus n graphs (Figures 21 and 22). It would be interesting to extend these measurements to higher temperatures and larger n to see if the Xe/alkanol systems become more like the Xe/alkane systems.

Entropy of solution for  $^{133}$ Xe in the alkanols is very close to that of Xe in the alkanes. The behavior of both  $\Delta S_2^0$  and  $\Delta S_2^{0p}$  as functions of n are the same as for the alkanes, and are about 10% larger in magnitude. We conclude that the Xe is either more constrained, or has less of a solvent disordering effect (or more of a solvent ordering effect), in the alkanols than in the alkanes.

We obtain from the data of Komarenko and Manzhelii,  $^{74}$  a value of  $\Delta S_2^{\circ} = -19.14$  cal/mol K for Xe in n-propanol at -55°C. Abraham<sup>75</sup> lists the entropy of solution for Ar, Kr, and Rn in methanol (-16.0, -17.4, and -22.4 cal/mol K) and Ar and Rn in ethanol (-15.1 and -18.1 cal/mol K) at 25°C. These compare favorably with our values for Xe in methanol and ethanol (-18.82 and -17.87 cal/mol K, respectively).

TABLE 6. Chemical potentials in the mole fraction scale,  $\Delta\mu_2^o$ , and in the number density scale,  $\Delta\mu_2^{o\,\rho}$ . The first row is  $\Delta\mu_2^o$  and the second row is  $\Delta\mu_2^{o\,\rho}$ . Units are cal/mol.

er of ons in kanol				·		
Δμ <sup>ο</sup> Δμ <sup>ο</sup> ρ	=	3076 ± 8 -507.4±8.4	3263 ± 9 -460.4±8.7	3452 ± 9 -411.5±9.0	3640 ± 9 -362.3±9.3	
		2800 -577.9	2983 -527.9	3163 -481.5	3341 -436.0	3515±10 -395.4±9.6
		2619 -621.3	2800 -567.7	2975 -521.3	3146 -478.9	3316 -437.4
		2501 -625.8	2677 -574.7	2849 -527.4	3019 -482.16	3187 -439.0
		2421 -613.3	2594 -561.3	2760 -516.5	2929 -469.7	3093 -427.2
		2343 -611.9	2515 -559.1	2680 -512.7	2844 -467.0	3011 -419.6
		2284 -601.6	2452 -594.4	2614 -503.3	2776 -457.5	2936 -413.5
		2234 -590.7	2401 -537.3	2563 -489.6	2721 -445.8	2877 -404.4
		2191 -577.5	2351 -530.5	2509 -484.5		
			2800 -577.9 2619 -621.3 2501 -625.8 2421 -613.3 2343 -611.9 2284 -601.6 2234 -590.7 2191	2800	2800	2800

TABLE 6 (cont'd.).

Temperature	10°C	20°C	30°C	40°C	50 <b>°</b> C
Number of carbons in n-alkanol					
10 Δμ <sup>ο</sup> = Δμ <sup>ο</sup> =	2151 -567.8	2311 -518.4	2464 -475.5	2618 -432.0	2773 -388.4
11		2286 <b>-</b> 496.2	2441 -449.8	2593 -406.3	2746 -363.8
12			2392 -453.5	2542 -410.8	2691 -369.6
14				2465 -404.0	2609 -364.8

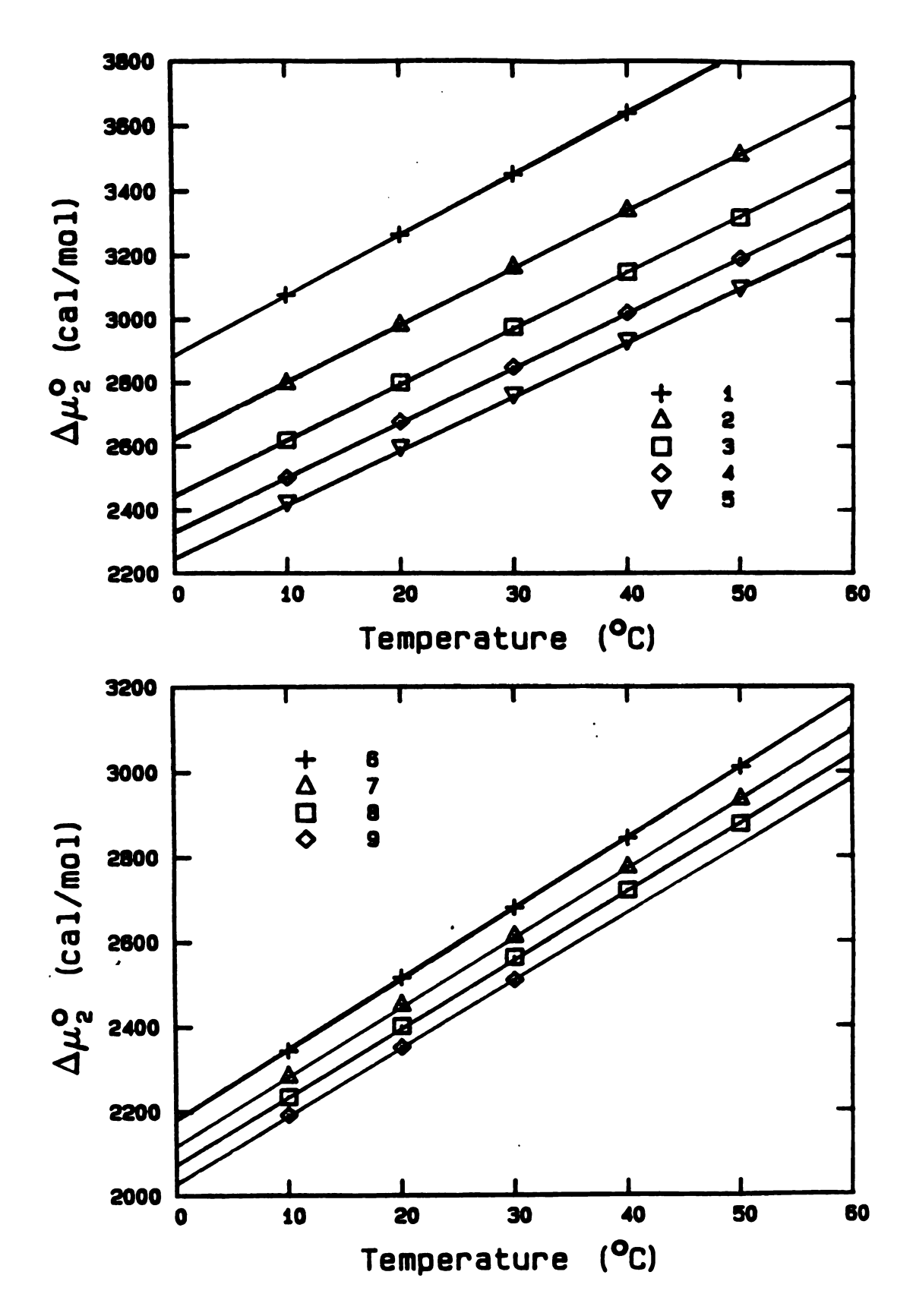


Figure 23.  $\Delta\mu_2^o$  vs. T for the n-alkanols. The numbers next to the symbols are the number of C atoms in the alkanol molecule.

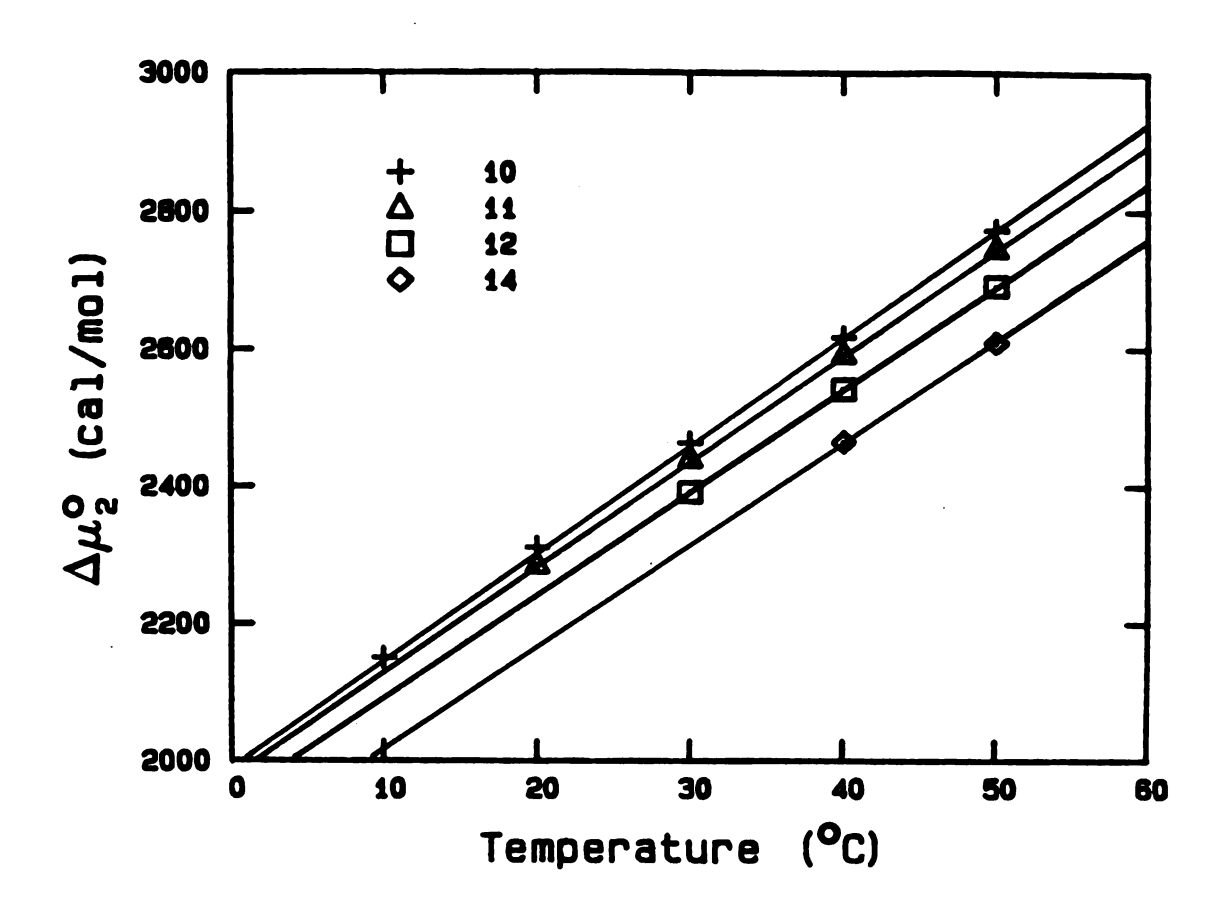


Figure 23. (cont'd.).

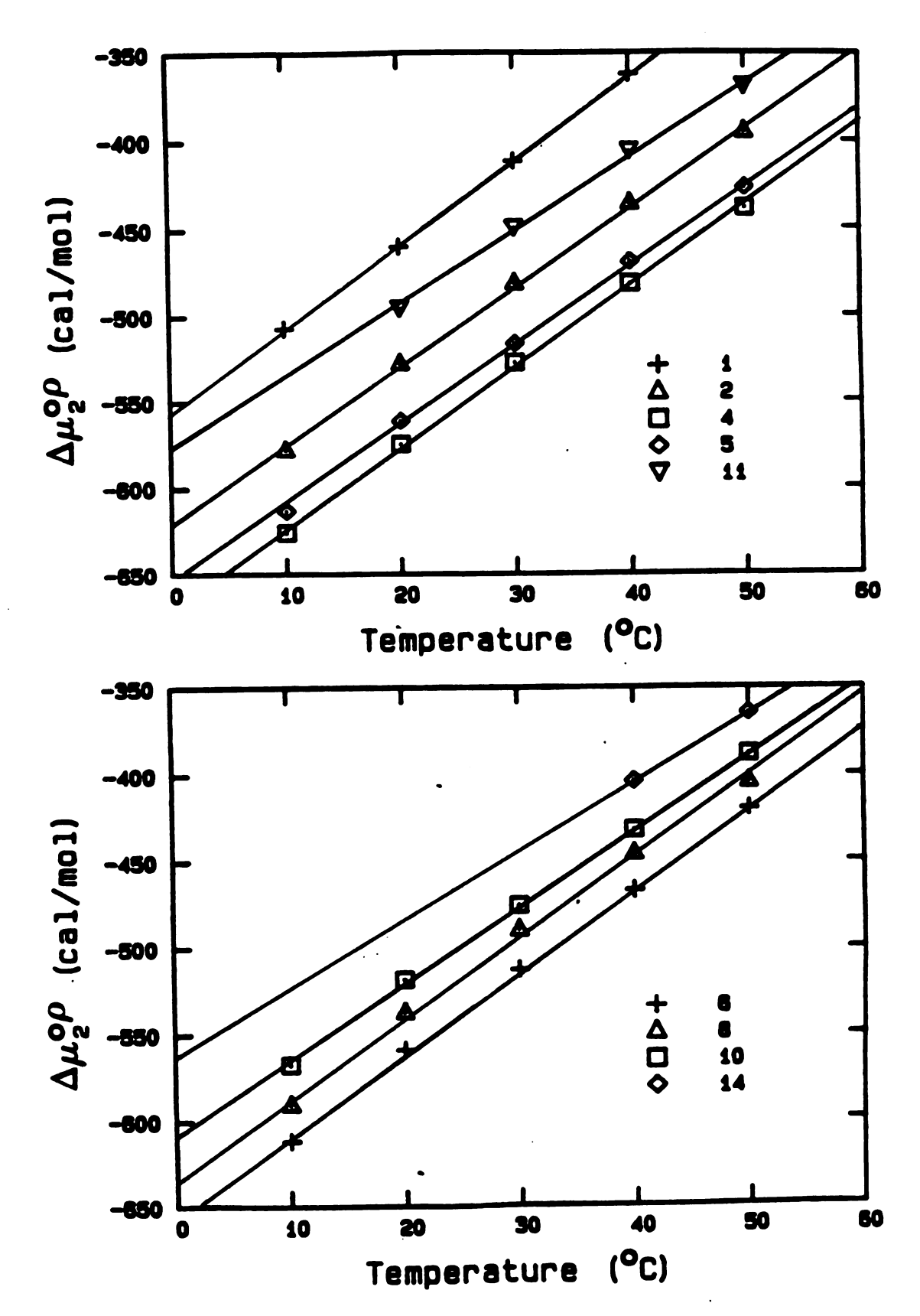


Figure 24.  $\Delta\mu_2^{\circ \rho}$  vs. T for the n-alkanols. The numbers next to the symbols are the number of C atoms in the alkanol molecule.

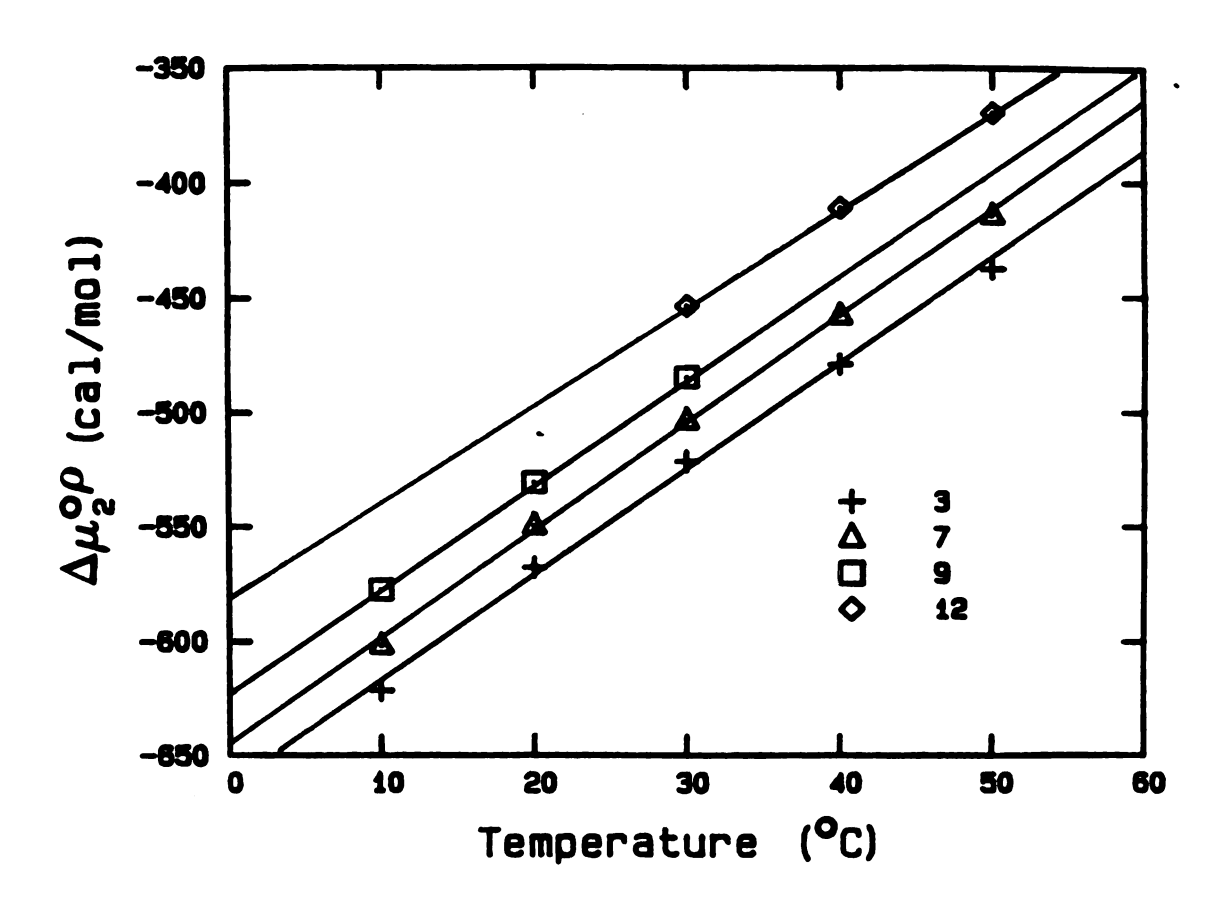


Figure 24. (cont'd.).

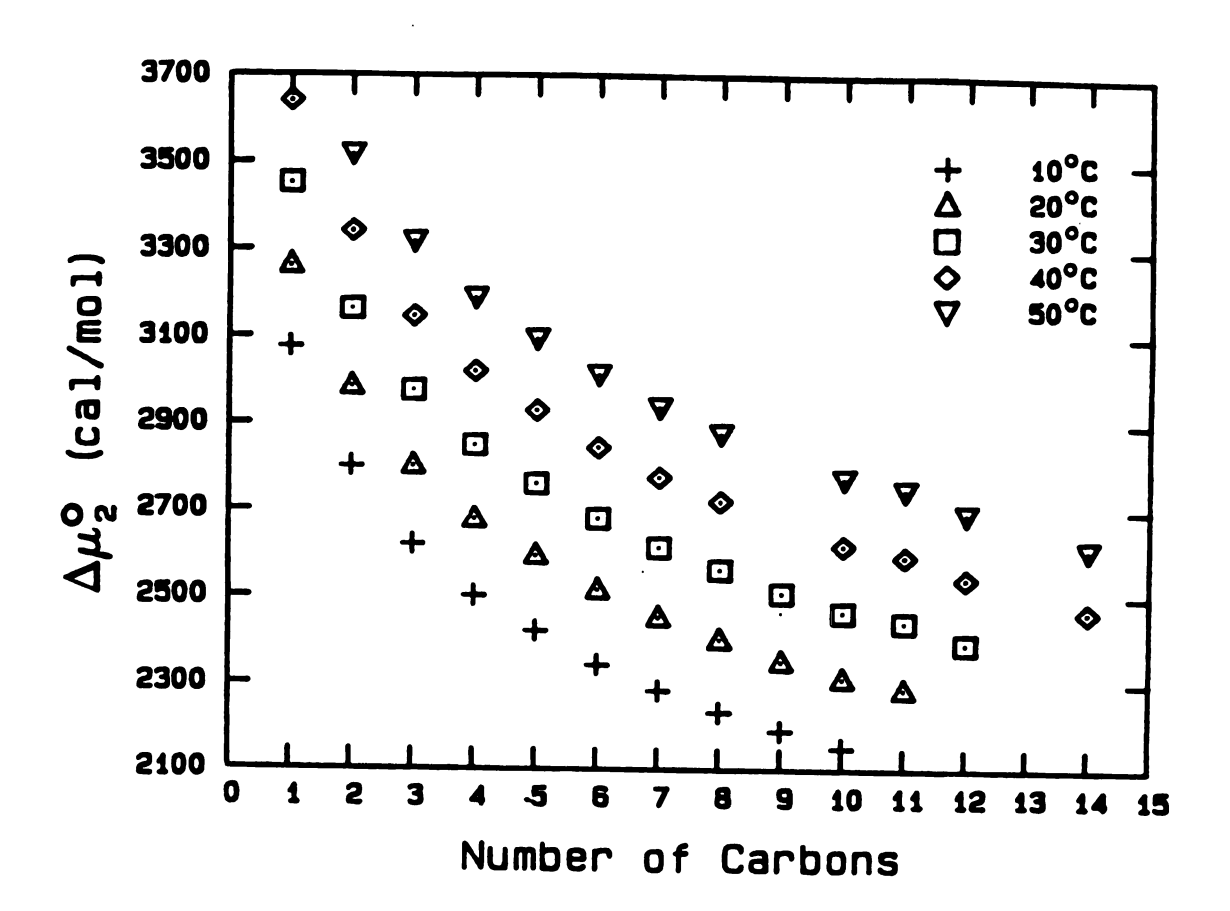


Figure 25.  $\Delta\mu_2^o$  vs. n for the n-alkanols at 5 temperatures.

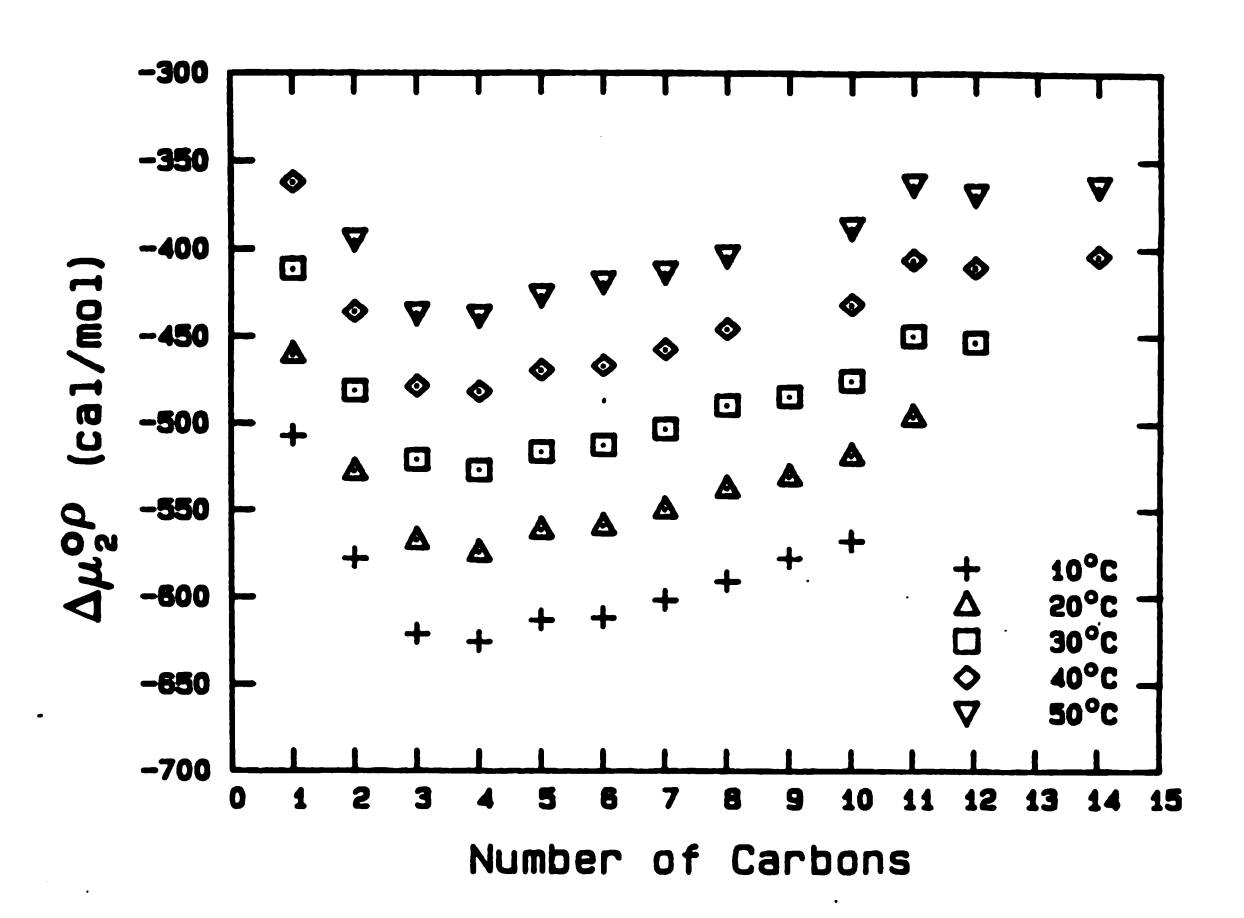


Figure 26.  $\Delta \mu_2^{op}$  vs. n for the n-alkanols at 5 temperatures.

TABLE 7. Entropy and enthalpy of solution in both the mole fraction scale and in the number density scale for solutions of  $^{133}$ Xe in the normal alkanols. (Table 2 of reference 69)

	Mole Fracti	on Scale	Number Densi	ty Scale	
Number of Carbons	Enthalpy of Solution AH <sub>2</sub> (cal/mol)	Entropy of Solution  AS <sup>o</sup> (cal/mol K)	Enthalpy of Solution  AH <sup>op</sup> (cal/mol)	Entropy of Solution AS (cal/mol K)	Temperature Range of Experiments
•	-2250 ± 120	-18.82 ± 0.40	-1880 ± 120	-4.84 ± 0.40	10 - 40°C
1	-2250 ± 120 -2257 ± 88	-17.87 ± 0.29	-1869 ± 88	-4.57 ± 0.29	10 - 50°C
2	-2300 ± 88	$-17.39 \pm 0.29$	-1910 ± 88	-4.57 ± 0.29	10 - 50°C
3 4	-2345 ± 88	-17.13 ± 0.29	-1943 ± 88	-4.66 ± 0.29	10 - 50°C
-	-2331 ± 88	-16.79 ± 0.29	-1943 ± 88	-4.64 ± 0.29	10 - 50°C
5 6	-2364 ± 88	-16.64 ± 0.29	-1959 ± 88	-4.77 ± 0.29	10 - 50°C
	-2317 ± 88	-16.26 ± 0.29	-1939 ± 88	-4.67 ± 0.29	10 - 50°C
7 8	-2304 ± 88	-16.05 ± 0.29	-1900 ± 88	-4.64 ± 0.29	10 - 50°C
9	-2310 ± 180	-15.90 ± 0.62	-1890 ± 180	-4.65 ± 0.62	10 - 30°C
10	-2234 ± 88	-15.50 ± 0.02	-1826 ± 88	-4.45 ± 0.29	10 - 50°C
11	-2210 ± 130	-15.35 ± 0.41	-1790 ± 130	-4.41 ± 0.41	20 - 50°C
		-14.96 ± 0.66	-1790 ± 130	-4.20 ± 0.66	30 - 50°C
12	-2140 ± 210				
14	-2040 ± 430	$-14.40 \pm 1.30$	-1630 ± 430	-3.90 ± 1.30	40 - 50°C

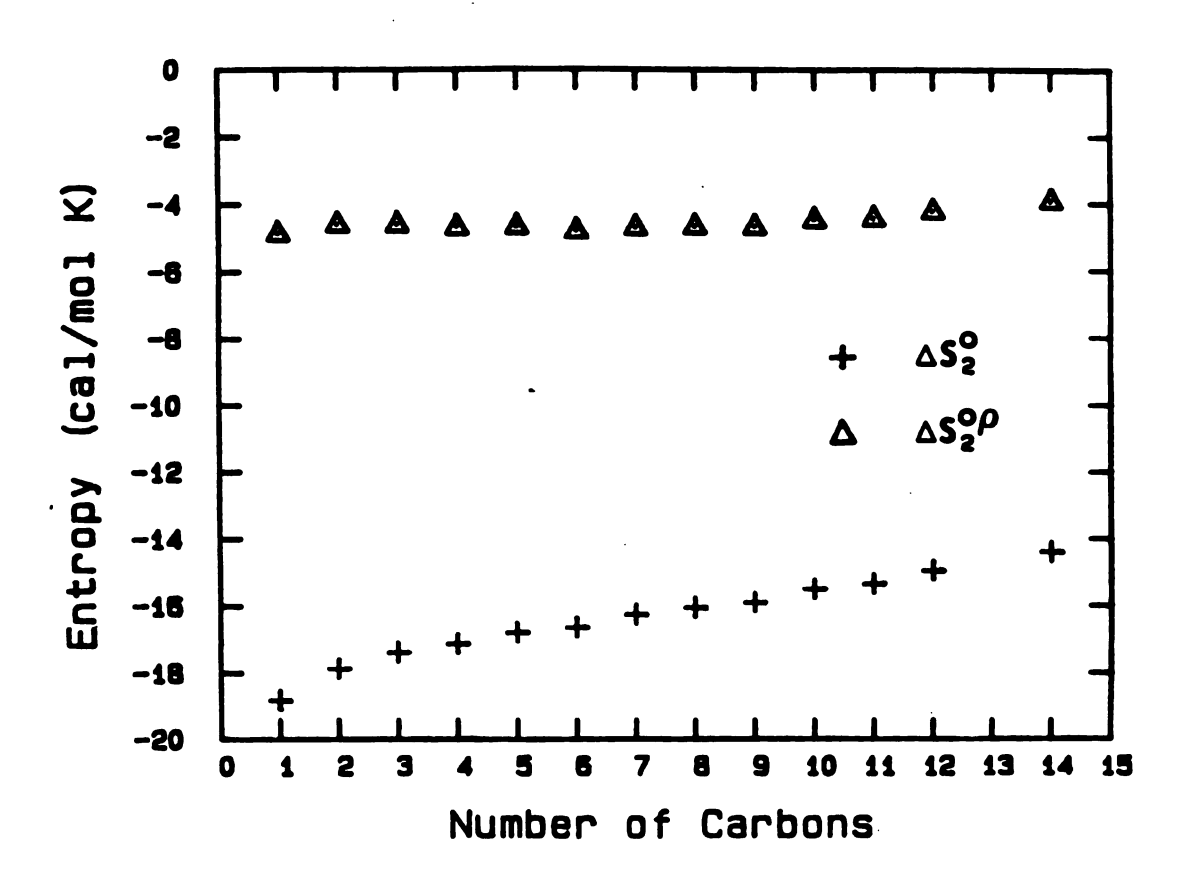


Figure 27. Entropy of solution for Xe in the n-alkanols.

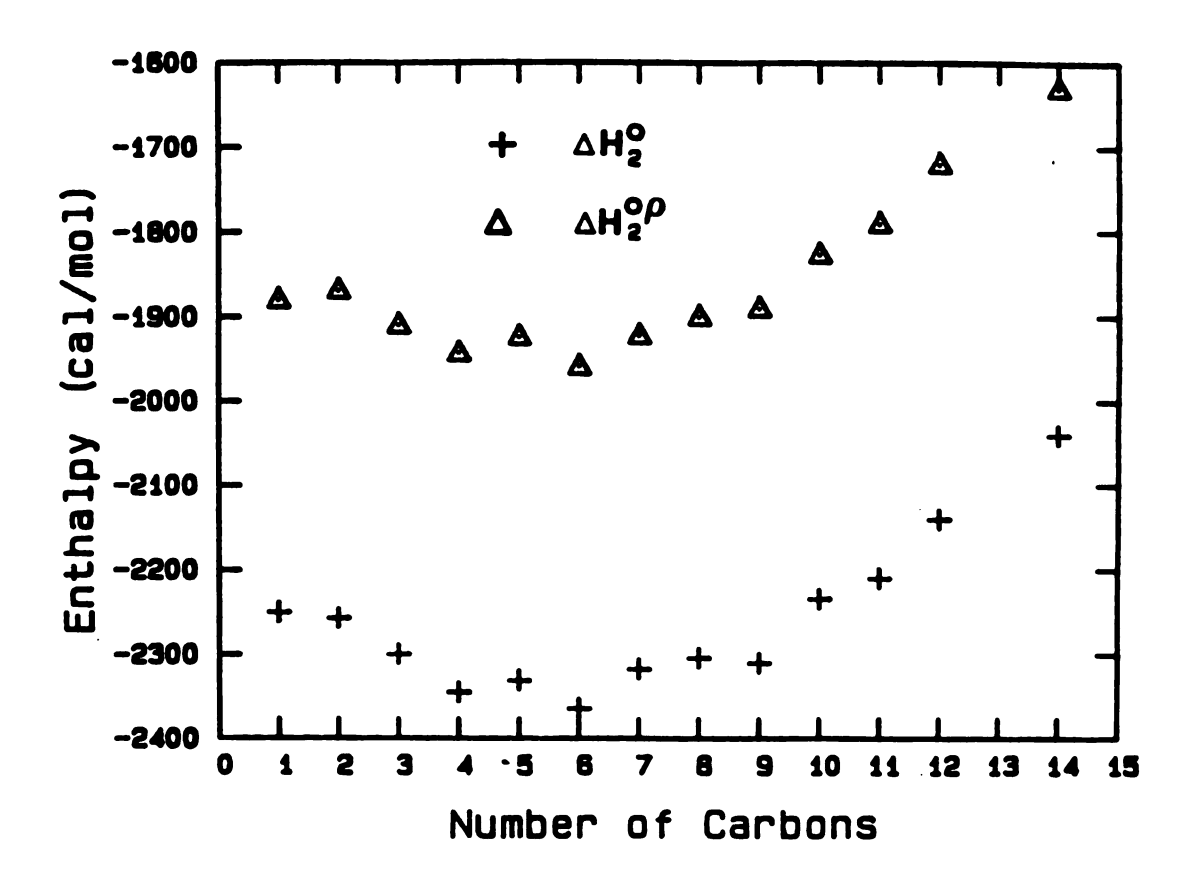


Figure 28. Enthalpy of solution for Xe in the n-alkanols.

The transitional behavior of the chemical potential as a function of n is thus due to the enthalpic contribution of the solvation process. This contribution is shown in figure 28. The initial decrease, followed by the increase, of enthalpy versus n contrasts with the Xe/alkane systems, where  $\Delta H$  is an increasing function of n.

Our value of  $\Delta H_2^{\circ}$  = -2250 cal/mol for Xe in methanol is intermediate in value to the data listed by Abraham<sup>75</sup> of -1170 and -3820 cal/mol for Kr and Rn in methanol, respectively. The data of Komarenko and Manzhelii<sup>74</sup> yield  $\Delta H_2^{\circ}$  = -2758 cal/mol for the system Xe/n-propanol at -55°C. Our value is -2300 cal/mol for the same system at 25°C.

The chemical potential in the mole fraction scale is dominated by the entropic contribution for the alkanols, just as for the alkanes. Here,  $T\Delta S_2^{\circ}$  is about twice  $\Delta H_2^{\circ}$ . The number density scale yields the opposite conclusion, namely that the solution process is enthalpically dominated.

Figure 29 is a plot of the three quantities in equation (64) for the alkanols methanol through n-dodecanol. The binding energy  $E_b$  was calculated from  $\Delta H_2^0$  and  $4\pi r_2^2 \gamma_1 N_A$  through rearrangement of equation (64). The average binding energy of the Xe/alkanol systems is about 3% higher than that of the Xe/alkane systems, and is due to the greater surface energy contribution. Table 8 lists both our experimental  $E_b$ , and  $E_b$  estimated from heat of vaporization data, for the normal alkanols. As with the alkanes, estimated values agree to within 20% of the experimental values. Here, too, the estimated values increase with n at a greater rate than the experimental values.

 ${\tt Abraham}^{75}$  has compiled values of the standard free energy, enthalpy, and entropy of solution for many gaseous nonpolar

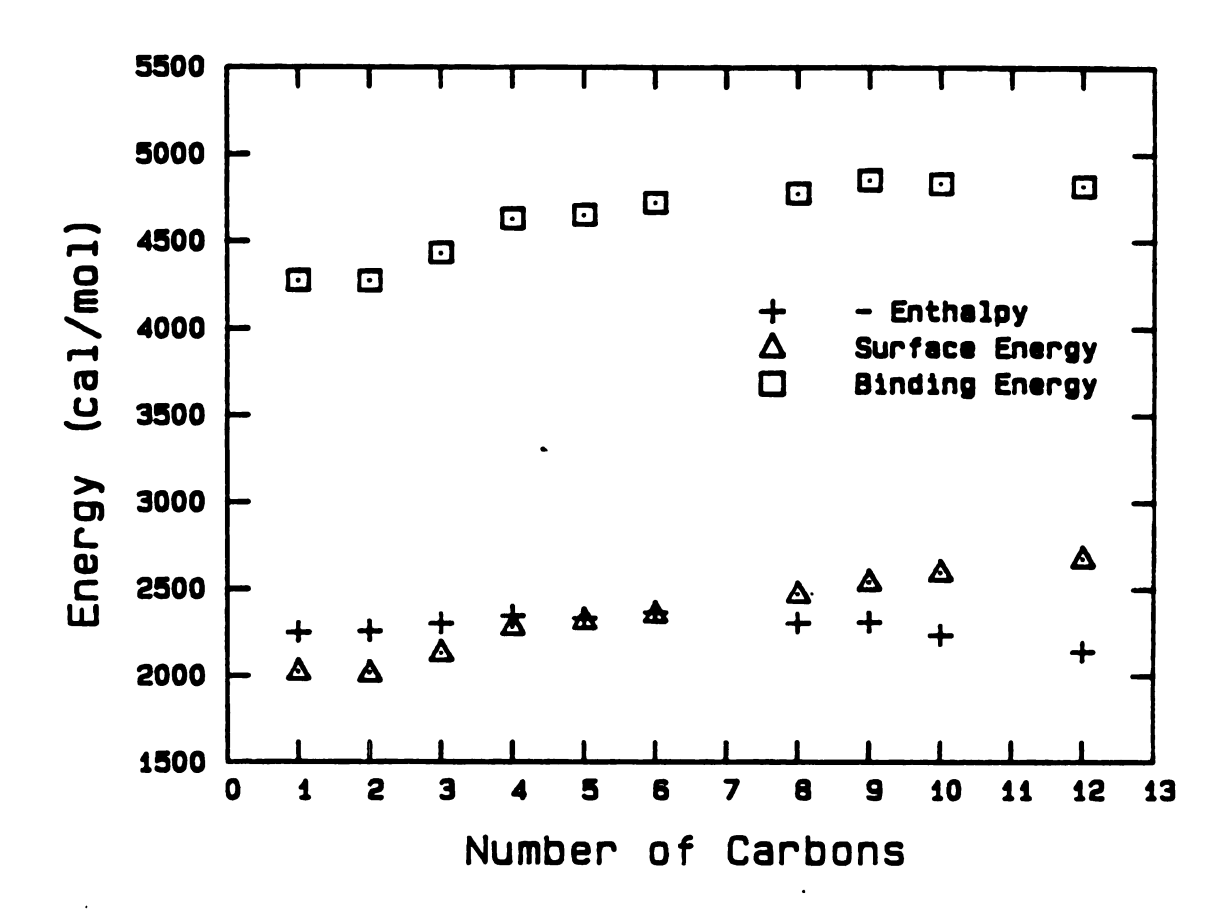


Figure 29. Binding energy, surface energy, and enthalpy of solution for the n-alkanols. (Figure 4 of reference 69).

TABLE 8. Comparison of experimental binding energies,  $E_b^{\text{exp}}$ , of Xe in the normal alkanols with binding energies estimated from the heats of vaporization of the solute and solvent,  $E_b^{\text{ext}}$ .

Number of	E <sup>exp</sup>	$\mathtt{E}^{ exttt{est}}_{ exttt{b}}$
Carbons	(cal/mol)	(cal/mol)
_	hogh	hro0
1	4274	4708 4990
2	4271 4432	5182
3 4	4432 4628	5266
5	4650	5358
6	4721	5579
7	,,,,,	5562
8	4777	5489
9	4853	5914
10	4831	5658

nonelectrolytes in a variety of nonaqueous solvents and in water. He found that the data could be correlated using an equation of the form:

$$\Delta P_2^0 = \Omega R + d \tag{86}$$

where P stands for the free energy G, enthalpy H, or entropy S. R is a parameter, close to the solute's radius in A, characteristic of the solute gas, and L and d characterize the solvent.

Table 9 lists the values of  $\Delta G_2^{\circ}$ ,  $\Delta H_2^{\circ}$ , and  $\Delta S_2^{\circ}$  at 25°C, calculated from Abraham's parameters for the solvents shown, using a value of 2.16 for R for Xe. The agreement with our experimental values is good. Calculated free energies of solution are about 10% too high for all solvents. The calculated enthalpies of solution are all within 10% of experiment, except for 1-decanol, which is 40% too small in magnitude. The agreement between calculated and experimental entropies is excellent, within 5% for both the alkanes and alkanols.

We can calculate the thermodynamics of solution from Pierotti's model. 33 From equation (33) above:

$$\ln(K_{H}) = \frac{\bar{G}_{c}}{RT} + \frac{\bar{G}_{i}}{RT} + \ln(\frac{RT}{V_{i}^{o}}),$$
 (87)

where

TABLE 9. Comparison of calculated and experimental thermodynamics of solution.

		calculated			Experime	ental
	ΔG° <sub>2</sub>	ΔH <b>°</b>	ΔS.°	ΔG° <sub>2</sub>	ΔH <b>°</b>	ΔS.º
Solvent	$(\frac{\text{cal}}{\text{mol}})$	$(\frac{\text{cal}}{\text{mol}})$	$(\frac{\text{cal}}{\text{mol } K})$	$(\frac{\text{cal}}{\text{mol}})$	$(\frac{\text{cal}}{\text{mol}})$	$(\frac{\text{cal}}{\text{mol } K})$
hexadecane decane hexane	2200 2210 2230	-2210 -2140 -2330	-14.7 -14.5 -13.7	1994 2100 2183	-2180 -2351 -2691	-14.00 -14.93 -16.37
1-decanol 1-octanol 1-butanol 1-propanol ethanol methanol	2710 2720 2930 3070 3220 3500	-1580 -2090 -2540 -2170 -2180 -2120	-15.5 -16.8 -17.9 -17.7 -18.1 -18.8	2398 2482 2763 2883 3073 3358	-2234 -2304 -2345 -2300 -2257 -2250	-15.50 -16.05 -17.13 -17.39 -17.87 -18.82

$$\frac{\bar{G}_{c}}{RT} = 6(\frac{y}{1-y})[2(\frac{r_{12}}{r_{1}})^{2} - (\frac{r_{12}}{r_{1}})]$$

+ 
$$18\left(\frac{y}{1-y}\right)^2\left[\left(\frac{r_{12}}{r_1}\right)^2 - \left(\frac{r_{12}}{r_1}\right) + \frac{1}{4}\right] - \ln(1-y)$$
 (88)

and

$$\frac{\bar{G}_{i}}{RT} = -3.555\pi\rho(\frac{\varepsilon_{12}}{kT})r_{12}^{3} . \tag{89}$$

If we compare equations (25) and (87), we see that

$$- lnL = \frac{\bar{G}_{c}}{RT} + \frac{\bar{G}_{i}}{RT} . \qquad (90)$$

We have for the free energy of solution in the mole fraction scale

$$\Delta \mu_2^{\circ} = -RT \ln \left[ \left( \frac{RT}{LV_1^{\circ}P_2} + 1 \right)^{-1} \right]$$
 (91)

The entropy of solution is given by equation (59),

$$\Delta S_2^{\circ} = -\frac{\partial}{\partial T} (\Delta \mu_2^{\circ})_{P,n} . \tag{59}$$

It is easy to show, assuming that  $r_1$ ,  $r_{12}$ , and  $\epsilon_{12}$  are independent of temperature, that

$$\Delta S_{2}^{o} = R \ln x_{2} + RT(x_{2}^{-1}) \left\{ \frac{1}{T} - \alpha_{p} - (\alpha_{p} + \frac{1}{T}) \frac{G_{1}}{RT} - \frac{\alpha_{p}}{1 - y} (\frac{G_{c}}{RT} + \ln(1 - y) - y + 18(\frac{y}{1 - y})^{2} [(\frac{r_{12}}{r_{1}})^{2} - (\frac{r_{12}}{r_{1}}) + \frac{1}{4}]) \right\}, \quad (92)$$

where  $\alpha_{\!{}_{\!{}^{\textstyle D}}}$  is the thermal expansivity of the solvent, and

$$\Delta H_2^0 = -RT \ln x_2 + T \Delta S_2^0 . \tag{93}$$

Using the Lennard-Jones parameters of Wilhelm and Battino,  $^{35}$  and equations (92) and (93), we can calculate the entropy and enthalpy of solution for some of the alkanes and alkanols. These calculated values are listed in Table 10, along with our experimental values for the same solvents. The agreement with experimental values is very good ( $\pm 10\%$ ), except for  $\Delta H_2^0$  for tetradecane ( $\pm 25\%$ ). Agreement is not as good for the two alkanols. Calculated entropies and enthalpies differ from experimental results by 20% and 50%, respectively.

The deviation of the theoretical values from the experimental results occur in the regions we might expect. For the alkanes, the largest deviations occur for the longer molecules. The free energy of cavity formation,  $\bar{G}_{c}$ , is calculated assuming the solvent molecules are hard spheres. Since the normal alkanes are decidedly non-spherical, such deviations are to be expected.

Methanol and ethanol also show large differences between calculated and experimental values. We believe the source of these

TABLE 10. Comparison of calculated and experimental values for the enthalpy and entropy of solution for mixtures of Xe in some of the alkanes and alkanols. Values were calculated using Pierotti's model, and the Lennard-Jones parameters of Wilhelm and Battino.

	Calculated	Values	Experimental	l Values
Solvent	Enthalpy of Solution AH (cal/mol)	Entropy of Solution $\Delta S_2^{\circ}$ (cal/mol K)	Enthalpy of Solution  AH <sup>o</sup> (cal/mol)	Entropy of Solution AS (cal/mol K)
Hexane	-2517	-16.57	-2691	-16.37
Heptane	-2495	-16.38	-2415	-15.36
Octane	-2432	-16.22	-2429	-15.34
Nonane	-2337	-15.97	-2378	-15.09
Decane	-1964	-15.60	-2351	-14.93
Dodecane	-2056	-15.61	-2278	-14.56
Tetradecane	-1738	-14.90	-2239	-14.30
Methanol	-3195	-22.76	<del>-</del> 2250	-18.82
Ethanol	-3158	-21.60	-2257	-17.87

differences is also the free energy of cavity formation term. The difficulty in this instance, however, is probably the strong dipole/dipole interactions of the alkanols. Because of these interactions, they are not "hard" spheres.

There are several possible directions in which this work might be extended. First, further studies should be done on Xe solubility in the normal alkanes and alkanols at higher temperatures, and with longer molecules. The goal here would be to see if the thermodynamics of the Xe/alkanol systems becomes more alkane-like for large n. It might also be interesting to study the solubility of Xe in solvents consisting of a normal alkane "doped" with one of the alkanols.

A second course of research would be to extend these studies to the solubility of Xe in other homologous series of nonpolar solvents, specifically the halogenated normal alkanes such as the perfluoroalkanes and perchloroalkanes. These liquids have stronger intermolecular interactions than the alkanes, as evidenced by increased melting and boiling points. However, these higher boiling points would permit solubility measurements to be made with the shorter, more spherical molecules.

A third direction for further research is to modify the hard sphere theory. Modifications would include the addition of an attractive potential to the hard sphere equation of state, similar to that of Longuet-Higgins and Widom. <sup>38</sup> This would take account of strong interactions between solvent molecules. A second possible modification of the theory might take into account the non-spherical shape of a solvent molecule.

## 4.3 AQUEOUS AMINO ACID SOLUTIONS

We measured the Ostwald solubility of  $^{133}$ Xe in aqueous solutions of NaCl, sucrose, and 20 amino acids at 25°C. Some of these results have recently been published.  $^{70}$  Values of L obtained are listed in Table 11. Also included in this table are the solution molarity (M), the solution pH, the total volume fraction of the solution that is water  $(v_{tw})$ , and the hydration number H as calculated from equation (66). Our values for the mean hydration number for each amino acid are listed in the column at the left of Table 12.

Our method for calculating  $v_{tw}$  has been described in section 1.7 above. The values of  $v_{tw}$  can also be calculated from the solution molarity M, and the partial molar volume  $v_{pm}$  of the amino acids, via the equation:

$$v_{tw} = 1 - Mv_{pm}/1000$$
 (87)

Using equation (87), and partial molar volumes of the amino acids at 25°C given by Lilley, <sup>76</sup> we can calculate the volume fraction water. Agreement with values obtained using our method is good.

For several of the amino acids, we were not able to obtain good values for the hydration numbers. These include isoleucine, leucine, phenylalanine, tyrosine, and tryptophan. The ILE data seem to fall into two different groups, with mean values of 13.3 and 5.8. We were unable to obtain a consistent value for this amino acid, since its solubility in water is too low.

TABLE 11. List of solubilities measured for Xe in aqueous solutions of the amino acids, sucrose, and NaCl. Also included are the solution molarities (M), the solution pH, the volume fraction water, and the hydration number calculated for each experiment.

Amino Acid	Ostwald Solubility L	Solution Molarity M	Solution pH	Volume Fraction Water <sup>V</sup> tw	Hydration Number H
Alanine	0.094	0.450	6.2	0.973	10.60
(Ala)	0.090	0.661	6.55	0.973	9.21
	0.088	0.873	6.35	0.946	7.34
m.w. 89.09	0.088	0.900	6.1	0.944	7.00
	0.076	1.350	6.27	0.917	8.20
	0.079	1.500	6.00	0.908	6.00
	0.070	1.800	7.03	0.889	7.03
Arginine	0.100	0.438	10.6	0.945	0.20
(Arg)	0.100	0.439	11.3	0.945	0.20
	0.093	0.919	10.8	0.884	0.40
m.w. 174.20	0.094	0.920	11.4	0.884	-0.17
	0.103	0.300	10.6	0.963	-1.60
	0.095	0.600	11.1	0.925	2.65
	0.098	0.760	11.0	0.905	-1.42
	0.094	0.760	11.0	0.905	1.33
Glycine	0.082	1.043	6.35	0.953	9.52
(Gly)	0.092	0.500	6.50	0.978	12.18
	0.085	1.066	6.0	0.953	7.85
m.w. 75.07	0.084	1.071	6.46	0.952	8.24
	0.075	1.500	6.2	0.934	8.36
	0.065	2.130	6.46	0.903	7.53
	0.068	2.131	5.8	0.904	6.82
	0.064	2.132	6.44	0.903	7.77

TABLE 11 (cont'd.).

Amino Acid	Ostwald Solubility L	Solution Molarity M	Solution pH	Volume Fraction Water <sup>V</sup> tw	Hydratior Number H
		10			
Hydroxyproline	0.094	0.548	6.0	0.953	6.69
(Hyp)	0.097	0.549	5.9	0.953	3.82
m 121 12	0.083	1.156	5.96	0.901	5.65
m.w. 131.13	0.086 0.078	1.160 1.589	5.8 5.9	0.901 0.864	4.28 4.46
	0.078	2.173	5.7	0.813	3.89
	0.069	2.173	5.6	0.790	3.35
	0.068	2.349	6.0	0.797	3.66
Lysine	0.094	0.510	9.9	0.945	6.32
(Lys)	0.088	0.511	9.5	0.946	12.54
	0.079	1.07	9.7	0.885	7.23
m.w. 146.19	0.082	1.094	10.0	0.880	5.38
	0.053	2.19	9.9	0.763	6.65
	0.064	2.19	10.3	0.756	3.84
	0.056	2.775	10.5	0.687	3.17
	0.054	2.800	10.3	0.687	3.51
Sucrose	0.097	0.250		0.948	7.28
	0.090	0.498		0.893	4.88
m.w. 342.3	0.085	0.750		0.841	2.89
	0.075	0.998		0.788	4.46
	0.062	1.500		0.679	3.47
	0.052	2.000		0.570	2.20
	0.046	2.250		0.516	2.02

TABLE 11 (cont'd.).

Amino Acid	Ostwald Solubility L	Solution Molarity M	Solution pH	Volume Fraction Water <sup>V</sup> tw	Hydration Number H
Proline	0.101	0.300	6.25	0.976	4.27
(Pro)	0.100	0.600	6.29	0.950	0.61
	0.098	0.600	6.26	0.950	2.35
m.w. 115.13	0.092	0.779	6.50	0.935	4.77
	0.096	0.900	6.19	0.925	1.19
	0.093	0.900	6.12	0.926	2.99
	0.091	1.199	6.18	0.901	1.96
	0.090	1.200	6.23	0.900	1.76
	0.086	1.600	6.24	0.867	1.93
	0.088	1.600	6.18	0.867	1.27
	0.078	2.098	6.25	0.825	2.35
	0.082	2.098	6.11	0.825	1.36
	0.073	2.884	6.26	0.758	1.33
	0.071	2.884	6.08	0.758	1.69
	0.069	3.151	6.15	0.737	1.51
	0.065	3.422	6.88	0.711	1.58
	0.063	3.518		0.703	1.71
	0.065	3.518	6.24	0.705	1.44
Serine	0.094	0.383	5.9	0 <b>.</b> 977	13.04
(Ser)	0.101	0.171	6.0	0.990	12.03
•	0.099	0.277	6.13	0.983	9.80
m.w. 105.09	0.095	0.383	6.1	0.977	11.67
	0.101	0.171	6.3	0.990	12.03
	0.104	0.085	6.1	0.995	9.03

TABLE 11 (cont'd.).

Amino Acid	Ostwald Solubility L	Solution Molarity M	Solution pH	Volume Fraction Water <sup>V</sup> tw	Hydratior Number H
Threonine	0.070	• h h h		0.007	9.60
(Thr)	0.070 0.090	1.444 0.680	6.0 6.1	0.887 0.947	8.69 7.97
(IIII)	0.090	0.680	6.1	0.947	7.97
m.w. 119.12	0.101	0.300		0.977	4.46
	0.084	1.060	5.9	0.918	6.56
	0.095	0.490	5.9	0.962	7.43
	0.081	1.250	6.15	0.903	6.15
	0.083	0.870	5.2	0.933	9.54
	0.098	0.300	5.6	0.977	9.68
	0.072	1.444	5.3	0.887	7.96
	0.105	0.150	6.5	0.988	
Cysteine	0.097	0.509	5.75	0.962	5.10
(Cys)	0.080	1.158	4.93	0.913	7.57
	0.097	0.509	6.0	0.963	5.21
m.w. 121.16	0.081	1.158	5.8	0.914	7.16
	0.091	0.680	5.2	0.949	7.37
	0.098	0.350	4.8	0.974	7.82
	0.086	1.000	5.5	0.925	6.29
	0.088	0.840	5.7	0.938	7.10
•	0.102	0.180	5.2	0.9870	7.61

TABLE 11 (cont'd.).

Amino Acid	Ostwald Solubility L	Solution Molarity M	Solution pH	Volume Fraction Water <sup>V</sup> tw	Hydration Number H
Valine	0.098	0.343	6.23	0.968	7.01
(Val)	0.097	0.344	6.45	0.969	8.67
m.w. 117.15	0.103 0.102	0.153 0.158	6.34 6.47	0.986	5.17
m.w.	0.102	0.156	6.0	0.985 0.969	7.96 5.64
	0.102	0.344	6.1	0.986	8.48
	0.102	0.155	6.1	0.978	7.66
	0.100	0.250	6.6	0.976	10.9
	0.1036	0.080	6.9	0.9932	10.9
Histidine	0.100	0.259	7.91	0.974	6.54
(His)	0.103	0.126	7.80	0.987	6.72
	0.100	0.259	7.25	0.974	6.54
m.w. 155.16	0.102	0.126	7.25	0.988	11.30
	0.101	0.192	7.32	0.981	8.12
	0.1025	0.126	7.88	0.9878	9.14
	0.103	0.060	7.15	0.994	20.57
	0.1034	0.0601	7.75	0.9947	17.68
Isoleucine	0.100	0.192	6.41	0.979	10.26
(Ile)	0.102	0.0943	6.78	0.990	16.28
•	0.099	0.192	6.2	0.980	13.27
m.w. 131.18	0.105	0.0470	6.3	0.9954	5.69
<b>.</b>	0.104	0.0939	6.2	0.9905	5.5
	0.1027	0.1430	6.6	0.9846	6.09
	0.1014	0.1921	6.73	0.9802	6.80
	0.1031	0.1430	6.69	0.9853	4.92

TABLE 11 (cont'd.).

Amino Acid	Ostwald Solubility L	Solution Molarity M	Solution pH	Volume Fraction Water <sup>V</sup> tw	Hydration Number H
Glutamine	0.098	0.219	5.0	0.979	13.77
(Gln)	0.102	0.100	5.30	0.990	16.35
4116 4	0.100	0.160	4.8	0.985	14.39
m.w. 146.15	0.0989	0.219	5.0	0.9801	11.90
	0.1041	0.0501	6.68	0.9960	15.36
	0.1033	0.0999	5.7	0.9910	9.14
	0.095	0.219	4.6	0.980	21.17
	0.100	0.100	4.7	0.991	26.35
	0.102	0.050	5.4	0.996	31.12
Methionine	0.101	0.215	5.8	0.977	6.22
(Met)	0.103	0.103	5.9	0.989	9.30
	0.101	0.160	5.6	0.984	10.78
m.w. 149.21	0.1000	0.215	6.17	0.9772	8.70
	0.1038	0.1029	6.35	0.9895	5.54
	0.100	0.103	5 <b>.7</b>	0.989	24.50
	0.103	0.050	5.9	0.995	25.79
	0.098	0.215	5.7	0.977	13.51
	0.1036	0.0501	6.78	0.9955	20.00
Asparagine	0.098	0.186	5.5	0.983	17.40
(Asn)	0.103	0.0758	5.6	0.9934	15.85
(	0.103	0.0759	5.5	0.9931	15.61
m.w. 150.14	0.101	0.131	6.1	0.988	14.86
	0.100	0.186	7.0	0.983	11.78
	0.104	0.0381	7.1	0.9970	23.05

TABLE 11 (cont'd.).

Amino Acid	Ostwald Solubility L	Solution Molarity M	Solution pH	Volume Fraction Water V	Hydration Number H
Leucine	0.103	0.154	6.40	0.983	4.06
(Leu)	0.1009	0.1540	6.9	0.9843	11.65
	0.1040	0.1150	6.7	0.9881	3.35
m.w. 131.18	0.1057	0.0369	6.95	0.9965	-1.00
	0.1024	0.0750	6.8	0.9922	19.3
	0.107	0.0751	6.67	0.992	-12.85
	0.0989	0.0750	6.7	0.9920	43.5
Phenylalanine	0.101	0.145	5.90	0.982	11.13
(Phe)	0.103	0.0686	6.51	0.991	15.57
	0.1029	0.1450	6.4	0.9818	4.22
m.w. 165.19	0.1051	0.0351	6.85	0.9963	7.55
	0.1052	0.0690	6.4	0.9913	-0.92
	0.1031	0.1070	6.4	0.9870	7.43
Sodium Chloride	0.088	0.500		0.991	17.80
(NaCl)	0.082	0.750		0.987	15.75
	0.075	1.000		0.981	15.13
m.w. 58.44	0.055	2.001		0.961	12.23
-	0.039	3.001		0.940	10.55
	0.023	4.000		0.917	9.69
	0.018	5.251		0.888	7.57
	0.098	0.250		0.996	15.72
	0.063	1.500		0.972	13.93
	0.090	0.500		0.991	15.71

TABLE 12. Hydration numbers of the amino acids.

Amino Acid	This Work	Reference (77)	Reference (78)	
		(11)	(70)	(79)
ALA	7.9 ± 0.6	3.3 ± 0.3	3.5 ± 0.2	3.35
ARG	$0.2 \pm 0.5$		4.1 ± 0.5	
ASN	$15.1 \pm 0.9$	$6.1 \pm 0.3$	~~~~~	
CYS	$6.8 \pm 0.3$		$4.3 \pm 0.2$	
GLN	$13.3 \pm 1.0$	$13.3 \pm 0.4$		
GLY	$8.5 \pm 0.6$	$8.2 \pm 0.3$	$3.4 \pm 0.3$	3.40
HIS	$7.4 \pm 0.5$	$35.6 \pm 2.8$	$4.6 \pm 0.8$	4.62
HYP	$4.5 \pm 0.4$	$16.2 \pm 0.8$		
ILE		$24.0 \pm 0.4$		
LEU		$8.3 \pm 0.4$	$4.3 \pm 0.2$	4.53
LYS	$6.1 \pm 1.1$	$20.1 \pm 0.5$		
MET	$8.1 \pm 1.0$	$21.1 \pm 0.8$	$4.5 \pm 0.5$	4.53
PHE			$4.6 \pm 0.2$	4.48
PRO	$2.0 \pm 0.2$	$29.9 \pm 1.6$	$3.3 \pm 0.3$	3.26
SER	$11.3 \pm 0.6$	$4.2 \pm 0.3$		4.04
THR	$7.6 \pm 0.5$			4.06
VAL	$8.0 \pm 0.7$	$4.9 \pm 0.4$	$3.8 \pm 0.2$	4.22
SUCROSE	3.9 ± 0.7	25.8 <sup>a</sup>		3.42
	_	-3	b	J + . =
NaCl	$16.2 \pm 0.5$		20.2 <sup>b</sup>	

a Reference (81); b Reference (59)

The difficulty with calculating a hydration number for these five amino acids stems from their low solubility in water. Consider equation (66):

$$H = \frac{55.3460}{M} \left[ v_{tw} - \frac{L(M)}{0.1060} \right] . \tag{66}$$

Since the experiments with LEU, PHE, TRP, and TYR all involved dilute solutions, with M  $\leq$  0.154, and the coefficient which multiplies the square bracket is large. For M << 1, both terms in the square brackets in equation (66) are within a few percent of unity. Thus, a 1% change in either  $v_{tw}$  or L(M) results in a large change in H. The uncertainty in our values of L(M) are of the order of 1%. This uncertainty is probably the source of the large variation in calculated H values for these five amino acids.

We must also mention a possible problem with the H values calculated for cysteine. In each of the runs, we observed a white precipitate forming during the course of the experiment. The precipitate is probably cystine, which forms from aqueous cysteine solutions in the presence of air. We estimate the mass of the precipitate to be about 0.56 g, which is the amount of cysteine which can form in the presence of 130 cm<sup>3</sup> of air  $(V_g^{(1)} = 70 \text{ cm}^3, V_g^{(2)} = 55 \text{ cm}^3, \text{ and the effective volume of } V_g = 5 \text{ cm}^3)$ . Cystine is very insoluble in water; a liter of water will dissolve only 0.112 g of cystine at 25°C. Thus, nearly all the cystine formed precipitates out of solution. We did not correct the measured solubilities for cysteine for changes in volume, molarity, or in  $v_{tw}$ , which occurred as a result of this effect.

The solubility data can be presented in several ways. Figure 30 is a plot of L versus M. Figure 31 is a plot of L versus  $v_{tw}$ . In both graphs, the data for each amino acid can be approximated by a straight line which passes through the point for pure water. The linear dependence of L on both the solution molarity and the volume fraction of water suggests that the hydration number for each amino acid is a constant, i.e., each additional amino acid molecule decreases the volume of water available to disolve Xe by a constant amount.

The assumption of constant H is borne out if we consider Figure 32, which is a graph of L/L<sub>0</sub> versus  $v_{tw} - \bar{H}M/55.346$ . The ordinate can be recognized as the volume fraction of free water as measured by Xe solubility. The abscissa is the volume fraction of free water in a solution of molarity M and volume fraction of water  $v_{tw}$ , assuming a constant mean hydration number  $\bar{H}$ . The data, for the most part, closely follow the line L/L<sub>0</sub> =  $v_{tw} - \bar{H}M/55.346$ . Deviations tend to be at high solution molarity, where we might expect, as in NaCl solutions, a deviation from a constant H.

What properties of amino acids determine the hydration number? Figure 33 is a plot of the mean hydration number as a function of the molecular weight of the amino acid, which is a rough measure of the size of the amino acid molecule. From this plot, we can see that there is no obvious correlation between H and the size of the molecule. The data are also broken down according to the type of side chain, whether it is nonpolar, polar, or positively charged. When viewed in this way, some observations do suggest themselves.

If we first consider the amino acids with nonpolar side groups, we see that the majority have hydration numbers in the range from 7 to

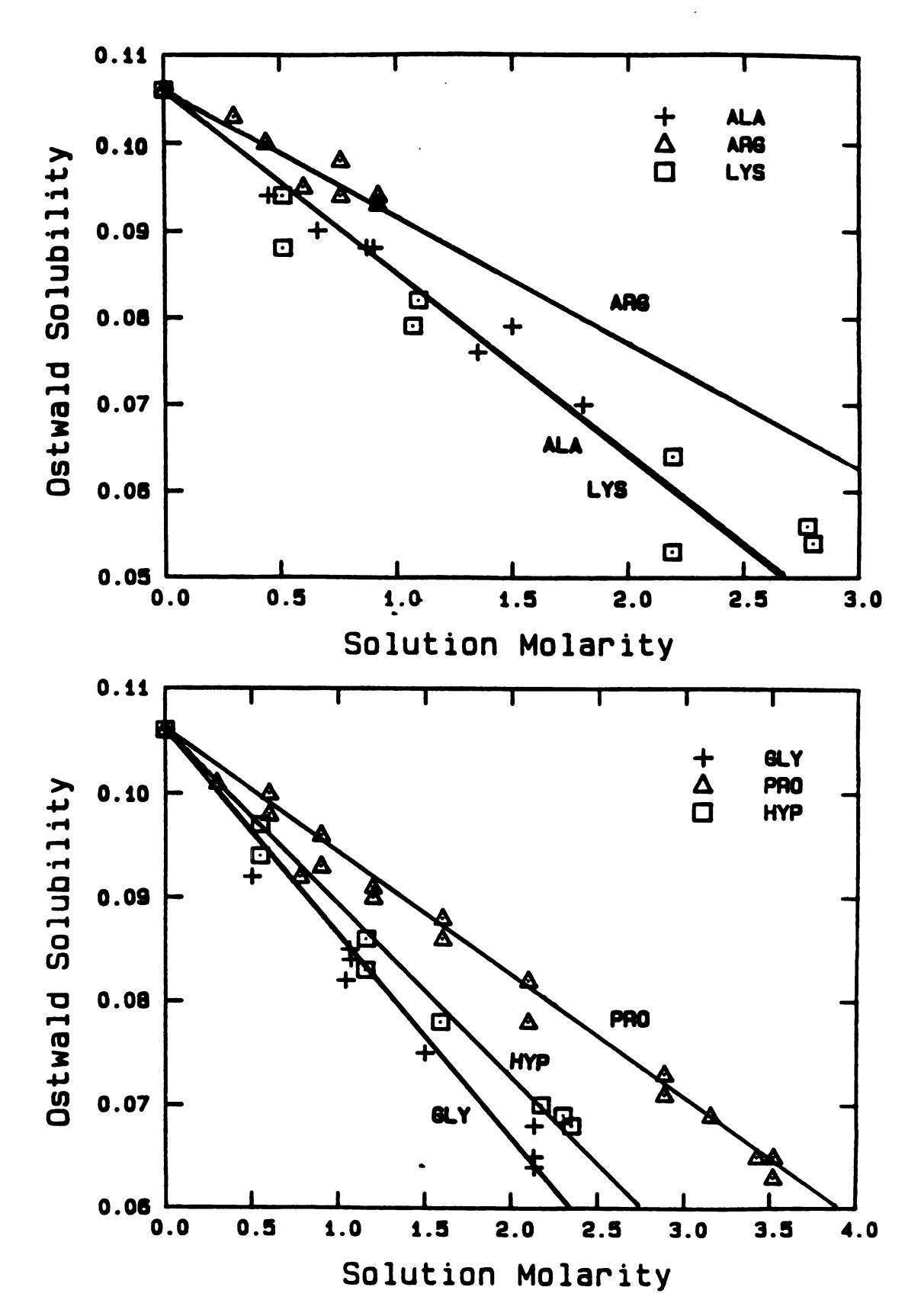


Figure 30. L vs. M for Xe in aqueous amino acid solutions.

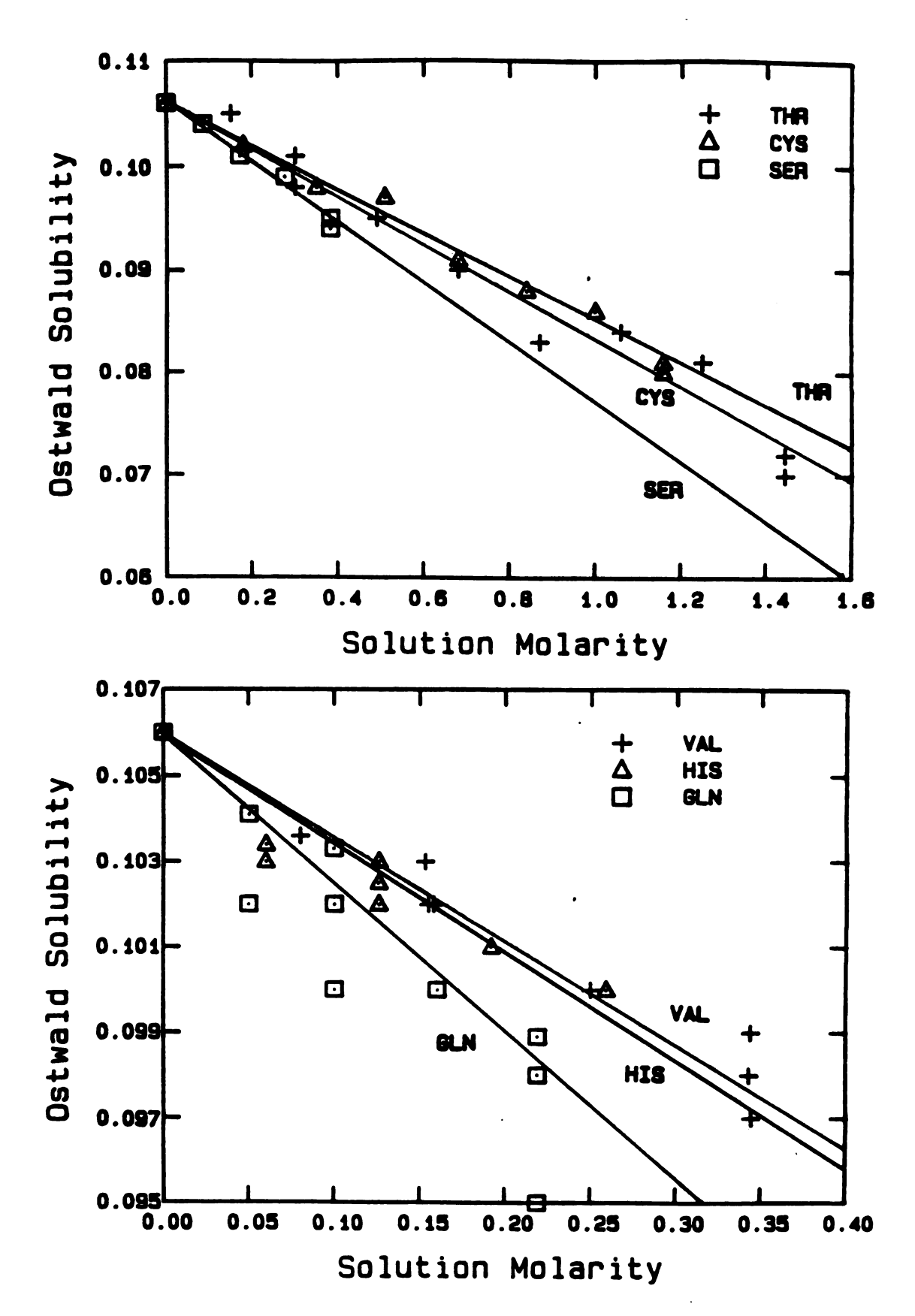


Figure 30. (cont'd.).

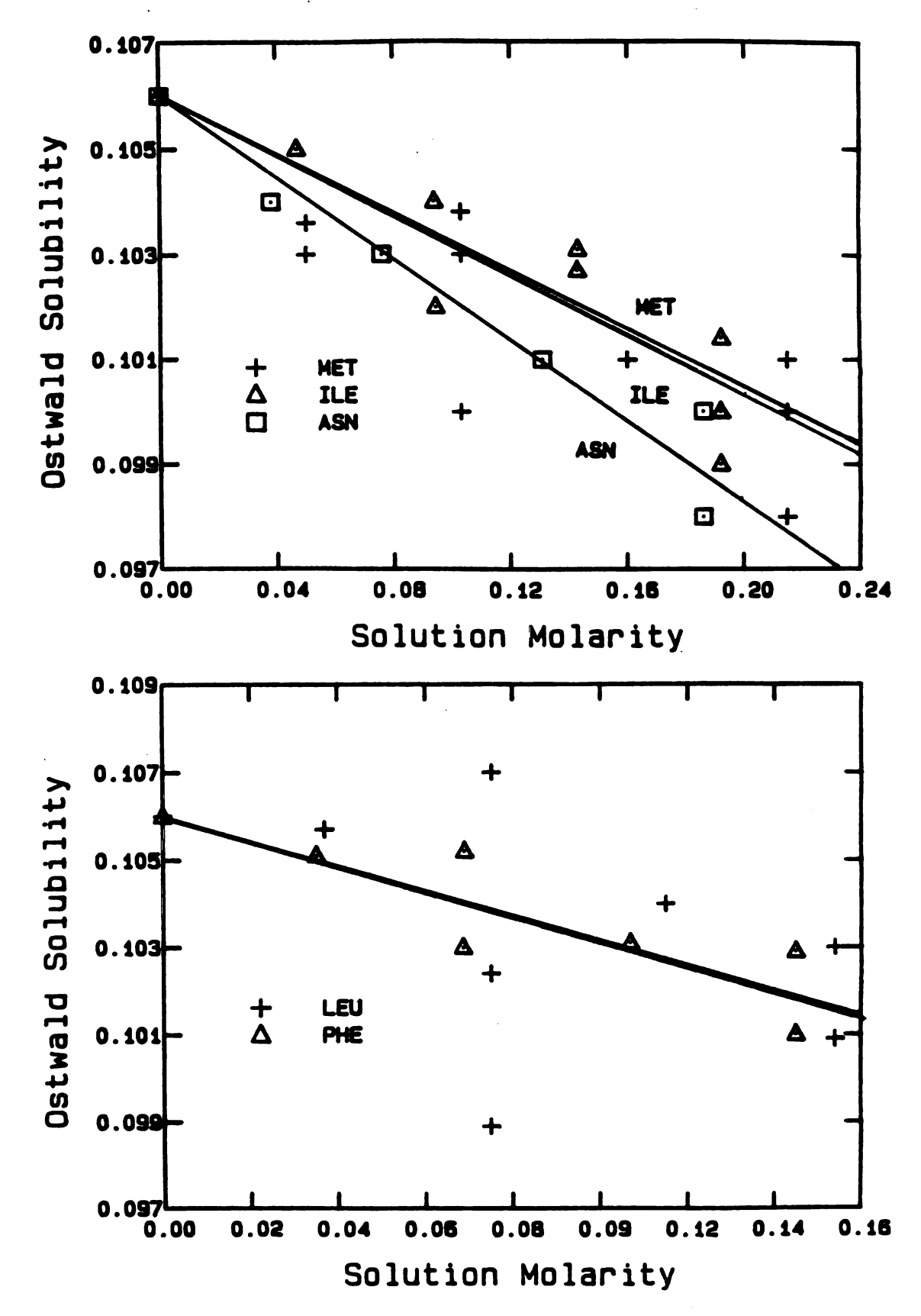


Figure 30. (cont'd.).

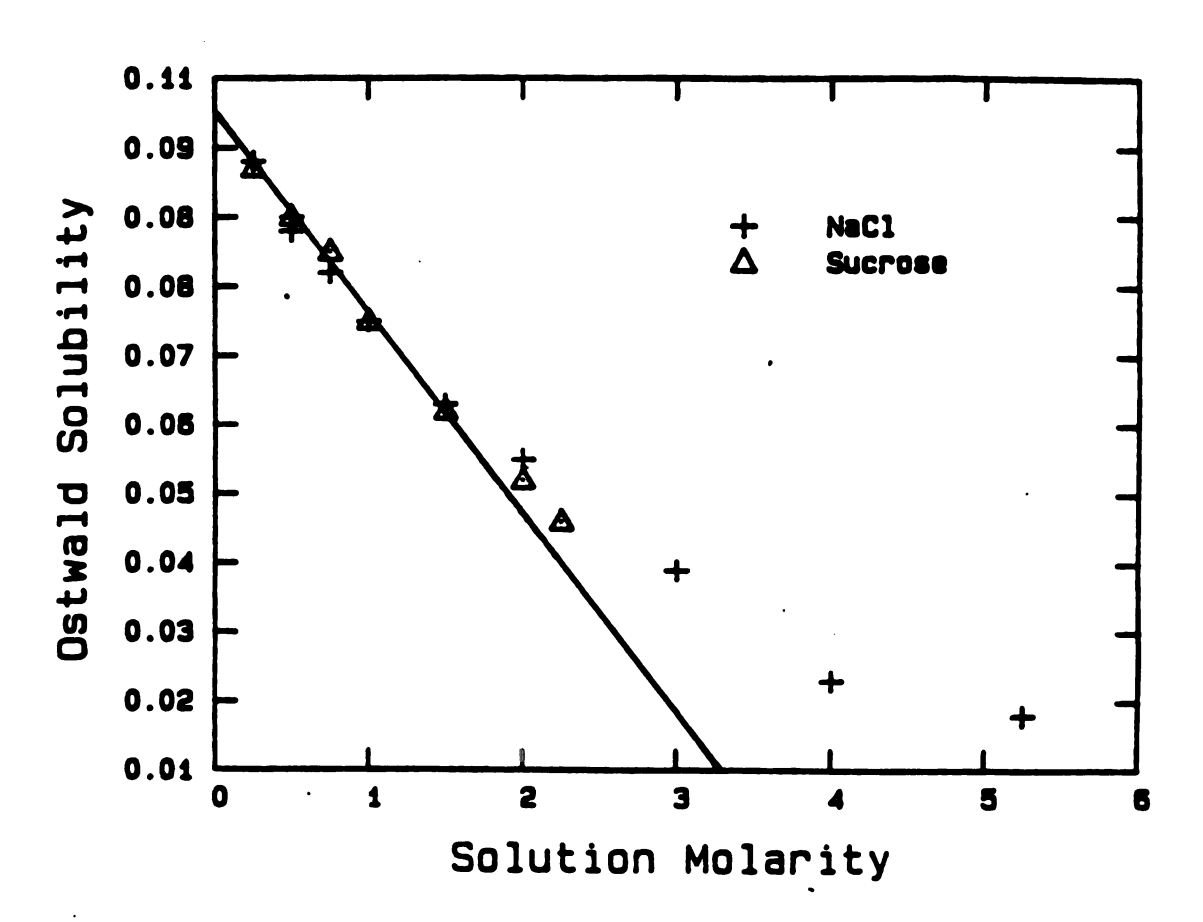


Figure 30. (cont'd.).

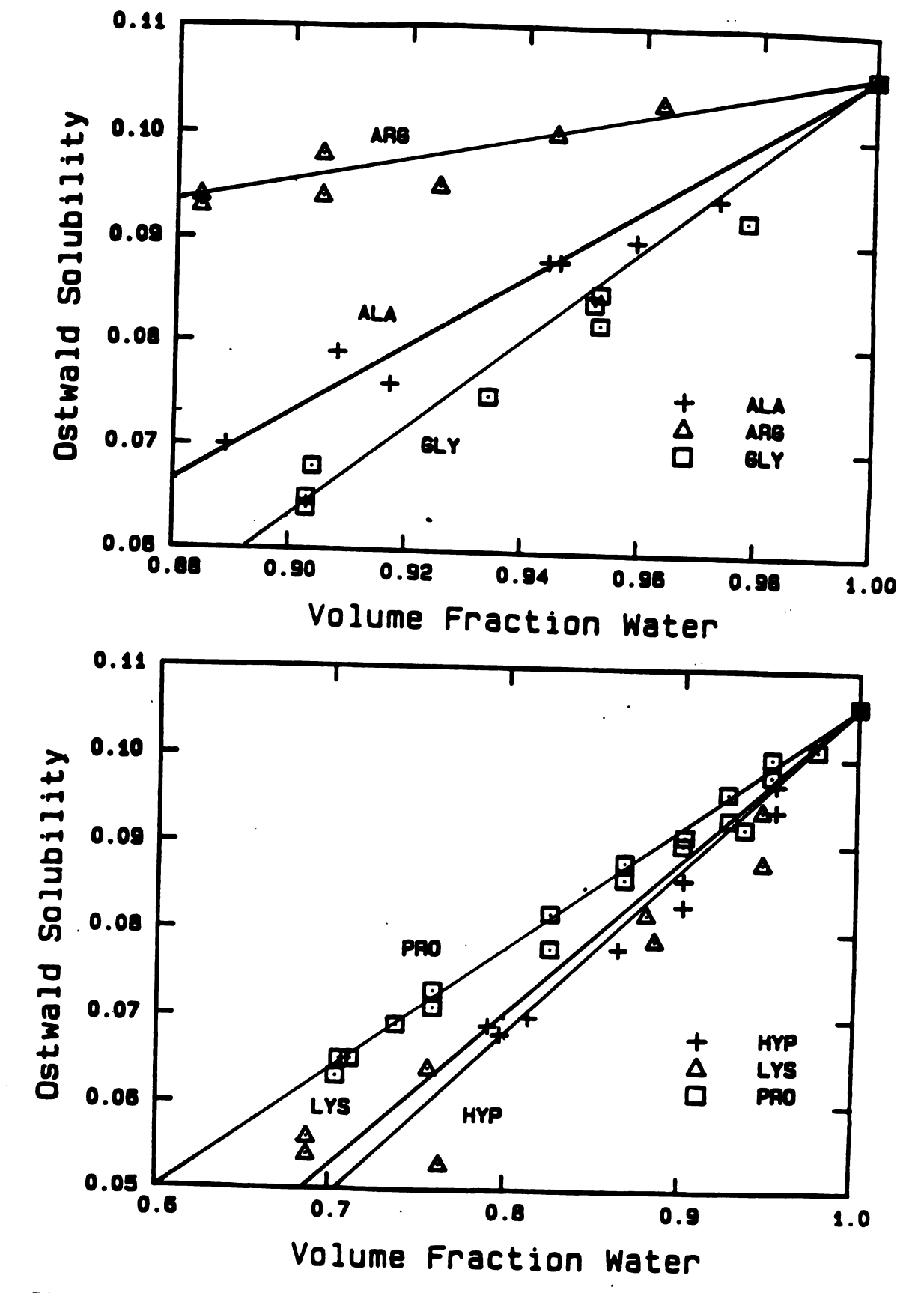


Figure 31. L vs.  $v_{tw}$  for Xe in aqueous amino acid solutions.

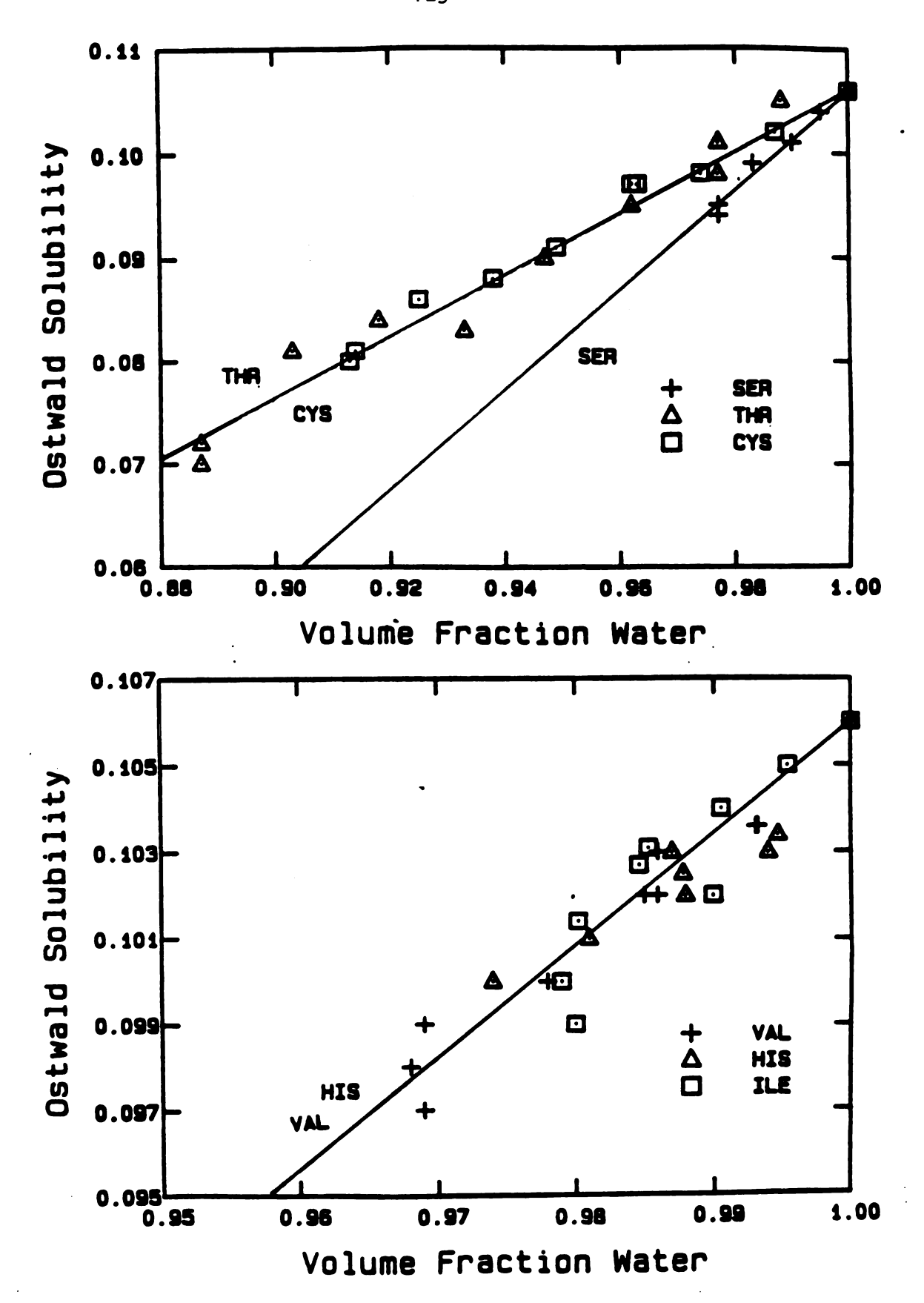


Figure 31. (cont'd.).

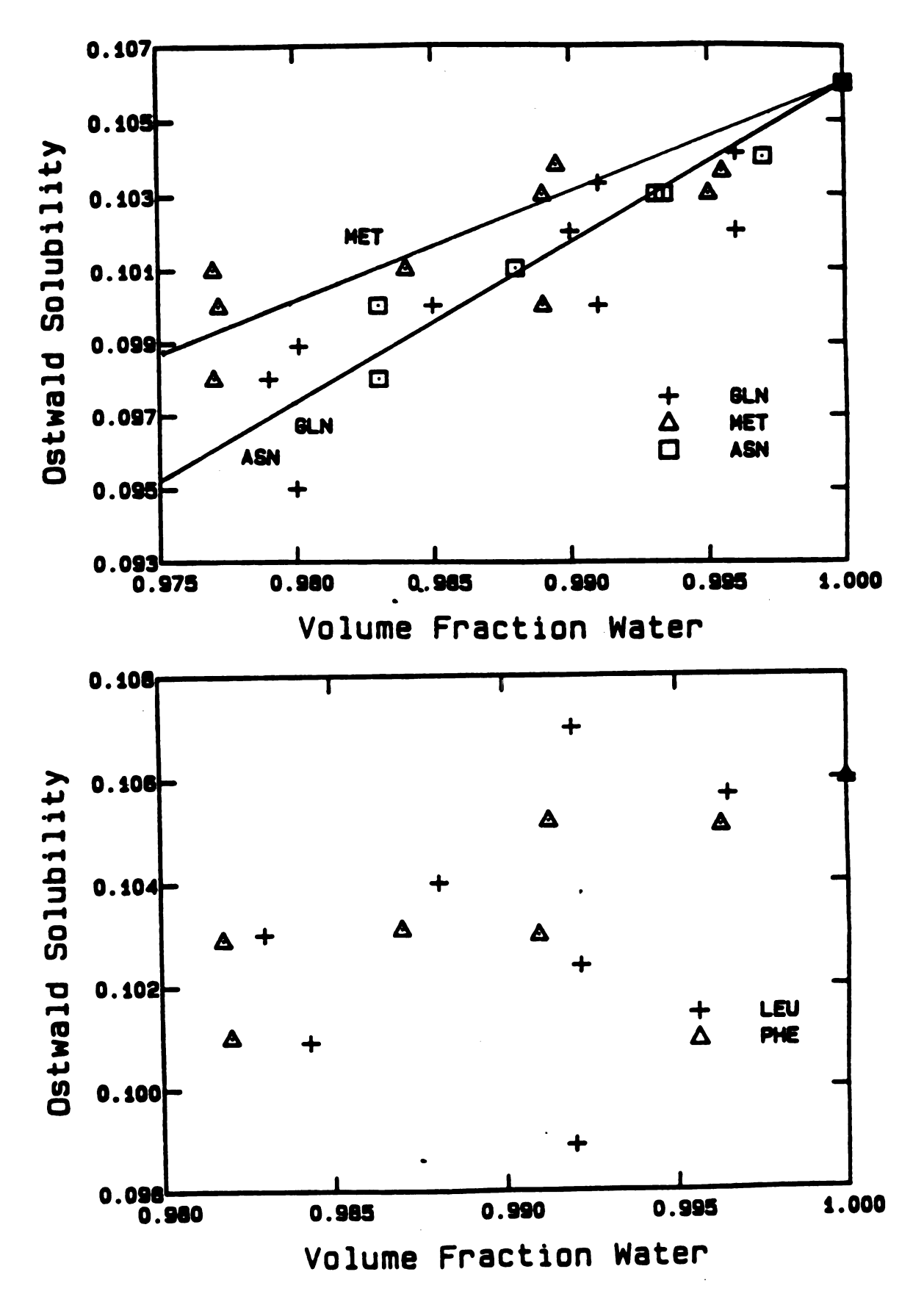


Figure 31. (cont'd.).

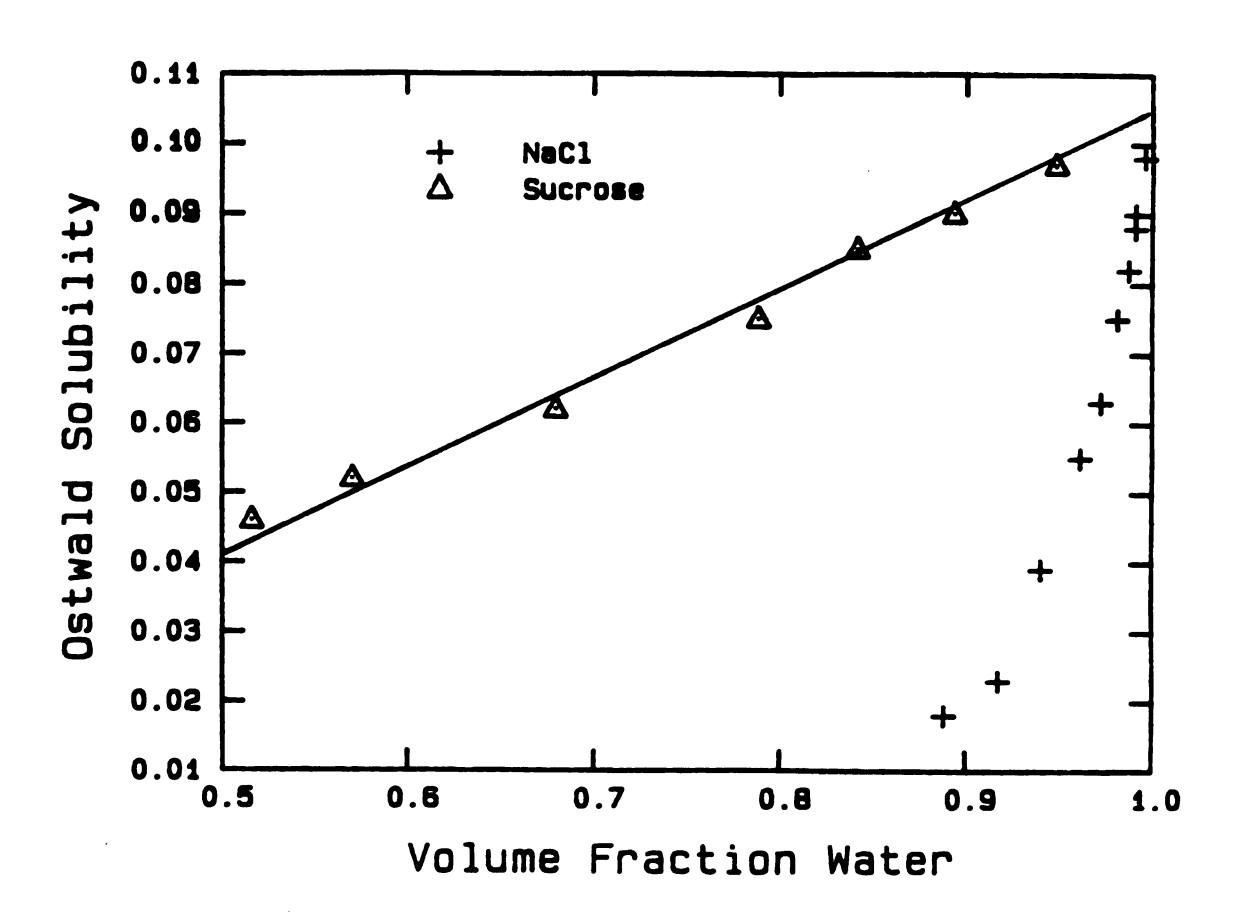


Figure 31. (cont'd.).

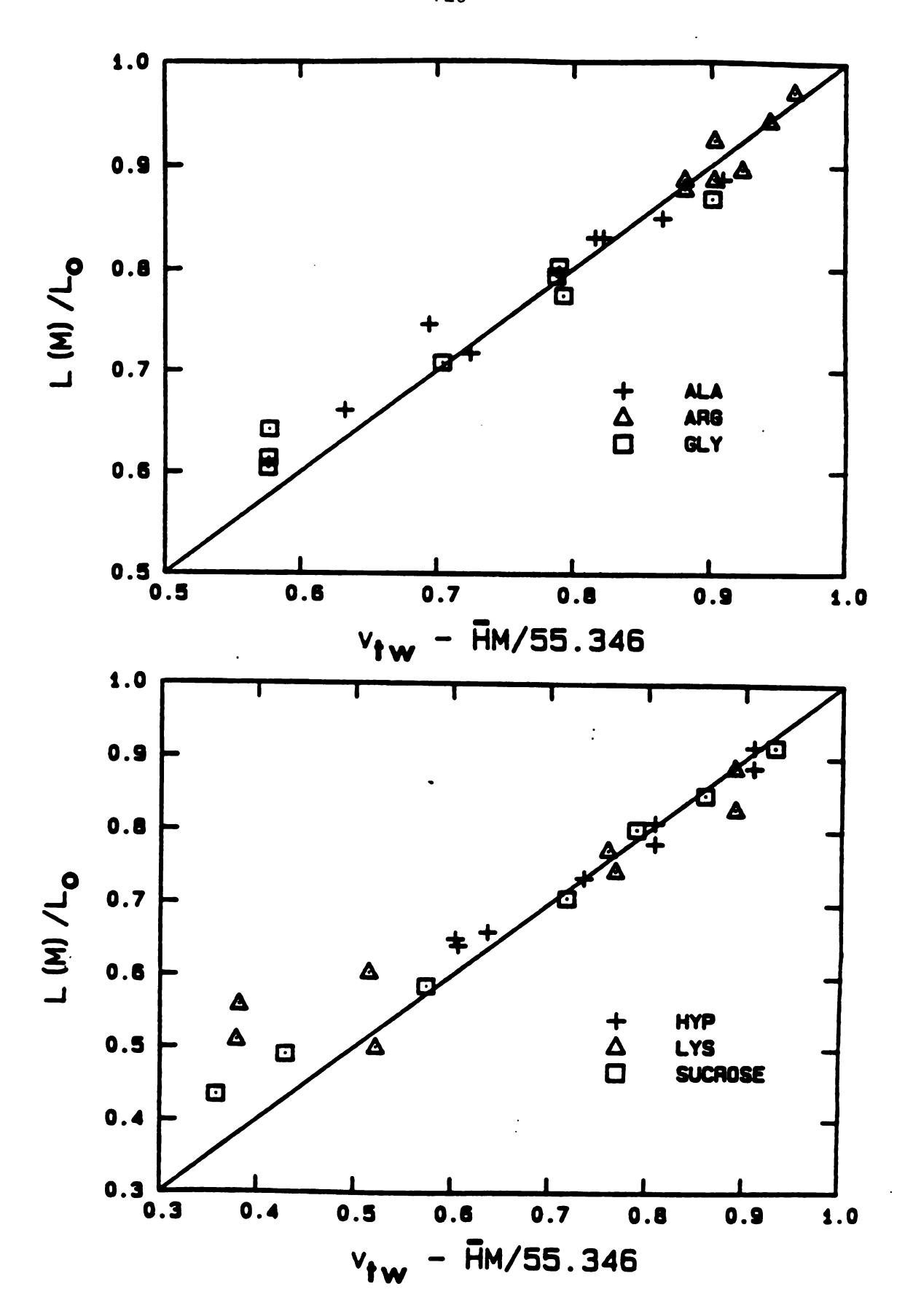


Figure 32.  $L/L_0$  vs.  $v_{tw}$  - HM/55.346 for amino acid solutions.

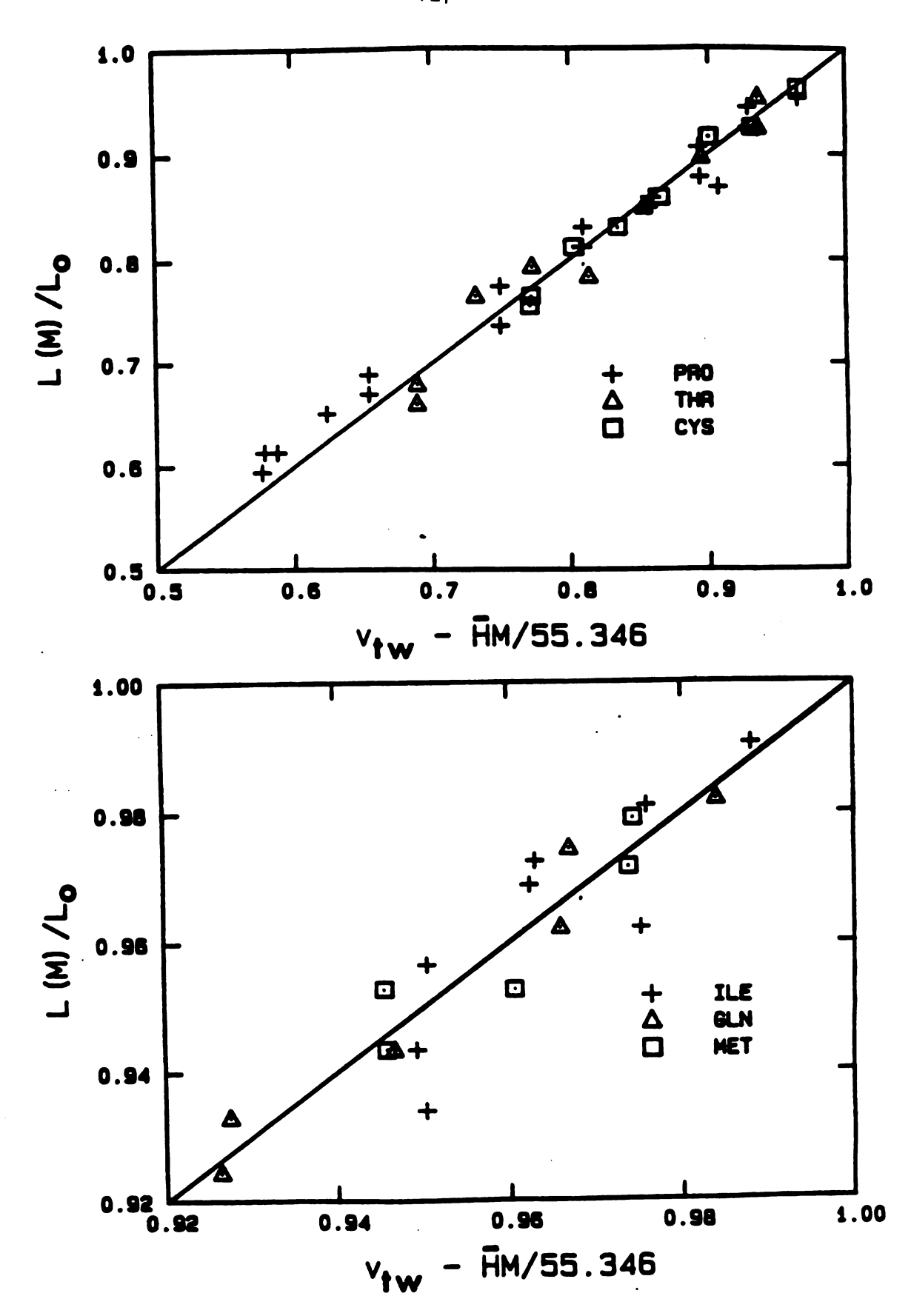


Figure 32. (cont'd.).

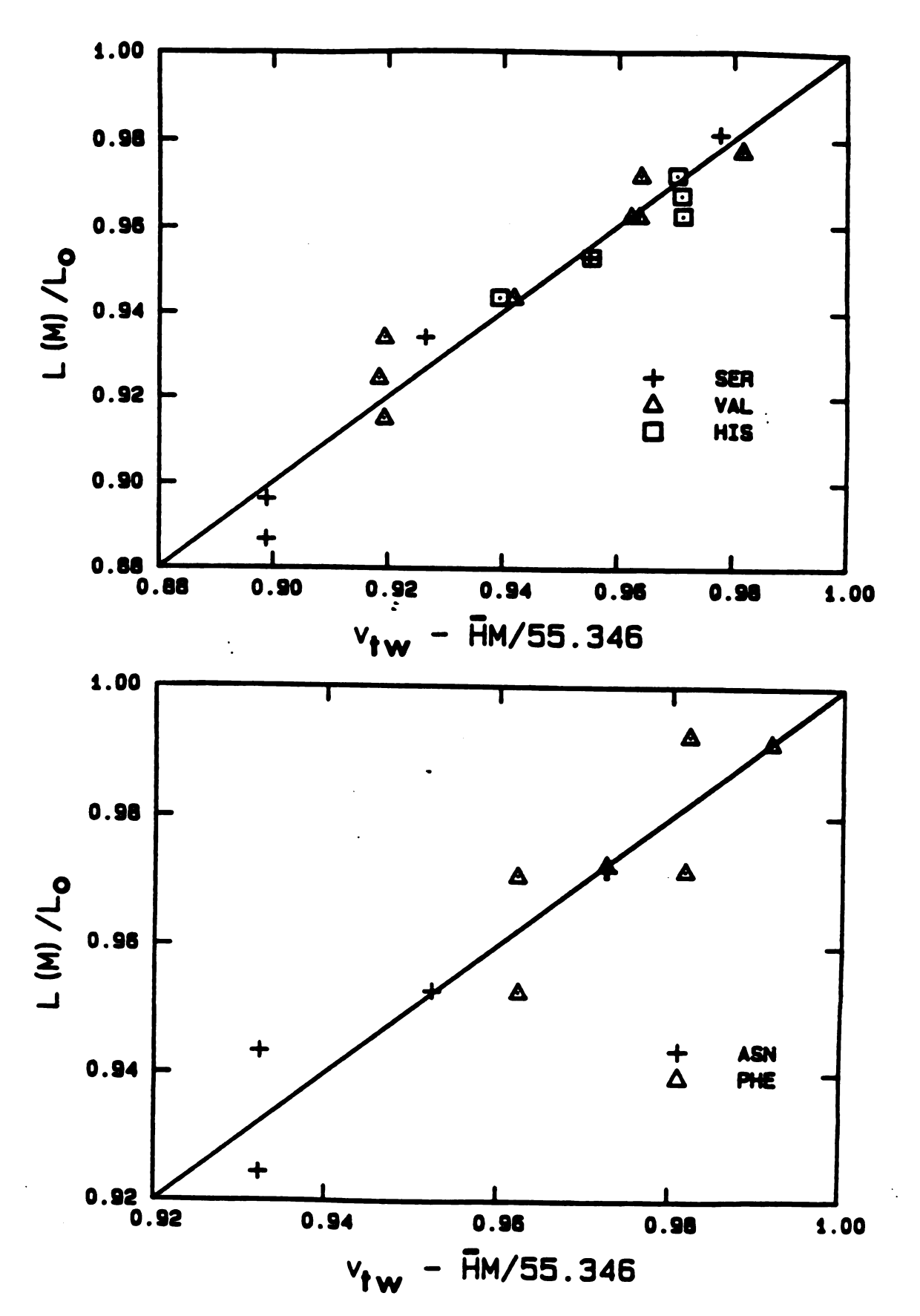


Figure 32. (cont'd.).

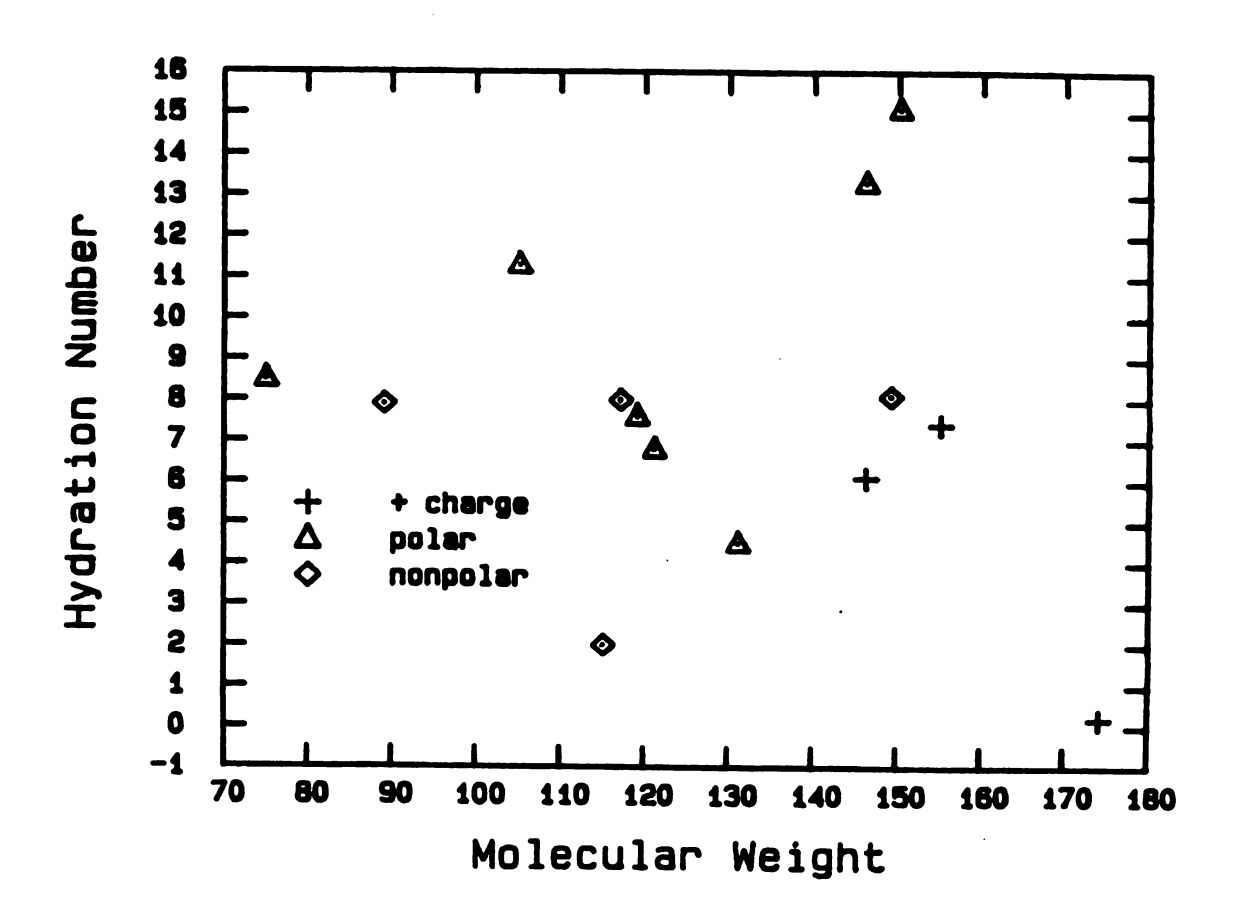


Figure 33.  $\bar{H}$  vs. molecular weight.

9. Glycine, which has a molecular weight of 75.07, has a hydrogen atom as its side group, and although it is included in the polar group, it might also be included in the nonpolar group. GLY has an H of 8.5, which is in the proper range.

The amino acids with polar side groups tend to have higher H values. The exceptions are THR, CYS, and HYP. Hydroxyproline will be discussed below. Cysteine has the difficulty discussed above, namely a large uncertainty in H due to the cystine precipitate. Threonine is the third anomalous amino acid in this group. We would expect, based on the similarity of structure of serine and threonine, that these two amino acids would have nearly identical hydration numbers. The large difference is puzzling.

The amino acids with positively charged side groups may have slightly lower hydration numbers than the nonpolar group. It is interesting to note that ARG and LYS display a large difference in H, despite a strong similarity in structure. Arginine, with H =  $0.2 \pm 0.5$ , probably has some affinity for Xe.

Proline differs from other amino acids in that the nitrogen atom in the amino acid head group is also bound to the side chain, forming a ring structure. Since it is bound, the amino group is no longer ionized in solution. The low hydration number for PRO,  $H = 2.0 \pm 0.2$ , could be due to either a Xe affinity, or to the loss of the dipolar charge of the amino acid head group. The slightly higher value of  $H = 4.5 \pm 0.4$  for hydroxyproline, which is a proline molecule with an additional hydroxyl (OH) group, could be due to the addition of the polar OH group.

Figure 34 shows  $\overline{H}$  versus pH, with the same breakdown according to R group as in Figure 33. There is no obvious correlation between H and

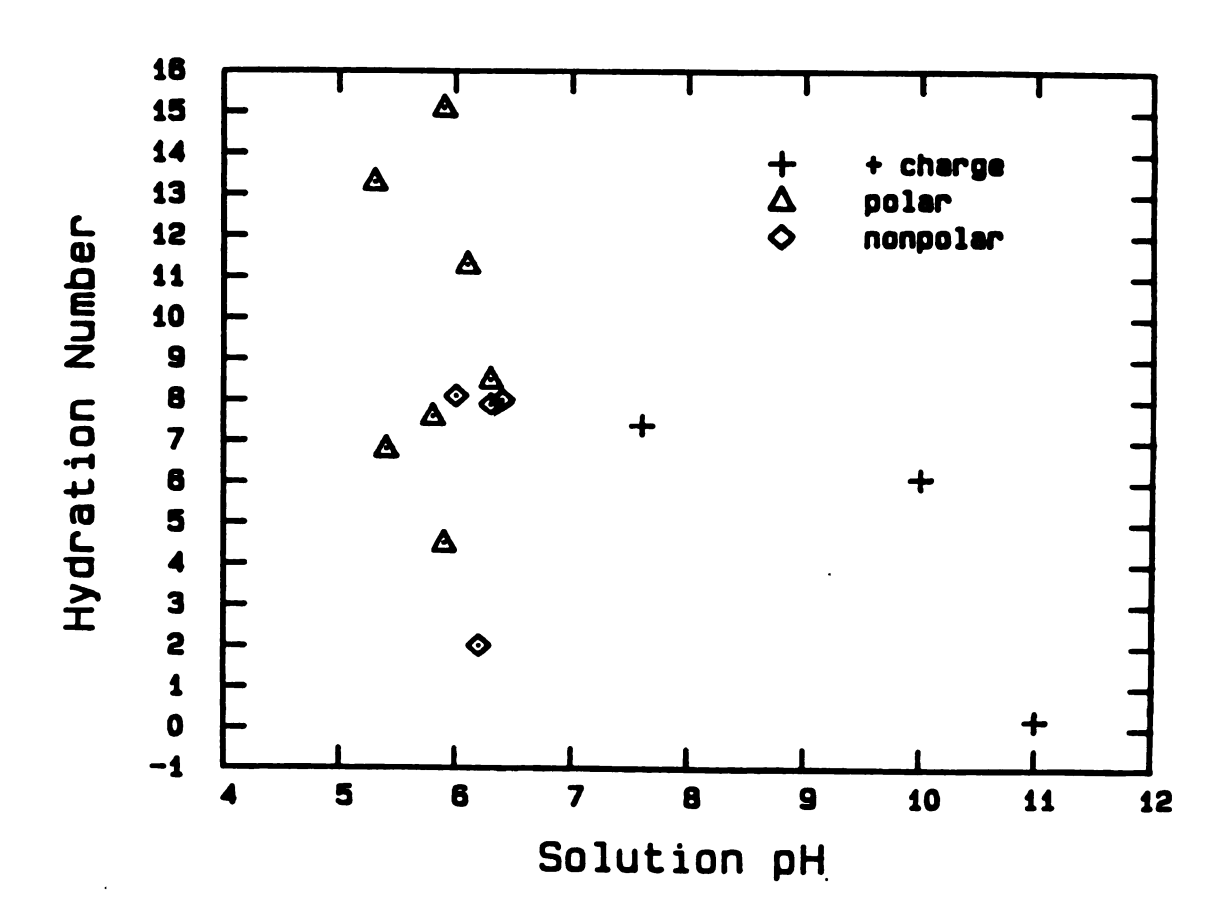


Figure 34.  $\overline{H}$  vs. solution pH.

pH, although there may be some decrease in H with increasing pH for pH > 7.

Eucken and Hertzberg<sup>59</sup> have measured the solubility of the rare gases in a variety of alkali/halide salt solutions. The calculated hydration number of NaCl is H = 20.2, which agrees favorably with our value of  $16.2 \pm 0.5$ . Goto<sup>80</sup> reports a hydration value of H = 22 for NaCl, calculated from effective volumes of electrolytes in aqueous solution.

There are several other methods which may be used to calculate hydration numbers. These methods include ultrasonic interferometry, near infra-red spectrophotometry, and analysis of molal volume and adiabatic compressibility data.

Hollenberg and Ifft<sup>77</sup> used the spectrophotometry method to measure hydration numbers of amino acids in solution. Hollenberg and Hall also used this method to measure hydration numbers of sugars. Some of their values are listed in Table 12. Also included in the table are hydration numbers from the work of Millero et. al.<sup>78</sup> and of Goto and Isemura.<sup>79</sup> The former analysed apparent molal volume and compressibility data, and the latter used ultrasonic interferometry. Our values are included for comparison.

The data of Hollenberg and Ifft are highly variable, even for similar molecules. For example, LEU and ILE have hydration numbers of  $8.3 \pm 0.4$  and  $24.0 \pm 0.4$ , respectively. This, along with other considerations, 82 probably indicate that we should discard their results.

What can we conclude about our hydration numbers? Why do our values differ so markedly from those of Millero et al. and Goto and Isemura? Our method of determining hydration numbers is quite different from that of either of these groups. Our values of H are actually a measure of many different effects. We assume that the excluded volume effect is the only process which causes a change in solubility. This is certainly a naive model, since we are working with a three component system, and interactions between the components are undoubtedly very complex. At the least, there is probably a second contribution to the hydration values from Xe/amino acid interactions, such as is hinted at by the hydration number of arginine.

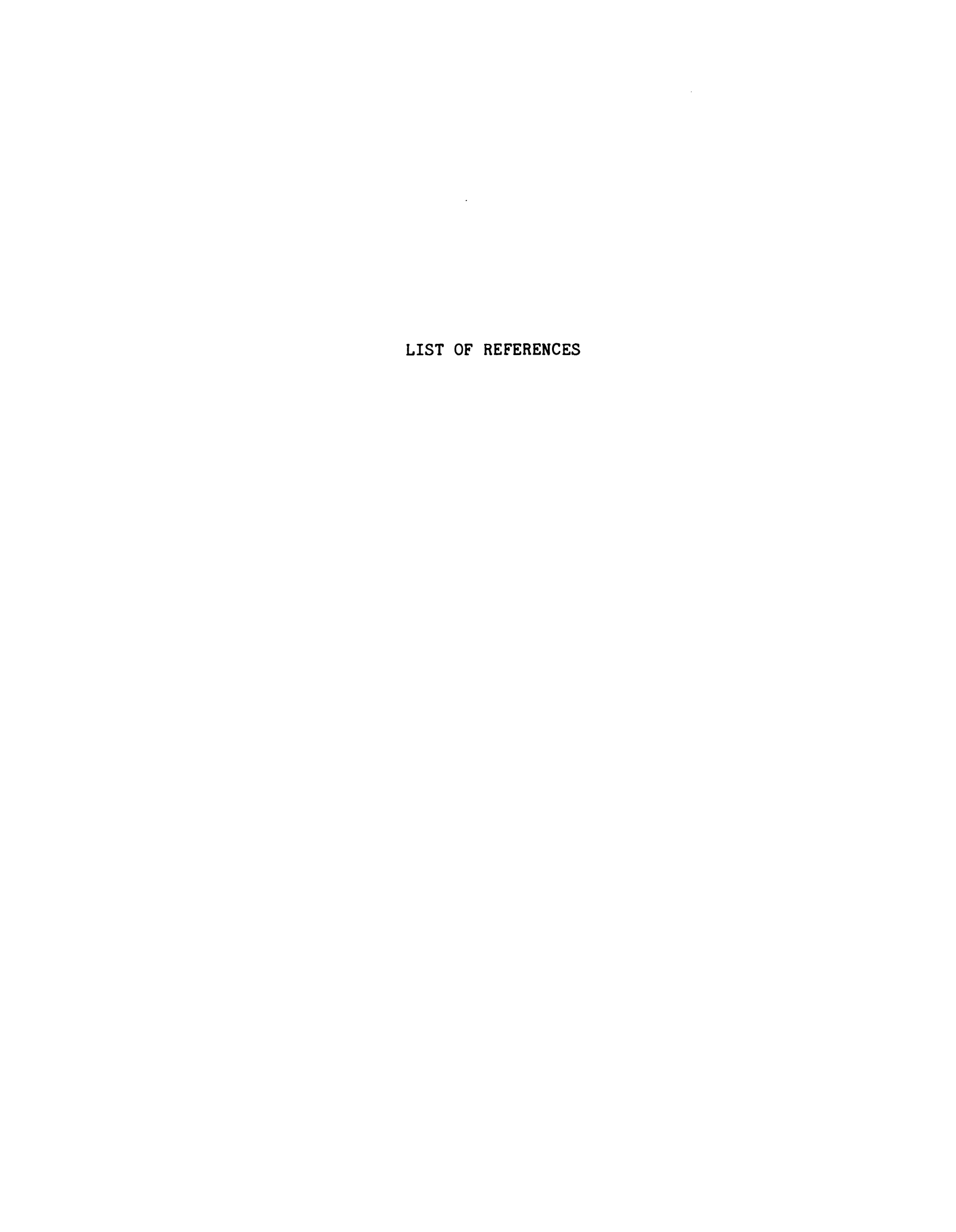
The difference between our values, and those of Millero et al. and Goto and Isemura, may be due to differences in the strength of the water/amino acid "bond". If water were tightly bound only to the polar head group of an amino acid, and not to the rest of the molecule, it is possible that only this tightly bound water would affect such bulk properties as the partial molal volume, adiabatic compressibility, and sound velocity.

Although our model of amino acid hydration is not altogether well defined, it does explain the linear dependence of L on solution molarity. It also shows that there may be an attractive interaction between Xe and arginine in aqueous solution.

There are several avenues of research to pursue here, also. First, a buffer might be added to the amino acid solutions to control the pH. This would be closer to physiological conditions in which the pH of the cell is controlled. A disadvantage to this approach is the addition of a fourth component to an already complex system.

Second, experiments could be done with polyamino acids in aqueous solutions. The advantage here is that the contribution to hydration from the polarity of the amino acid head group is eliminated, since these groups are bound to each other in the formation of the polypeptide bonds. These experiments would be very expensive to undertake at the present time, but as improvements are made in the production process, the cost of polyamino acids should decrease.

Third, studies might be done on the solubility of Xe in solutions of the amino acids in the normal alkanes and alkanols, or in olive oil, which is a biological, nonpolar solvent. The liquid environment in these solvents is similar to that in the interior of a cell membrane.



## LIST OF REFERENCES

- 1. G. L. Pollack, Rev. Mod. Phys. 36, 748 (1964).
- 2. M. L. Klein and J. A. Venables, eds., Rare Gas Solids, vol. 1 and 2, (Academic Press, London, 1976).
- 3. G. A. Cook, ed., Argon, Helium, and the Rare Gases (Interscience, New York, 1961).
- 4. G. L. Pollack, U. S. Nuclear Regulatory Commission, Accession No. 8008190073, September, 1979; Accession No. 8004160039, March 1980.
- 5. M. J. Halsey, R. A. Millar, and J. A. Sutton, eds., Molecular Mechanisms in General Anesthesia (Churchill Livingston, Edinburgh, 1974).
- 6. D. E. Metzler, <u>Biochemistry the Chemical Reactions of Living Cells</u> (Academic Press, New York, 1977).
- 7. L. Stryer, Biochemistry (W. H. Freeman and Company, San Francisco, 1975); A. L. Lehninger, Biochemistry (Worth Publishers, New York, 1972).
- 8. J. Timmermans, Physico-Chemical Constants of Pure Organic Compounds, Volume 1, (Elsener Publishing Co., New York, 1950).
- 9. R. C. Wilhoit and B. J. Zwolinski, J. Phys. Chem. Ref. Dat., 2, Supplement 1, (1973).
- 10. R. S. Berry, S. A. Rice, and J. Ross, <u>Physical Chemistry</u> (John Wiley and Sons, New York, 1980).
- 11. G. Boato, G. Scoles, and M. E. Vallauri, Nuovo Cimento 14, 735 (1959).
- 12. H. C. Weber and H. P. Meissner, <u>Thermodynamics for Chemical</u> Engineers (John Wiley and Sons, New York, 1959).
- 13. M. Tribus, Thermostatics and Thermodynamics (Van Nostrand, New Jersey, 1961).
- 14. R. H. Davies, A. G. Duncan, G. Saville, and L. A. K. Staveley, T. Farad. Soc. 63, 855 (1967).
- 15. J. C. G. Calado and L. A. K. Staveley, T. Farad. Soc. <u>67</u>, 289 (1971).
- 16. T. D. O'Sullivan and N. O. Smith, J. Phys. Chem. 74, 1460 (1970).

- 17. A. Ben-Naim, <u>Water and Aqueous Solutions</u> (Plenum Press, New York, 1974).
- 18. G. J. Yevick and J. K. Percus, Phys. Rev. 101, 1186 (1956).
- 19. J. K. Percus and G. J. Yevick, Phys. Rev. 101, 1192 (1956).
- 20. J. K. Percus and G. J. Yevick, Nuovo Cimento 5, 65 (1957).
- 21. J. K. Percus and G. J. Yevick, Nuovo Cimento 5, 1057 (1957).
- 22. J. K. Percus and G. J. Yevick, Phys. Rev. 110, 1 (1958).
- 23. E. Thiele, J. Chem. Phys. 39, 474 (1963).
- 24. M. S. Wertheim, Phys. Rev. Let. 10, 321 (1963).
- 25. J. L. Lebowitz, Phys. Rev. A 133, 895 (1964).
- 26. H. Reiss, H. L. Frisch, and J. L. Lebowitz, J. Chem. Phys. <u>31</u>, 369 (1959).
- 27. H. Reiss, H. L. Frisch, E. Helfand, and J. L. Lebowitz, J. Chem. Phys. 32, 119 (1960).
- 28. E. Helfand, H. Reiss, H. L. Frisch, and J. L. Lebowitz, J. Chem. Phys. 33, 1379 (1960).
- 29. H. H. Uhlig, J. Phys. Chem. 41, 1215 (1937).
- 30. D. D. Eley, T. Farad. Soc. 35, 1281, 1421 (1938).
- 31. H. Reiss, Advances in Chem. Phys. 9, 1 (1964).
- 32. H. Reiss and S. W. Mayer, J. Chem. Phys. 34, 2001 (1961).
- 33. R. A. Pierotti, J. Phys. Chem. 67, 1840 (1963).
- 34. R. A. Pierotti, J. Phys. Chem. 69, 281 (1965).
- 35. E. Wilhelm and R. Battino, J. Chem. Phys. 55, 4012 (1971).
- 36. S. J. Yosim and B. B. Owens, J. Chem. Phys. 39, 2222 (1963).
- 37. S. J. Yosim, J. Chem. Phys. 40, 3069 (1964).
- 38. H. C. Longuet-Higgins and B. Widom, Mol. Phys. 8, 549 (1964).
- 39. N. S. Snider and T. M. Herrington, J. Chem. Phys. 47, 2248 (1967).
- 40. J. G. Kirkwood and F. P. Buff, J. Chem. Phys. 19, 774 (1951).
- 41. I. Prigogine, The Molecular Theory of Solutions (North Holland Publishing Company, Amsterdam, 1957).

- 42. K. Watanabe and H. C. Anderson, J. Phys. Chem. 90, 132 (1986).
- 43. A. Michels, T. Wassenaar, and P. Louwerse, Physica 20, 99 (1954).
- 44. A. Ben-Naim, J. Phys. Chem. 82, 792 (1978).
- 45. A. Ben-Naim and Y. Marcus, J. Chem. Phys. 80, 4438 (1984).
- 46. M. C. A. Donkersloot, J. Soln. Chem. 8, 293 (1979).
- 47. K. J. Patil, J. Soln. Chem. 10, 315 (1981).
- 48. K. Kojima, T. Kato, and H. Nomura, J. Soln. Chem. 13, 151 (1984).
- 49. H. Schneider in Solute-Solvent Interactions, J. F. Coetzee and C. D. Ritchie eds., (Marcel Dekker, New York, 1969).
- 50. D. D. Van Slyke, J. Biol. Chem. 30, 347 (1917).
- 51. D. D. Van Slyke and J. M. Neill, J. Biol. Chem. 61, 523 (1924).
- 52. S. Y. Yeh and R. E. Peterson, J. Pharm. Sci. 52, 453 (1963).
- 53. S. Y. Yeh and R. E. Peterson, J. Appl. Physiol. 20, 1041 (1965).
- 54. P. K. Weathersby and L. D. Homer, Undersea Biomed. Res. 7, 277 (1980).
- 55. J. Setschenow, Z. Physik. Chem. (Leipzig) 4, 117 (1889).
- 56. S. K. Shoor and K. E. Gubbins, J. Phys. Chem. 73, 498 (1969).
- 57. W. L. Masterton and T. P. Lee, J. Phys. Chem. 74, 1776 (1970).
- 58. W. L. Masterton, J. Soln. Chem. 4, 523 (1975).
- 59. A. Eucken and G. Hertzberg, Z. Physik. Chem. 195, 1 (1950).
- 60. C. M. Lederer, J. M. Hollander, and I. Perlman, <u>Table of Isotopes</u>, sixth edition, (Jlhn Wiley & Sons, New York, 1967).
- 61. D. D. Hoppes and F. J. Schima, eds., NBS Special Publication 626, "Nuclear Data for the Efficiency Calibration of Germanium Spectrometer Systems", (NBS, January 1982).
- 62. R. T. Morrison and R. N. Boyd, Organic Chemistry (Allyn and Bacon, Boston, 1975).
- 63. R. R. Dreisbach, Physical Properties of Chemical Compounds. II. (American Chemical Society, Washington, D.C., 1959).
- 64. M. Windholz, ed., The Merck Index (Merck & Co., New Jersey, 1976).
- 65. K. Siegbahn, ed., Alpha-, Beta-, and Gamma-ray Spectroscopy, volume 1, (North Holland, Amsterdam, 1965).

- 66. H. G. Cuming and C. J. Anson, <u>Mathematics and Statistics for</u> Technologists (Chemical Publishing Co., New York, 1967).
- 67. G. L. Pollack, J. Chem. Phys. <u>75</u>, 5875 (1981).
- 68. G. L. Pollack and J. F. Himm, J. Chem. Phys. 77, 3221 (1982).
- 69. G. L. Pollack, J. F. Himm, and J. J. Enyeart, J. Chem. Phys. 81, 3239 (1984).
- 70. G. L. Pollack and J. F. Himm, J. Chem. Phys. <u>85</u>, 456 (1986).
- 71. J. Makranczy, K. Megyery-Balog, L. Rusz, and L. Patyi, Hung. J. Ind. Chem. 4, 269 (1976).
- 72. H. L. Clever, R. Battino, J. H. Saylor, and P. M. Gross, J. Phys. Chem. 61, 1078 (1957).
- 73. H. L. Clever, J. Phys. Chem. 62, 375 (1958).
- 74. V. G. Komarenko and V. G. Manzhelii, Ukr. Phys. J. 13, 273 (1968).
- 75. M. H. Abraham, J. Am. Chem. Soc. <u>104</u>, 2085 (1982).
- 76. T. H. Lilley, in Chemistry and Biochemistry of the Amino Acids, G. C. Barrett, ed., (Chapman and Hall, London, 1985).
- 77. J. L. Hollenberg and J. B. Ifft, J. Phys. Chem. <u>86</u>, 1938 (1982).
- 78. F. J. Millero, A. Lo Surdo, and C. Shin, J. Phys. Chem. <u>82</u>, 784 (1978).
- 79. S. Goto and T. Isemura, Bull. Chem. Soc. Jpn. 37, 1697 (1964).
- 80. S.Goto, Bull. Chem. Soc. Jpn. 37, 1685 (1964).
- 81. J. L. Hollenberg and D. O. Hall, J. Phys. Chem. 87, 695 (1983).
- 82. J.Jayne, J. Phys. Chem. 87, 527 (1983).

